

**The Large Scale Understanding of Natural Organic
Matter: Processes and Application**

Jessica Louise Adams

BSc (Hons)

Lancaster Environment Centre

Lancaster University

Submitted for the degree of Doctor of Philosophy

April 2017

Declaration

I declare that the work produced for this thesis is my own, and has not been presented to obtain any other degree. Collaborations with other researchers are fully acknowledged.

Jessica Louise Adams

Lancaster University, April 2017

Statement of authorship

This thesis is prepared in the alternative format, as a series of four papers, one of which is published in a peer reviewed journal and is presented as the final copy before journal editing. The rest are submitted to journals or intended for submission, with the exception of the consolidated bibliography at the end of the thesis, and where the manuscripts refer to other chapters. All papers have several authors. Their contributions to each paper are detailed below, and have been approved by my supervisors. Chapters 1, 2 and 7 include an introduction, literature review discussion respectively, and are not intended for submission.

Chapter 3 is in review in the journal *Plant and Soil* (special issue S69 – OP2016) (submitted 31/03/2017) as:

JL Adams, E Tipping, A Lawlor, JN Quinton (2017) Density fractionation of soil organic phosphorus.

JLA set up the experiment, carried out the lab work, analysed the data and prepared the manuscript. ET gave advice on experimental design and analysis, and contributed significantly to revisions of the manuscript. AL also carried out analyses on the samples and provided data for certified reference standards. JNQ gave advice on data analysis and interpretation and contributed to manuscript revisions.

Chapter 4 is published as:

JL Adams, E Tipping, CL Bryant, RC Helliwell, H Toberman, JN Quinton (2015)
Aged riverine particulate organic carbon in four UK catchments. *Science of the Total Environment*. 536, 648-654.

JLA carried out the sampling, processing and data analysis, and prepared the manuscript. ET also collected samples, gave advice on data analysis and contributed significantly to manuscript revisions. CLB carried out radiocarbon analysis of the samples. RCH executed sampling of one of the catchments, and provided data. HT provided data on the radiocarbon content of the catchment soils. JNQ contributed significantly to manuscript revisions and gave advice on data analysis.

Chapter 5 is intended for publication as:

JL Adams, E Tipping, R Helliwell, N Pedentchouk, R Cooper, S Buckingham, E Gjessing, P Ascough, C Bryant and M Garnett (2017) Quantifying sources of dissolved organic radiocarbon in rivers.

JLA collected and processed samples, collated and analysed the data and prepared the manuscript. ET also collected samples and contributed significantly to the revised manuscript. RH collected samples from one of the catchments and provided data. NP, RC, SB and EG all contributed unpublished data. PA and MG carried out database searches of the NERC radiocarbon facility, and provided data. CB carried out the radiocarbon analyses and provided data.

Chapter 6 is in review in the journal *Inland Waters* (submitted 16/03/2017) as:

JL Adams, E Tipping, H Feuchtmayr, H Carter, P Keenan (2017) The contribution of algae to freshwater dissolved organic matter: implications for UV spectroscopic analysis.

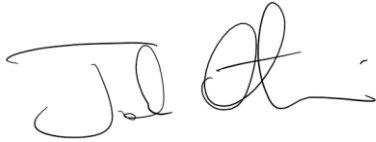
JLA collected and processed the samples, analysed the data and prepared the manuscript. ET and HF also collected samples, provided data and contributed significantly to the revised manuscript. HC and PK carried out analyses of the samples.

I hereby agree with the above statements:

A handwritten signature in black ink on a light grey background. The signature appears to be 'E. Tipping' written in a cursive, slightly stylized font.

Prof. Edward Tipping

Centre for Ecology and Hydrology, Lancaster

A handwritten signature in black ink on a light grey background. The signature is highly stylized and cursive, appearing to be 'John N. Quinton'.

Prof. John N Quinton

Lancaster Environment Centre, Lancaster University.

Acknowledgements

This process would have not been possible without the support from a fantastic network of colleagues and friends. I was convinced that I would not be capable of achieving a PhD qualification. I have Dr. Niall McNamara to thank for convincing me otherwise. I am most grateful to Prof. Ed Tipping and Prof. John Quinton for agreeing to supervise me, and for their invaluable support and guidance, which has made me into the more confident scientist that I am today. I carried out my PhD full time while in full time employment at the Centre for Ecology and Hydrology (CEH) as a research associate. I am most appreciative of my line manager, Steve Lofts for his patience and understanding throughout. My project was part funded by CEH and Lancaster University, for which I am very grateful. Thanks are due to my examiners – Prof. Pippa Chapman and Dr. Peter Wynn for their constructive comments.

I have so many people to thank, whose kind words, patience and willing to listen have carried me forward during the tough stages. Rebecca, Ian, Susan, Kim, Jacky, Jess R, Jess D, Alona, Jeanette, Kate and the rest of the lunch time crew have provided valuable help, advice and friendship. My mum and John approached my PhD woes with good humour and wise perspectives. My dad never let me forget how proud of me he is. Of course, I have to mention my cat, Roux, who always let me know it was time for a break by lolling over my keyboard and running off with my pens.

Finally, I leave the most important person till last. Dafydd Elias has experienced my tears, tantrums and self-doubts at first hand, and has always responded with empathy and love. His calming nature, logic and quiet, can do attitude has been invaluable, not to mention the constant stream of tea and food. Daf, I will return the favour when you're writing up!

Abstract

Natural biogeochemical cycles of the macronutrient elements carbon (C), nitrogen (N) and phosphorus (P) have been transformed by food and fuel production, through atmospheric pollution and climate change. Further, land disturbance has led to considerable losses of nutrients from terrestrial ecosystems. This investigation aims to explore and address several barriers to understanding natural organic matter cycling across terrestrial and aquatic ecosystems.

Soil organic matter (SOM) turnover models are often constrained by C and N, while data on organic P is lacking. Twenty UK soils were used to provide the first investigation of organic P in density fractionated SOM pools. Organic matter in the mineral fraction was considerably more enriched in oP. Stoichiometric ratios agreed with a new classification model, which provides important constraints for models of nutrient cycles.

Radiocarbon (^{14}C) measurements of aquatic OM indicates sources and turnover on different timescales. Here, the first analysis of particulate O^{14}C in UK rivers suggested topsoil was the major source. Significantly depleted material was found in a catchment with historical mining activity. Global, temporal analysis of dissolved O^{14}C enabled quantification of different OM sources, and highlighted the importance of assessing the data against the changing atmospheric ^{14}C signal. New dissolved O^{14}C data for rural, arable and urban catchments were more depleted than the global averages.

In industry, there is a growing need to manage aquatic nutrient enrichment through rapid and reliable monitoring. A model of UV absorbance was tested against freshwaters that were biased towards eutrophic conditions. The results

demonstrated the weak absorbing components of algal DOM, and new variable model parameters were introduced, which quantified the contribution of algal DOM. This could have implications on model predictions of DOC concentration, and a generally applicable spectroscopic model is questionable.

This investigation considerably expands the dataset available for modelling large scale biogeochemical cycles, highlights the importance of an integrated approach, and considers the implications involved with applied modelled predictions of aquatic DOC.

Table of Contents

Declaration	2
Statement of authorship	3
Acknowledgements	7
Abstract	8
List of Tables	16
List of Figures	18
1. Introduction	24
<i>1.1 Thesis Aims and Objectives</i>	25
2 Literature Review	29
<i>2.1 Part I - Anthropogenic influences on terrestrial nutrient cycling</i>	29
<i>2.2 The nature and formation of soil organic matter</i>	31
<i>2.2.1 Biological processes of soil organic matter</i>	32
<i>2.2.2 The chemistry of soil organic matter</i>	33
<i>2.3 The physical state of soil organic matter</i>	35
<i>2.3.1 Selective preservation</i>	36
<i>2.3.2 Stabilization by spatial inaccessibility</i>	37
<i>2.3.3 Association with mineral matter</i>	38

2.4 <i>Soil organic matter turnover.</i>	39
2.5 <i>Soil organic matter Stoichiometry</i>	42
2.6 <i>Fractionated soil organic matter</i>	43
2.7 <i>Part II – Transport, fate and behaviour of natural organic matter in aquatic ecosystems</i>	46
2.7.1 <i>Nutrient transfer from land to freshwater</i>	46
2.7.2 <i>Dissolved and particulate organic carbon: Rivers and Estuaries</i>	48
2.7.3 <i>Nutrient cycling in lakes and reservoirs</i>	51
2.8 <i>Quantifying DOC in freshwater systems</i>	52
2.9 <i>Overview</i>	56
2.9.1 <i>Quantification</i>	57
2.9.2 <i>Spatial scale</i>	57
2.9.3 <i>Technology</i>	59
3. Density fractionation of soil organic phosphorus	65
3.1. <i>Introduction</i>	66
3.2. <i>Methods</i>	70
3.2.1. <i>Sample selection</i>	70

3.2.2. <i>Analysis of the bulk soil samples</i>	70
3.2.3. <i>Aggregate separation by density</i>	71
3.2.4. <i>Extraction of the heavy fraction</i>	72
3.3. <i>Fractionated soil: Analyses</i>	73
3.3.1. <i>C:N</i>	73
3.3.2. <i>P analysis</i>	73
3.4. <i>Results</i>	74
3.4.1. <i>Composition of C, N and P in the fractions</i>	74
3.4.2. <i>Element recovery and distribution</i>	75
3.4.3. <i>Stoichiometry</i>	76
3.5. <i>Discussion</i>	77
3.6. <i>Conclusions</i>	81
3.7. <i>Acknowledgements</i>	82
4. Aged riverine particulate organic carbon in four UK catchments	95
4.1 <i>Introduction</i>	96
4.2 <i>Methods</i>	99

4.2.1 <i>Field sites</i>	99
4.2.2 <i>Sampling and analysis</i>	100
4.2.3. <i>Soil radiocarbon data</i>	103
4.3 <i>Results</i>	103
4.4 <i>Discussion</i>	106
4.5 <i>Conclusions</i>	110
4.6. <i>Acknowledgements</i>	111
5. Quantifying sources of dissolved organic radiocarbon in rivers	120
5.1 <i>Introduction</i>	121
5.2 <i>Methods</i>	123
5.2.1 <i>Original data for the UK and Norway</i>	123
5.2.2 <i>Collection and analysis</i>	125
5.2.3 <i>Collation of the dataset</i>	126
5.2.4 <i>Land classifications</i>	127
5.2.5 <i>Application of modelled SOM pools</i>	128
5.3 <i>Results</i>	130
5.3.1 <i>Original data for the UK and Norway</i>	130

<i>5.3.2 Applying the UK data to the international data</i>	132
<i>5.3.3 Temporal analysis of riverine DO¹⁴C</i>	133
<i>5.4 Discussion</i>	135
<i>5.5 Conclusions</i>	138
<i>5.6 Acknowledgements</i>	138
6. The contribution of algae to freshwater dissolved organic matter:	
Implications for UV spectroscopic analysis	149
<i>6.1. Introduction</i>	150
<i>6.2. Methods</i>	153
<i>6.2.1. Model explanation</i>	153
<i>6.2.2. Sample collection and processing</i>	154
<i>6.2.3. Analyses</i>	156
<i>6.3. Results</i>	157
<i>6.3.1 Estimating extinction coefficients for DOM derived from freshwater algae</i>	157
<i>6.3.2 Natural water samples</i>	159
<i>6.3.3 Modification of the three-component model of UV absorption</i>	160

6.3.4 DOM derived from algae in freshwater samples	161
6.4. Discussion	162
6.5. Conclusions	166
6.6. Acknowledgements	167
7. Discussion	178
7.1: Quantification of natural organic matter	178
7.2: Large scale data	180
7.3: Technological advances: past, present and future	183
7.4 Conclusions	184
7.5 Future work	185
8. References	188
Appendix	See USB provided

List of Tables

Table 2.1. A summary of the main structural components of SOM, their sources and how they are detected. Information was sourced from Simpson and Simpson (2012) and Kögel-Knabner (2002).	61
Table 3.1: Information about the soil samples.	83
Table 3.2. Concentrations of the light fraction, heavy fraction and bulk soil for carbon (C) nitrogen (N), total P (TP) inorganic P (IP) and organic P (OP). S and D refer to shallow (0.15 cm) and deep (15-40 cm) respectively. Concentrations are presented as %. Data for TP IP and oP are mean values (n=4).	85
Table 3.3. Masses and recoveries of soil, C, N and TP for the bulk soil, light and heavy fractions. Mass is presented in grams. Recovery of the soil, C, N and TP is presented in %. Shallow (s) and deep (d) are for depths of 0-15 cm and 15-40 cm respectively.	87
Table 3.4. Distribution of the soil mass, C, N, oP, TP and IP measured across the light fraction and heavy fraction, measured by %.	89
Table 4.1. Catchment information. Discharge data are from records of between 35 and 50 years up to the present. Geology, soil type and land use are presented in order of importance.	113
Table 4.2. Mean concentrations of SPM and OC contents of SPM. Values in brackets are standard deviations, and reflect both natural variation and the averaging of results obtained by different methods (Section 3.2.2).	114

Table 4.3. Isotope data for POM in high-flow samples. Values are given of ^{14}C (pMC), $\delta^{13}\text{C}$ (‰ vPDB) and conventional radiocarbon age (years BP). The errors in ^{14}C are expressed as $\pm 1\sigma$ (pMC) where σ is the overall analytical uncertainty. Bracketed values of $\delta^{13}\text{C}$ are not necessarily representative of the original combusted material (see Section 4.2.2). 115

Table 5.1. Catchment information. Discharge data are from records between 35 and 50 years up to the present. Geology, soil type and land use are arranged in order of dominance. Information for Doe House gill was obtained from Tipping et al. (2007). Catchment information for the Ribble, Dee, Avon and Conwy catchments can be found in Adams et al. (2015) (chapter 4). 140

Table 5.2. Isotopic data for the original and unpublished UK dataset. Values are given of ^{14}C (pMC), $\delta^{13}\text{C}$ (‰ vPDB) and conventional radiocarbon age (years B.P). Errors of the ^{14}C are expressed as $\pm 1\sigma$ (pMC) where σ is the analytical uncertainty. 141

Table 5.3. Number of samples in each of the land categories that fall above the 50:50 fast pool (1 year and 20 years) or fall below the 2000 year pool. 142

Table 6.1. Summary of [DOC], pH, conductivity and [Chla] for the field sites. 168

Table 6.2. Calculated extinction coefficients for phytoplankton derived material in the mesocosms and the open ocean. Model extinction coefficients for components A and B are parameters obtained from Carter et al. (2012). Mesocosm extinction coefficients were derived from data in Figure 6.2. Open ocean extinction coefficients were derived from data provided in Helms et al. (2008) and Guo et al. (1995). The Yangtze basin samples were obtained from Zhang et al. (2005), the

axenic culture from Nguyen et al. (2005) and the non- axenic culture from Henderson et al. (2008). 169

Table 6.3. Calculated fractions of A, B and C2 using the new parameters derived from the mesocosm experiments and the corresponding proportions of [DOC] in mg/L. Samples are listed by their specific ID – site names and locations can be found in Appendix 6.1. 170

List of Figures

Figure 1.1: An illustration of the different elements of the thesis and how they fit together. Each box represents an element of an integrated model of macronutrient cycles. The processes explored in this thesis are shown in red. Nutrient stability and stoichiometry are explored in chapter 3 and would aid better understanding of nutrient retention and release in soils. Exploring sources and ages of dissolved organic matter in rivers will aid our understanding of nutrient losses from soil (chapters 4 and 5). Finally, instream processing and analytical detection of aquatic organic matter will contribute towards a UV spectroscopic method that could be applied to industrial water treatment strategies (chapter 6). 28

Figure 2.1. A simplified illustration of the global carbon cycle. Fluxes are shown by the red arrows and red values, all presented in Pg C a^{-1} (10^{15} g C). Arrows are approximately proportional to the magnitude of the flux. Pools are either shown in the black or white writing, and are measured in Pg C (10^{15} g C). Values for land use change, fossil burning, litter fall, rivers, atmospheric pools and oceanic pools were quoted from Schlesinger and Andrews (2000). Soil pools and fluxes were quoted from Batjes (2014) and Raich and Potter (1995) respectively. Sediment storage was quoted from Cole et al. (2007). 62

Figure 2.2. Examples of the carboxyl, carbonyl, aromatic and phenolic compounds present in SOM. Illustrations are redrawn from (Kögel-Knabner, 2002). 63

Figure 2.3. Example of the radiocarbon bomb peak as the result of atmospheric weapons testing. The figure has been redrawn based on (Hua, Barbetti and Rakowski, 2013), up to the year 2010. Data was extrapolated to extend the values to 2016. 63

Figure 2.4. A schematic of the multi-component model of absorbance, redrawn and modified from Carter et al (2012). The top column represents the sample being analysed. The model apportions the sample into the two components. Component A (bottom left) accounts for strongly absorbing material, which results in higher extinction coefficients. Component B (bottom right) represents weakly absorbing material, which has lower extinction coefficients. The model can then find the total DOC concentration [DOC] of the sample, and the fraction of component A. 64

Figure 3.1. Schematic of the fractionation procedure. 90

Figure 3.2. Average concentrations of the elements C, N, and oP for the light and heavy fractions. The light fractionation is shown by the grey block and the heavy fraction by the dotted block. Standard deviations are shown by the error bars. Concentrations are shown in %. 91

Figure 3.3. Concentrations of total P (TP), inorganic P (IP) and organic P (oP) for the light fraction (upper panel) and the heavy fraction (lower panel). Standard errors are shown by the error bars. 92

Figure 3.4. Soil mass and element distributions between the light the heavy fractions. 93

Figure 3.5. The N:C (upper plot) and oP:C (lower plot) against C for the light and heavy fractions. The black line shows the modelled values for the entire bulk dataset of the UK soil survey. Light fractions are shown by the hollow circles. Heavy fractions are shown by the grey circles. 94

Figure 4.1. Location map showing the study catchments. For the Dee and Ribble, black triangles indicate sampling sites. The Avon and Conwy sampling sites were at the tidal limit. 116

Figure 4.2. Average $PO^{14}C$ (pMC) for suspended sediment collected at high flow at the 9 sampling sites. Error bars represent standard deviations. Greyed bars show the two sites for which the $PO^{14}C$ values differ significantly from the others. 117

Figure 4.3. Soil radiocarbon plotted against soil depth for 296 samples of UK soils. Depths are plotted as the weighted average of sampling depths. The horizontal bars are standard deviations in ^{14}C , the vertical bars are ranges of sampling depth. See Appendix 5.1 for details. 118

Figure 4.4. Radiocarbon contents of POM, i.e. $PO^{14}C$, plotted the against OC content of SPM (%) and [SPM]. Global data collated by Marwick et al. (2015) are represented by the open circles. Data for the 7 rurally-dominated UK sites are shown by filled circles. Values for the Rivers Calder and Ribble B are shown by filled triangles. 119

Figure 5.1. Atmospheric ^{14}C content (black line) (Hua, Barbetti and Rakowski, 2013), extrapolated to 2016 and the two modelled SOM pools. The upper blue line represents the average of the 1 year and 20 year pool. The lower line is the 2000 year SOM pool assuming steady state conditions. 144

Figure 5.2. Average DO^{14}C content of the original and previously unpublished data for rivers in the UK. The white blocks are arable sites (A), the dotted blocks are forested sites (F), light grey blocks are not wetland, forest or arable sites (NWFA), dark grey blocks are mixed sites with urban influence (NWFAU) and diagonally lined blocks are wetland sites (W). Standard deviations are shown by the error bars. Starred bars show the nine sites that were significantly different. 145

Figure 5.3. DO^{14}C and DOC concentration for all data available for the UK. The black markers show the original dataset presented in this study. The grey markers show data available in the literature. 146

Figure 5.4 DO^{14}C and DOC concentration for the global dataset, classified by land use. A is arable, F is forested ecosystems, NWFA is catchments not dominated by wetland, forest or arable, NWFAU is the latter but with considerable urban influences, and W is wetland ecosystems. The black markers show the original UK dataset presented in this study. The grey markers show the global data available in the literature. New data on the forested UK catchment is not shown as DOC concentration was not available. 147

Figure 5.5. DO^{14}C values for the global dataset, plotted by year and classified by land use. The upper blue line represents the average of the 1 year and 20 year pool. The lower line is the 2000 year SOM pool assuming steady state

conditions. The black markers show the original dataset presented in this study. The hollow grey markers show data available in the literature. The filled grey markers show the previously unpublished Norwegian forested data. 148

Figure 6.1. Locations of the sites where surface water samples were collected. Site Co-ordinates are provided in Appendix 6.1. 172

Figure 6.2. [DOC] and absorbance plotted through time for A) mesocosm 4, B) mesocosm 7, C) mesocosm 15 and D) mesocosm 20. [DOC] measured and [DOC] modelled are shown on the primary axis and are represented by the hollow and filled squares respectively. Absorbance at 270 nm and 350 nm are on the secondary axis and are represented by the filled and hollow triangles respectively. 173

Figure 6.3. Extinction coefficients (E) at 270 nm (upper panel) and 350 nm (lower panel) against [DOC] measured across the entire sampling period for the mesocosms. Mesocosm 4 is marked by the hollow triangle, the black triangle represents mesocosm 7, the black circle mesocosm 15 and the hollow circle mesocosm 20. 174

Figure 6.4. Modelled [DOC] plotted against the measured [DOC] for all samples collected in this study. Hollow circles represent the mesocosm samples and triangles for the field sites. Filled triangles show seven Shropshire – Cheshire meres sites that were not satisfactorily explained by the model. The 1:1 line is shown. 175

Figure 6.5. Modelled [DOC] plotted against measured [DOC] for the Shropshire – Cheshire mere water samples (triangles). Filled triangles show the seven sites that were unsatisfactorily predicted. Data collected for Chinese lakes

are shown by the hollow squares (Zhang et al. 2005). The 1:1 line is shown.

176

Figure 6.6. The fraction of the variable component C2 (f_{C2}), vs the $[DOC_{C2}]$ for the whole sample set, including the Yangtze basin samples.

177

1. Introduction

The man-made production of food and fuel have modified virtually every major global biogeochemical cycle (Falkowski et al., 2000). The synthesis of ammonia and the mining of phosphorus manufactured into nutrient rich fertilizers has eradicated the natural restrictions of food production, which has been one of the main drivers of global population increase, reaching 7 billion in 2011. By 2050, the population is expected to reach 9 billion, which will inevitably increase the pressure on the management of land for fuel and food production, and of water for drinking, sanitation and irrigation.

Terrestrial ecosystems that previously had near-closed cycles of nitrogen (N) and phosphorus (P) now export considerable loads of these nutrients, which leads to eutrophication and acidification of surface waters. Further, ecosystems that remain nutrient limited are enriched and less biodiverse. Agricultural practices and managed semi-natural systems has affected natural carbon (C) cycling through changes in net primary productivity and carbon storage through N deposition. However, the effects of these impacts, and how they interact between the different nutrient cycles over large scales, is poorly understood (Vitousek et al., 1997) and it remains uncertain how these processes will respond to future change. Simple, mechanistically based integrated models of atmosphere, land and water can enhance understanding of past, and therefore future pools and fluxes of C, N and P. Considerable gaps in the knowledge of the processes involved across different ecosystems hinders further development of this approach.

Therefore, in order to improve the sustainability of agriculture, preserve carbon stocks, control eutrophication, reduce nutrient delivery to the sea and reduce greenhouse gas emissions to the atmosphere, we need to understand the processes

and interactions between these nutrients, and the linkages between atmospheric, terrestrial and aquatic environments.

1.1 Thesis Aims and Objectives

This project aims to explore several gaps in the knowledge of OM function across different ecosystems, thus aiding more effective integrated model predictions of macronutrient cycling. The thesis is structured using a sequence beginning with exploring terrestrial nutrient stability and stoichiometry, followed by the transfer of DOC and POC in freshwaters and ending with the application of spectroscopic methods for different freshwater DOC components (Figure 1.1). In doing so, I will gain a wider understanding of nutrient cycling, storage and the linkages between terrestrial and freshwater ecosystems.

Thus, I will aim to address the following research questions:

- **How is organic phosphorus distributed between different soil organic matter fractions, compared to the more widely researched macronutrient elements? (Chapter 3).**

Extensive information is available describing and quantifying the distribution of C and N in soil organic matter (SOM) pools, which is mostly measured using the N content (through C:N ratios). This data has been widely used to construct simple models of long term SOM turnover (Jenkinson et al. 1990; Sohi et al. 2001). However, no studies report the distribution of organic phosphorus (oP) in SOM pools. Thus, a quantitative analysis of the distribution of oP in SOM is necessary for further understanding and improved modelling of nutrient cycling and stability.

- **What is the time elapsed between terrestrial C fixation and entry into the water course? (Chapter 4 & 5)**

Chapter 3 addressed some of the mechanisms involved in nutrient stabilization in soil. Chapters 4 and 5 explore the terrestrial sources of particulate and dissolved organic matter present in rivers using radiocarbon (^{14}C), which is a powerful tracer of the origins of C pools and organic matter (OM) turnover. To date, no data is available on particulate organic carbon in UK rivers, and very little information is available for dissolved organic carbon. Therefore, understanding the origins of the terrestrial OM entering rivers should improve our ability to model the terrestrial-freshwater C cycle, and the mechanisms behind carbon transfer to the atmosphere and oceans.

- **Using optical absorbance, how well does a multi-component model algorithm predict DOC concentration in eutrophic waters, and what modifications can be made? (Chapter 6)**

In the water treatment industry, there is a growing need for rapid and reliable measurements, largely due to the widespread observed increases in concentrations and fluxes of dissolved organic carbon (DOC) (Monteith et al., 2007), which has implications for ecology and water treatment costs. However, complex in-stream processing of terrestrially derived organic matter and algal production make it difficult to quantify the different OM components and sources. This chapter explores the efficacy of a multi-wavelength model of DOM absorbance in eutrophic waters, and the feasibility of this approach for future in-situ measurements.

This thesis addresses the scientific questions using a range of environments and experimental design. Both laboratory and field simulations are used, and the thesis consists of four experimental chapters to address the following objectives:

- To develop a physiochemical fractionation method suitable for use across a wider range of soils, semi natural, managed and arable areas of land. The macronutrient elements of each fraction will be analysed, with a focus on the distribution of organic P across the fractions, compared with C and N (Chapter 3).
- To carry out a yearlong river water sampling campaign across four major UK catchments. Samples are to be collected at high flow, for the analysis of dissolved and particulate radiocarbon by accelerator mass spectrometry (Chapter 4 and 5).
- To identify field environments and collect samples where algal derived organic matter may dominate over terrestrially derived material. Two measurements of DOC concentration using the algorithm and a conventional laboratory analysis will be carried out to assess the differences between the data generated. Controlled mesocosms are also used to take samples at set time increments to monitor the changes in the prediction of DOC concentration over time (Chapter 6).

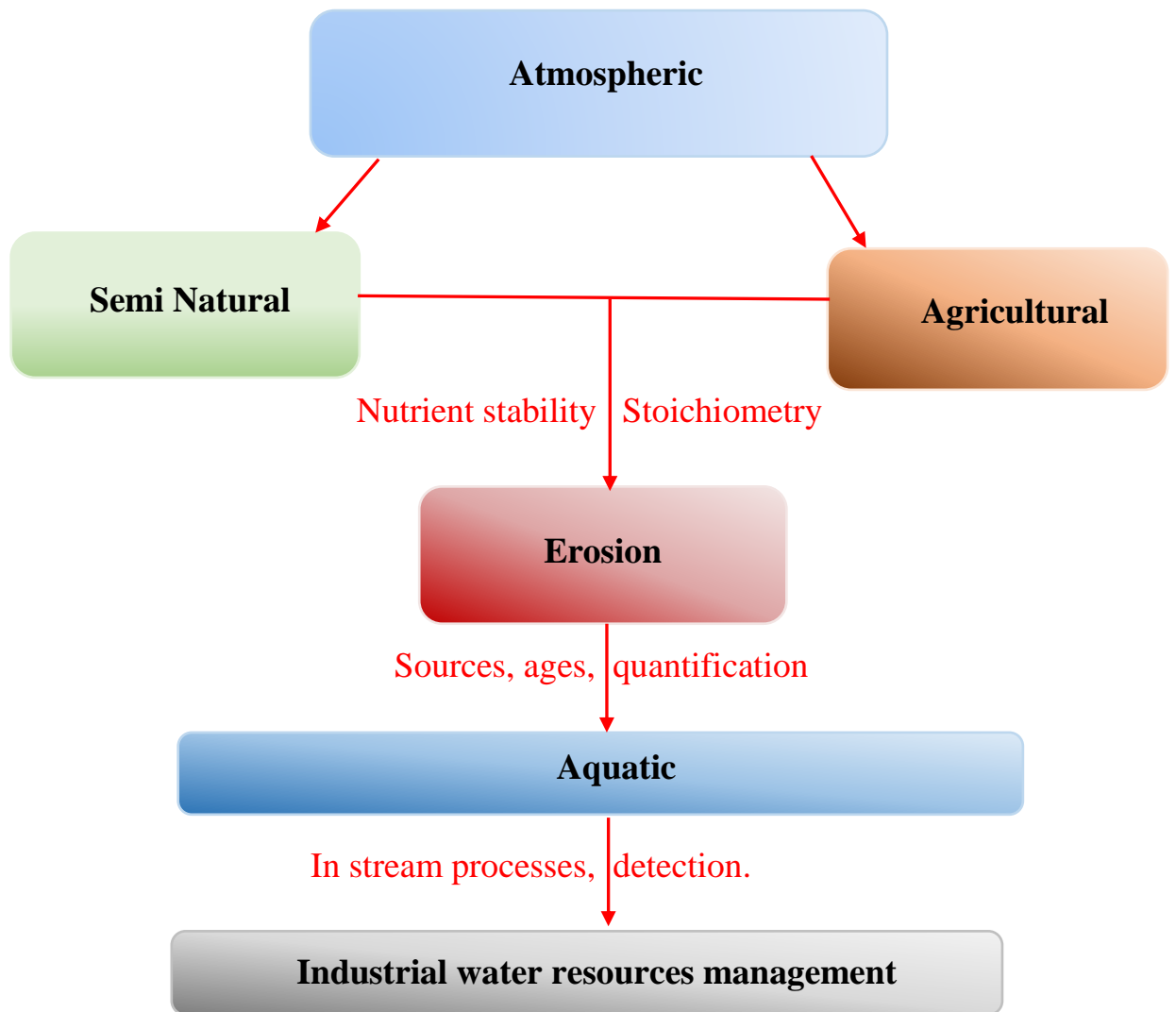


Figure 1.1: An illustration of the different elements of the thesis and how they fit together. Each box represents an element of an integrated model of macronutrient cycles. The processes explored in this thesis are shown in red. Nutrient stability and stoichiometry are explored in chapter 3 and would aid better understanding of nutrient retention and release in soils. Exploring sources and ages of dissolved organic matter in rivers will aid our understanding of nutrient losses from soil (chapters 4 and 5). Finally, instream processing and analytical detection of aquatic organic matter will contribute towards a UV spectroscopic method that could be applied to industrial water treatment strategies (chapter 6).

2. Literature Review

2.1 Part I - Anthropogenic influences on terrestrial nutrient cycling

Soils represent both a significant source and sink of C within the global carbon cycle, with an estimated 2157-2293 Pg C stored in the upper 100 cm (Batjes, 2014) and an estimated flux of 76.5 Pg C a⁻¹ to the atmosphere through soil respiration (Raich and Potter, 1995). Plants add 50-60 Pg C a⁻¹ to the soil pool through litterfall and contributes 59 Pg C a⁻¹ to the atmosphere through respiration, while photosynthesis fixes 120 Pg C a⁻¹ from the atmosphere. However, land disturbance and clearance for agricultural practices, including livestock grazing and food production was in the region of 5x10⁹ ha in 2000 (1.5x10⁹ ha for crops and 3.5x10⁹ ha for pasture) (Tilman et al., 2001), which increases the total atmospheric flux by 1 Pg C a⁻¹ (Schlesinger and Andrews 2000). Additionally, the combustion of fossil fuels contributes an extra 6-7 Pg C a⁻¹ to the atmosphere, all of which have collectively contributed towards an increase in global temperature and atmospheric CO₂ emissions (Schlesinger and Andrews, 2000). Natural hazards contribute a very small flux of C to the atmosphere, at 0.1 Pg C a⁻¹. A diagram of the carbon cycle can be seen in Figure 2.1, with the aquatic C cycling described further in section 1.7. Long term predictions indicate that by the end of the current century, global mean temperatures will increase by approximately 2 - 7 °C due to atmospheric greenhouse gas concentrations, CO₂ especially (Wu et al., 2011). In semi natural ecosystems, C cycling has also been altered through changes in net primary productivity and the ability to store C, through the increase of N deposition (Hagedorn, Spinnler and Siegwolf, 2003).

Pre-industrial patterns of biologically fixed N were in the region of 3 Tg N a^{-1} (Galloway et al., 1995). Production of synthetic fertilizers, cultivation of N fixing crops and the deposition of fossil fuel associated N are effectively in the same order of magnitude as natural biological N fixation (Galloway et al., 1995; Falkowski et al., 2000). Industry and fossil fuel combustion has contributed to atmospheric NO_x emissions of $\sim 0.05 \text{ Pg a}^{-1}$ and 0.11 Pg a^{-1} in methane (CH_4) emissions (Galloway et al., 2004). Phosphorus compounds are almost entirely supplied by the parent material of unfertilized soils through weathering and is mostly cycled in geological timescales, which leads to P limitation in terrestrial systems (Walker and Syers, 1976). Thus, phosphorus compounds are also mined for fertilizer, which has led to an approximately four fold increase in P inputs to the biosphere (Falkowski et al., 2000; Elser and Bennett, 2011). However, P differs from atmospheric emissions of C and N in that it does not have a stable gaseous form. Thus, fluxes of P to the atmosphere are much less than C and N, and is mostly in aerosol form (Mahowald et al., 2008) or fine biological debris transported over shorter distances (Tipping et al., 2014). However, some changes have been observed, as the result of biogenic and biomass burning (Mahowald et al. 2008; Baker et al. 2006), though these fluxes are small in comparison to C and N. Fluxes of biospheric P to the atmosphere are in the region of 0.001 Pg a^{-1} , 5% of which is anthropogenic (0.07 Tg a^{-1}) (Mahowald et al., 2008). More recent research by Tipping et al (2014) estimated a total annual transfer of P to and from the atmosphere of 3.7 Tg a^{-1} . In terrestrial ecosystems, P is accumulating at between $10.5\text{-}15.5 \text{ Tg a}^{-1}$ which will cause an increase in the rate of biological processes such as primary productivity, which in turn can create N limitations (Vitousek et al., 2010). Further, inputs of P from terrestrial diffuse (agricultural)

and point sources (sewage effluent) are hazardous to freshwaters, with the latter source providing the most significant risk of eutrophication in rivers (see part II) (Jarvie, Neal and Withers, 2006; Withers and Jarvie, 2008). In turn, nitrogen inputs have been found to accelerate phosphorus cycling rates across a range of different terrestrial ecosystems (Marklein and Houlton, 2012).

Biotic sinks of CO₂ and the rate of C sequestration into soil requires nitrogen and phosphorus in addition to carbon, creating close linkages in the main macronutrient elements. Limited availability of both nutrients are predicted to reduce future carbon storage by natural ecosystems during the 21st century (Peñuelas et al., 2013). Therefore, it is important to understand the linkages between C, N and P over the long term, and on large scales.

2.2 The nature and formation of soil organic matter

Much of the organic carbon and nitrogen in soil is stabilised within soil organic matter (SOM), with different plant functional types contributing towards the distribution of soil organic carbon (SOC) with depth. Globally, SOC in the top 20cm averaged 33% 42% and 50% relative to the first meter of soil for shrublands, grasslands and forests respectively, in a study of global terrestrial C storage (Jobbágy and Jackson, 2000). Soil OM contains two thirds of the world's terrestrial C stores, which is more than twice the amount of atmospheric C (Simpson and Simpson 2012; Schlesinger 1997; Batjes 2014), with the remainder stored as inorganic C (Scharlemann et al., 2014). As well as being an important source of soil C, SOM is a key functional component in soil, regulating contaminant uptake by crops and leaching into groundwater (Lehmann and Kleber, 2015), pH and conductivity, and influencing the cycling of other macronutrient elements. Organic

matter retains plant available water and nutrients and promotes the formation of soil structure, making it a central component in soil fertility, agricultural productivity and global food security (Lehmann and Kleber, 2015). Structural components of SOM are summarised in Table 2.1.

2.2.1 Biological processes of SOM

Microbes regulate the production of soil organic matter. They decompose plant residues and organic compounds of animal or microbial origin, to access C, N, P, sulphur (S) and other micronutrients, to fuel metabolism. A proportion of this C is retained within microbial biomass whilst the rest is respired as CO₂ or returned to the soil as exudates or metabolites. Plant material is rapidly respired, with a turnover of approximately 1 year, meaning that only a small proportion enters the SOM pool (Mills et al., 2013). However, vascular plant material does account for a major proportion of soil organic N (Kögel-Knabner, 2002). Microbial detritus is also a major component of SOM, which accounts for around 60% of the total P in the form of orthophosphate diesters from DNA and RNA (Turner et al., 2002; Kögel-Knabner, 2006).

The non-living aspect of SOM – notably humic substances are formed by the transformation of decomposing cellular material to non-cellular organic matter (humus), through microbial activity, and can account for around 50% of the total OM (Rice, 2001), and contains about 96% of the total organic N (Kögel-Knabner, 2006). Humic substances are extremely chemically heterogeneous and amorphous in nature, perhaps the most complex natural mixture on earth, which confounds the study of its structure and reactivity in the environment (Simpson et al. 2011; Simpson and Simpson 2012; Schlesinger and Bernhardt 2013).

2.2.2 *The chemistry of SOM*

Critical to understanding SOM formation and stability is the identification of the molecular components of which it is comprised, with research commencing as far back as the early 20th century (Waksman 1936). As a result, the main structural components of soil organic matter are accepted as being principally comprised of components from lignin, carbohydrates and sugars, cutin, suberin, peptides, microbially derived decomposition by-products and black carbon. A summary of the OM constituents, their origins and how they can be measured are summarised in Table 2.1.

Technological advances in nuclear magnetic resonance (NMR), mass spectrometry and biomarker techniques have led to a greater understanding of the composition of SOM (Simpson and Simpson 2012). These methods provide basic structural information on the sample and are widely favoured due to the lack of sample pre-treatments (Kögel-Knabner, 2000). The ¹³C-NMR technique involves the separation of active nuclei in a strong magnetic field, by the variation in nuclear spin energy levels, which will refer to the different electron densities surrounding each nucleus in the sample (Hatcher et al., 2001). The typical structural information obtained for SOM by ¹³C-NMR methods include alkyl, *o*-alkyl, aromatic and phenolic compounds, and carboxylic and carbonyl components (Simpson and Simpson 2012) (Figure 2.2).

Studies using the solid state ¹³C-NMR technique have shown that the humin component contains similar functional groups to the sample from which it originated, although the humin fraction tends to be higher in aliphatic carbon and lower in aromatic carbon compared to other humic acids (Almendros and Guadalix

1996). In peat soils for example, the bulk sample and the humin fraction vary as little as 2% in terms of their composition (Simpson and Johnson, 2006). Kang et al (2003) found 70% of aliphatic carbon in a sample of humin from Western Massachusetts. Simpson and Johnson (2006) demonstrated the presence of an amorphous, polymethylene - rich component in all of the six humin samples analysed, indicating a high affinity for hydrophobic compounds. In grassland soils, the insoluble SOM fraction showed some variation in comparison to the original sample. Larger aliphatic signals were found in the humin fraction, which are derived from components found in plant cuticles. This is thought to result from the highly hydrophobic nature of cuticular components (Kögel-Knabner 2002; Sachleben and Hatcher 2004; Simpson et al. 2002) although the preferential adsorption of their aliphatic compounds to clays may contribute to their persistence in some soils (Hayes et al 2009).

Biomarkers involve the fingerprinting of OM compounds that can be traced to a specific plant, microbial or anthropogenic source due to the retention of their specific carbon composition during decay (Simpson and Simpson 2012; Amelung et al. 2008). This has greatly improved the understanding of OM composition and the ecological responses to climate change (Simpson and Simpson 2012) and provides an additional step in molecular characterisation of OM by NMR.

Biomarkers also provide information on the stage of decomposition, and thus the turnover rates of OM components (Simpson and Simpson 2012; Otto and Simpson 2005; Feng et al. 2008). Some biomarkers that have been used for OM characterisation include n-alkanes, n-alkanols, n-alkanolic acids and phospholipid fatty acids (PLFA) sourced from plant waxes, bacteria and fungi (Simpson and Simpson 2012) (Table 2.1). However, biomarker methods only capture a small

proportion of the total OM composition in comparison to NMR methods, with approximately 17% of the total OM characterized compared to 52-79% respectively (Otto and Simpson 2007; Simpson and Simpson 2012).

Despite the recognised importance of the role of SOM in soil stability, a large proportion of the molecular constituents of SOM remain uncharacterised, largely due to the limitations associated with current analytical techniques (Hatcher et al. 2001; Hedges et al. 2000; Simpson and Simpson 2012).

2.3 The physical state of soil organic matter

The large reservoir of carbon sequestered in SOM has received widespread research interest due to its potential vulnerability to climate change. Pool sizes may be altered directly as a result of changes in temperature, soil moisture and pH, or indirectly through vegetation and land use change which all have the potential to alter atmospheric CO₂ concentration and the global climate (von Lutzow et al. 2006). Despite this, the mechanisms by which the SOM pool is maintained are poorly understood, making conceptual model simulations on ecosystem response and management difficult and uncertain (Von Lutzow et al. 2006; Parton 1996). Further, the term recalcitrance may hinder progress of SOM characterisation. For instance, some definitions of recalcitrance are based on the material property, while others refer to the specific turnover time or how it is operationally decomposed during laboratory incubation experiments (Kleber and Johnson 2010). The state at which SOM is maintained in the soil is largely dependent on the soil type, and studies on single soil classifications cannot easily be related to others. Von Lutzow et al. (2006) defined all stabilization mechanisms that have been

suggested to occur in different temperate soils and identified three main categories of stabilization discussed below.

2.3.1 Selective preservation

The process of selective preservation ultimately leads to the accumulation of molecules that are resistant to degradation and are considered to be recalcitrant. Several categories of preservation occur including primary, originating from above and below ground litter decomposition, and secondary, which mostly includes microbial products, but also humic polymers and charred material (Von Lutzow et al. 2006). In primary preservation, the polymers most resistant to degradation are largely regarded as aromatic in character including lignin, lipids and waxy residues (Von Lutzow et al. 2006; Derenne and Largeau 2001). The aliphatic compounds present in lignin are not readily decomposed, leading to an accumulation in the initial phases of decomposition. Investigations in both the field and laboratory have confirmed that such components are selectively preserved during degradation (Kögel-Knabner et al. 2008; Kalbitz et al. 2003a; Kalbitz et al. 2003b). However, the way in which lignin compounds are depolymerized is not entirely understood and results are restricted to specific habitats, including forested soils (Von Lutzow et al. 2006). In agricultural soils, lignin concentrations in topsoil are small, indicating that lignin is decomposed more readily under these conditions (Kögel-Knabner, 2000). For clay soils, alkyl C compounds are generally more abundant in comparison to whole soils and coarse soil fractions (Mahieu, Randall and Powlson, 1999). Studies on the accumulation of alkyl C in soils are inconclusive and it is not certain which of the OM structural properties, hydrophobicity or association to clay mineral surfaces are the main drivers (Von Lutzow et al. 2006).

Secondary selective preservation has previously been considered a minor aspect of SOM stabilization, accounting for between 0.3 % and 7 % of the OC content (Wardle 1992). However, more recent research has suggested a much greater input of microbial biomass to SOM, with a contribution of >50 % to extractable SOM, equating to >80 % of soil nitrogen (Simpson et al., 2007). Microbial residues that accumulate in soils include murein, chitin and lipids (Kögel-Knabner, 2002; Kiem and Kögel-Knabner, 2003). Fungi and bacteria also produce melanins which persist in soils, although their fate and decomposition in soils is unresolved (Von Lutzow et al. 2006). In some soils, labile microbial compounds including polysaccharides and proteins have also been found in 'old' OM, indicating stabilization, though the mechanisms behind this are still subject to debate (Kiem and Kögel-Knabner, 2003; Knicker, 2011).

2.3.2 Stabilization by spatial inaccessibility

The fate of SOM is highly dependent on several soil characteristics, including the location of OM in the soil profile and aggregate composition. In temperate soils, much evidence exists that suggests soil structure is responsible for the protection of OM against degradation (Six, Elliott and Paustian, 2000; Six et al., 2002). Soil biota are also driving agents for occlusion, whereby microbial cells, secretions and root exudates act as cementing agents, which are consequently occluded with the soil aggregates (Six, Elliott and Paustian, 2000; Six et al., 2002). Occluded SOM is therefore resistant to decomposition because of reduced access for microbial decomposers, reduced enzymatic diffusion and restricted aerobic decomposition due to reduced diffusion of oxygen, all of which are largely governed by soil pore size (Von Lutzow et al. 2006). The stabilization of OM in aggregated soil is highly

responsive to land management practices with continuous nutrient input, including fertilizer application and cropping in agriculturally managed soils (Lutzow et al., 2006). Labile components may also be resistant to degradation through encapsulation by hydrophobic components of humic substances (Piccolo, 2002; Knicker, 2011). However, limited evidence of this occurrence is available, due to the difficulty of measuring encapsulation in situ (Von Lutzow et al. 2006).

2.3.3 Association with mineral matter

The resistance of labile OM substances to degradation is often the result of binding with mineral surfaces through adsorption, and research supports the concept that small molecules adsorbed to mineral surfaces cannot be utilized by microorganisms (Chenu and Stotzky 2002; Kalbitz et al. 2005). The stabilization of OM constituents in different soils is largely governed by the specific surface area (Saggar et al., 1996), with preferential adsorption occurring on clay-sized particles (<2 μ m), iron oxides (3-10nm) and amorphous aluminium oxides (<3nm). Kaiser and Guggenberger (2003) also demonstrated that preferential sorption occurs at sites such as rough surfaces and micro-pores where Fe and Al-OH groups are exposed.

There are several mechanisms that are considered to be involved during the interaction of OM with mineral surfaces, which includes ligand exchange, weak interactions including hydrophobic interactions and complexation of metal ions (Von Lutzow et al. 2006). Ligand exchange involves anion exchange between hydroxyl (OH⁻) groups on the mineral surface, carboxyl and phenolic compounds of OH⁻ groups, and forms strong organo-mineral association (Fe-O-C bonds for example) (Von Lutzow et al. 2006). These reactions have been observed to

increase with decreasing pH, with maximum sorption occurring in mineral rich, acidic soils at between pH 4.1 and 6.5 (Gu et al., 1994). Weak hydrophobic interactions occur as the result of the absence of non-polar residues such as aromatic compounds and alkyl-C in water, forcing non-polar groups together through Van der Waals forces (Von Lutzow et al. 2006). Hydrophobic interactions again favour lower pH soils where hydroxyl and carboxyl groups are protonated. Stabilization of OM through complexation with metal ions is well known and has been extensively researched, and it is accepted that interaction of soil aluminium (Al) and iron (Fe) is the main driver of stable SOM in podzols (Lundström, van Breemen and Bain, 2000; Zysset and Berggren, 2001; Nierop, Jansen and Verstraten, 2002). However, a detailed, mechanistic understanding of why sorption to minerals reduces decomposition and quantification of OM stability is lacking, largely due to the lack of established methods available for in situ measurements.

2.4 Soil organic matter turnover

The turnover of soil organic matter is often quantified by the mean residence time (MRT), which is the average time an element or compound resides in the pool at steady state (Six and Jastrow, 2002). Quantifying the turnover of SOM, conventionally through the SOM-C content can be estimated through several techniques including simple first order modelling, natural abundance ^{13}C and radiocarbon (^{14}C) dating.

Considerable technological advances in the ^{14}C dating technique has greatly improved the accessibility of OM measurements across all ecosystems, through the development of the accelerator mass spectrometer. Early work by Libby et al (1949) demonstrated ^{14}C analysis by placing a modern source in a radiation

detector and counting its counts per minute, scaling up to 1g samples for over 12 hours, giving a precision of 1%. Later work by Bennett et al (1979) demonstrated that the analysis of ^{14}C in natural samples could be done using a mass spectrometer, coupled with a tandem electrostatic particle accelerator. Since then, accelerator mass spectrometry has become a widely used and powerful technique in the quantitative analysis of SOM turnover using ^{14}C , by the measurement of atom abundance.

Radiocarbon has a half-life of approximately 5700 years and naturally occurring ^{14}C is present in minute concentrations in the atmosphere ($\sim 1.2 \times 10^{-10} \%$) (Hua, 2009), which gives the ability to measure turnover on centennial and millennial timescales. During the atmospheric weapons testing period of the 1950s and 60s, large quantities of ^{14}C were produced in the atmosphere, in the region of 630×10^{26} ^{14}C atoms (Hesshaimer, Heimann and Levin, 1994). This caused increases in the $^{14}\text{C}:^{12}\text{C}$ ratio in atmospheric CO_2 leading to disequilibrium in the atmosphere, biosphere and oceans. Following the testing, $^{14}\text{CO}_2$ changes were documented, which has given the ability to use bomb ^{14}C as a unique tracer on decadal timescales (Hua, 2009) (Figure 2.3). Generally, ^{14}C is presented as years BP, although variations in units are frequently reported. Commonly, results are presented in $\Delta^{14}\text{C}$ (‰) or fraction modern carbon (fMC), although percent modern (%), or pMC) has been used throughout this study (see chapters 4 and 5). The units can be converted using the equations below, where x is the value of the dated sample in ‰, $\lambda = 1/8267 \text{ a}^{-1}$ and y is the year of the sample collection:

$$fMC = \left(\left(\frac{x\text{‰}}{1000} \right) + 1 \right) \exp^{\lambda(y-1950)} \quad (1)$$

$$pMC = 100 + \left(\frac{x\%_{00}}{10} \right) \quad (2)$$

Extensive research into SOM turnover has deduced that OM varies significantly in its turnover and age (Trumbore, 2009; Mills et al., 2013), such that the quantification of SOM by MRT will only ever provide an approximate value. Detailed simulation models of SOM turnover now use a multi-compartmental approach, with several organic matter pools, defined by different turnover rates (Six and Jastrow, 2002). A more recent example of large scale analyses of soil C turnover is that by Mills et al., (2013). In a synthesis of data from approximately 250 sites, a two pool, steady state model was applied for semi natural and forested areas for both the UK and globally. It was found that forested soils are significantly more enriched in radiocarbon than non-forested soils, indicating a faster turnover of C in these areas, when steady state conditions are assumed. The mean residence times for the topsoil samples included a slow pool of about 20 years and a passive pool of 1000 years. A fast pool comprised of rapidly decomposing material with a turnover of seconds to years includes recently deposited labile plant material (Amundson, 2001; Trumbore, 2009). Wide scale results of soil C turnover as described, can provide new constraints to quantitative models and complement smaller scale investigations of soil C cycling.

With the exception of large scale studies such as Mills et al. (2013), investigation into C cycling using ^{14}C has largely dominated at the plot scale, where differences in turnover has been characterised in terms of soil horizons (Richter et al. 1999; Leifeld et al. 2009; Schulze et al. 2009). For more reliable models of global nutrient cycles, quantification of soil carbon turnover needs to be characterised at

regional and global scales and over a wider range of soil classifications (Mills et al., 2013).

2.5 Soil organic matter Stoichiometry

The biogeochemical cycles of the macronutrient elements C, N and P are interlinked with SOM turnover, due to the continual alteration of their stoichiometric relationships. Since early research by Redfield (1958) observed an average ratio of CNP 106:16:1 in marine planktonic biomass, similar elemental ratios have been explored in terrestrial environments, with limited outcome. However, more recent research suggests parallel interactions between terrestrial biomass and the terrestrial environment (Cleveland and Liptzin 2007). While quantifying the stoichiometric relationships of SOM provides important model constraints, full understanding of the elemental relationships are lacking. This is partly due to the lack of data available on the elements P and sulphur (S), whilst information on the CN relationships across different soils is abundant. A diverse range of soil types is also not available, or has not been included in past data meta-analyses. For instance, Kirkby et al. (2011) presented a meta-analysis of more than 500 different soils internationally, but restricted the analyses to data with lower C:N ratios (16.5 or less) and to mineral soil. A similar approach was used by Cleveland and Liptzin (2007). Earlier research by Walker and Adams (1958) only focussed on grassland soils in New Zealand.

Improving the understanding of element stoichiometry in SOM is nevertheless reflected in more recent research. From analysis of data obtained with the Hedley fractionation procedure (Hedley et al, 1982), Yang and Post (2011) found that C and N in SOM were closely linked, but that P was correlated to neither C nor N,

and they concluded that OP is decoupled from OC and ON. However, Tipping et al (2016) provided stoichiometric analyses of C, N, P and S in SOM for approximately 2000 different soil samples globally. Strong negative correlations ($P < 0.001$) were observed for N:C, P:C and S:C ratios and % organic carbon, in all soils that were not characterised as peat. Tropical soils also follow the same pattern, but tend to have lower P:C ratios. This showed that SOM in soils with a low OC content tends to be richer in N, P and S. Strong relationships occur between C and N, due to their presence in many of the same molecules, including proteins, while phosphorus originates from other sources including DNA and RNA (Turner et al, 2002). Tipping et al (2016) therefore derived a simple mixing model to describe this relationship, based on the parameters of nutrient poor SOM (NPSOM) ($\geq 50\%$ C) and nutrient rich SOM (NRSOM) ($\leq 0.1\%$ C), which gave rounded CNPS stoichiometries of 919:36:1:5 and 61:7:1:1 respectively. Therefore, nutrient rich (mineral) SOM contains compounds preferentially selected based on their strong adsorption to mineral matter, providing a new quantitative framework for SOM classification and important constraints to conceptual SOM modelling.

2.6 Fractionated soil organic matter

The organo-mineral interactions and quantitative pools of SOM can be operationally defined by the physical or chemical separation of different SOM fractions; a technique which has been used for almost 50 years. The fractionation procedure essentially separates the SOM into discrete fractions of differing stability (Crow et al., 2007). These usually include an organic matter fraction referred to as the light fraction (LF) or particulate organic matter (POM), and the heavy fraction (HF), which is exclusive of OM bound to mineral matter (Golchin

et al., 1994; Six et al., 1998; Sohi et al., 2001). There are two common types of fractionation procedure, which can also be used together in the same method. Physical fractionation of soil according to particle size is generally achieved through varying degrees of dispersion and separation to break aggregate bonds, and can include dry or wet sieving to different aggregate sizes, or sonication of soil suspensions (Kirkby et al., 2011). Density separation involves the dispersion of aggregates using a heavy solution, commonly sodium polytungstate (Schrumpf et al., 2013). Due to the diversity of fractionation techniques, there has been a steady increase in the development and use of density fractionation methods over the past two decades, applied to a range of chemical and ecological research areas (Crow et al. 2007; Christensen 2001).

Fractionation methods have been commonly used to measure the transformations of C and N ratios associated with SOM decomposition, to provide simple turnover models based on the measurable, fractionated pools (Sohi et al., 2001). In an analysis of 12 sites of varying land uses, Schrumpf et al (2013), coupled density fractionation with ^{14}C analysis of the fractionated SOM, which showed that the mineral fractions are chemically more degraded and are older than that of the light fraction, suggesting that association with minerals was the single most important mechanism of SOM stabilization, and is more apparent in deeper soils. In an analysis of global soils combined with new data from agricultural soils in Australia, Kirkby et al (2011) demonstrated a relatively constant CNPS stoichiometry for the stable portion of soil organic matter. Almost all studies report low C:N ratios within the HF and high C:N ratios in the LF. However, measurements of the distribution of oP in both the LF and HF are not readily

available in the literature, although several studies report oP contents in the LF (Rodkey et al. 1995; O'Hara et al. 2006; Wick & Tiessen 2008).

The study of Kirkby et al (2011) also made important comparisons of the different methods available in soil fractionation, highlighting the implications involved with the wealth of non-standardized methods available. While removal of the light fraction with any of the stated methods produced similar CNPS ratios, the sieving and winnowing method consistently produced a more complete removal of the light fraction, as shown by the slightly lower C:N, C:P and C:S ratios of soils fractionated using this method. These ratios were comparable to size fractionation using wet dispersion and washing, as described in Crow et al (2007) and Kaiser et al (2009), although it is likely that more nutrients are lost during this process.

Considerable differences have been observed during the isolation of organic components, especially organic phosphorus; oP (Kirkby et al., 2011). As highlighted in Agbenin et al (1998) analysis of oP from the same soil using two different extraction methods (H₂SO₄ and Ethylenediaminetetraacetic acid – EDTA) gave average C:oP ratios of 193 or 309 respectively, suggesting that careful consideration is needed when analysing the stoichiometric relationship of C:oP in SOM fractions (Kirkby et al., 2011).

Though the study of SOM function has expanded substantially in recent decades, there are considerable gaps in the information available, which will inevitably limit the efficacy of terrestrial nutrient cycling models. For instance, modelling SOM turnover is restricted by the lack of soil types, and disregard the complete range of the macronutrient elements present in SOM. While it is beneficial to have a range of fractionation methods available for operationally defining SOM, a lack of diversity in soil type, and variation between published results evidently limits the

comparability of the studies (Cerli et al., 2012). Thus, for detailed and effective large scale modelling of SOM dynamics, there is evidently a need for a fractionation method that is tested over a range of different soil types and can be applied to measuring soil P as well as C and N. Further, conceptual models of SOM turnover are constrained by the terrestrial environment, raising fundamental questions on the linkages between transfer of OM between terrestrial and aquatic environments, and the important chemical transformations that occur.

In summary, advances in analytical technology has led to a wealth of information on the composition of SOM, enhancing our understanding of SOM stability and turnover. The macronutrient elements of SOM, including C, N and P are closely linked with SOM turnover due to the constant changes involved in the elemental stoichiometry. Thus, to improve large scale models of SOM turnover, quantitative information is needed on the distribution of P in different soil organic matter pools, and its relationship relative to C and N, which is lacking in the data currently available in the literature.

2.7 Part II – Transport, fate and behaviour of natural organic matter in aquatic ecosystems

2.7.1 Nutrient transfer from land to freshwater

The physical and chemical erosion of soil are the most widespread mechanisms of soil degradation, with a global estimate of 1094 M ha of land affected by water erosion (Lal, 2003), which equates to a flux of $\sim 2.7 \text{ Pg C a}^{-1}$ transported, mineralized and buried by inland waters (Battin et al., 2008). Anthropogenic stresses on the land have increased the global flux of carbon from land to

freshwater ecosystems by 0.1 to 0.2 Pg C a⁻¹, largely as a result of deforestation, agricultural intensification and human wastewater effluent (Butman et al., 2015). Inland waters carry multiple forms of carbon, including dissolved organic and inorganic carbon (DOC and DIC), particulate organic and inorganic carbon (POC and PIC) and dissolved CO₂ (Meybeck and Vörösmarty 1999), which can occur at almost all interfaces through drainage, erosion and overland flow. Rivers in particular carry 0.8 Pg C a⁻¹ to the oceans, contributing to the largest carbon sink of 38000 Pg C which also includes 92 Pg C a⁻¹ from the atmosphere through assimilation. Approximately 0.01 Pg C a⁻¹, including that transported by rivers, is buried within oceanic sediments, while oceanic loss through outgassing contributes 90 Pg C a⁻¹ to the atmosphere. Outgassing of CO₂ from inland waters to the atmosphere is also an important component of the global C cycle, though conventional ‘top down’ approaches to modelling carbon cycling is often constrained to terrestrial ecosystem respiration (Battin et al., 2008), making it difficult to predict the actual flux from inland waters alone. However, recent research has placed the global CO₂ flux at 2.1 Pg C a⁻¹, larger than previous estimates which frequently report values at only 1 Pg C a⁻¹ (Cole et al., 2007; Battin et al., 2008; Aufdenkampe et al., 2011; Raymond et al., 2013).

Agricultural and urban activities make up the two major sources of phosphorus and nitrogen to aquatic ecosystems, with atmospheric deposition of N contributing a much smaller source (Carpenter et al., 1998). Approximately 150 Tg N a⁻¹ is applied to the Earth’s land surface, predominantly by fertilizer application.

Research estimates show that approximately 23% of the N applied to land is lost to inland waters (van Breemen et al., 2002) much of which is denitrified in the coastal zone, returning to the atmosphere as N₂ (Seitzinger et al., 2006). The four fold

increase in P addition to the land has inevitably increased the losses to inland freshwater systems, leading to an accumulation of P in freshwaters of approximately 15.5 Tg a⁻¹ (Bennett et al. 2001). As a consequence, growth and reproduction of photosynthetic biota and large scale ecosystem primary production are frequently limited by N and P, having considerable implications on biological diversity and ecosystem function (Smith, Tilman and Nekola, 1998; Elser et al., 2007). Over-enrichment further leads to eutrophication in freshwaters and coastal regions, creating large coastal ‘dead zones’ such as in the Gulf of Mexico, which averages more than 17,000 km² (Elser and Bennett, 2011). While more recent research has successfully identified the major molecular constituents (Lam et al., 2007), understanding the linkages between the terrestrial landscape and inland waters is essential in characterizing the impacts of climate and land use change on freshwater biogeochemical functioning (Aufdenkampe et al., 2011).

2.7.2 Dissolved and particulate organic carbon: Rivers and Estuaries

Despite the prominence of organic carbon in aquatic systems, the pool is difficult to characterize due to the heterogeneous mixture of molecules, some of which remain unidentified (Fry et al., 1998). Common methods for determining the isotopic composition of aquatic DOC include persulfate oxidation, high-temperature sealed-tube combustion (HTC) and total carbon analyzers, all of which undergo continual development (Gandhi et al., 2004).

Analysis of the stable isotope ¹³C is commonly measured by elemental analysers, coupled with isotopic ratio mass spectrometry (Gandhi et al., 2004; Bouillon et al., 2006). Stable isotopic signatures are distinct and therefore give the ability to estimate carbon sources of terrestrial material, owing to the differences in the

isotope fractionation associated with photosynthetic pathways (Bouillon et al., 2006). Photosynthetic pathways of major C₄ plant fixers are commonly identified by a $\delta^{13}\text{C}$ range of between -13 ‰ and -10 ‰. Ancient OC can be in the region of -32 ‰ to 17 ‰, with signals from carbonate rocks in the region of -2.5 ‰ to 0 ‰ (Marwick et al., 2015). However, some $\delta^{13}\text{C}$ signatures of different sources can overlap, such as modern C₃ plant fixers and recently assimilated soil OM (between -32 ‰ and -24 ‰). One of the major advantages of characterizing the ¹⁴C content of aquatic C reservoirs by AMS is that it provides an additional resolution in terms of the sources, where overlapping $\delta^{13}\text{C}$ signals cannot (Marwick et al., 2015).

In a recent synthesis of global riverine DO¹⁴C data, rivers and streams were found to be enriched in ¹⁴C, with an average $\Delta^{14}\text{C}$ enrichment of 22-46 ‰ (equivalent to 102-105 pMC) which indicates recently assimilated carbon originating from the atmospheric weapons testing period (Marwick et al., 2015). At the catchment scale, streams draining directly from urban areas have shown depleted ¹⁴C signals, representing anthropogenic sources such as wastewater effluent (Griffith, Barnes and Raymond, 2009a). In a global analysis of riverine DO¹⁴C data across 135 watersheds, DO¹⁴C was depleted, which can be attributed to an increased mobilisation of aged carbon to rivers by anthropogenic disturbance, including land use change to agriculture and urban settlements (Butman et al. 2015). Catchment size dependency was also observed, with larger catchments typically transporting more enriched ¹⁴C, but in situ mineralization and dilution of aged C with modern sources make interpretation difficult (Caraco et al., 2010; Butman et al., 2015). In contrast, global data for PO¹⁴C is almost always depleted, with an average of $\Delta^{14}\text{C}$ -204 ‰ (equivalent to ~80 pMC or 1800 years B.P), suggesting a different source than DO¹⁴C, and one which originates from stable terrestrial C sources. However,

interpreting depleted PO^{14}C sources is complicated by the metabolism of labile particulate matter, leaving an average overall depleted signal in the stream. Further, variations in the atmospheric ^{14}C signal through time, as the result of atmospheric weapons testing, does not make individual ^{14}C samples directly comparable. Despite the growing use of ^{14}C , the meta-analysis of Marwick et al (2015) is only one of very few attempts to fully synthesise global DO^{14}C and PO^{14}C data, although temporal variations were not addressed. However, substantial bias in the selection of sites was found. Most of the available data are based on areas of particularly high erosion including some of the largest rivers in the world (Mayorga et al., 2005; Galy, France-Lanord and Lartiges, 2008; Spencer, Butler and Aiken, 2012). Larger catchments with relatively moderate erosion rates, such as the African catchments added to the synthesis by Marwick et al (2015), are mostly overlooked.

In the UK, available data on both DO^{14}C and PO^{14}C are focussed on small, upland catchments, draining predominantly peatlands. Here, all analyses of DO^{14}C draining from these upland streams were enriched during high flows (Billett, Garnett and Harvey, 2007; Tipping et al., 2010). As argued in Butman et al. (2015), additional research in lowland, urban catchments is important when quantifying the proportion of aged carbon mobilized from the landscape and understanding its impact on large scale carbon cycling and within river processes. There are no known data on PO^{14}C in larger, lowland catchments and the first such dataset is presented in Chapter 4.

2.7.3 Nutrient cycling in lakes and reservoirs

Inland waters store a significant stock of OC, with an estimated 820 Pg OC buried in the sediment bed (Einsele, Yan and Hinderer, 2001; Cole et al., 2007). Lakes and reservoirs generate approximately 0.65 Pg C a⁻¹ in lake gross primary production (Tranvik et al., 2009), although this is only a fraction of the global primary productivity of 100–150 Pg C a⁻¹ (Randerson et al., 2002). The exact number of lakes around the globe quoted in the literature is variable (Downing et al. 2006; Verpoorter et al. 2014). However, all studies show an abundance of lakes within the smallest category by area (typically 0.001-0.01 km²) (Downing et al. 2006; Verpoorter et al. 2014; Messenger et al. 2016). Therefore, most lakes are typically shallow, allowing an abundance of light and nutrient sources, placing them among the most productive systems on earth (Wetzel, 2001). However, the mechanisms by which OM entering these systems is stabilized is subject to debate. While the stabilizing factors of SOM are largely considered as extrinsic (Schmidt et al., 2011), the same cannot be said for OM in lakes and reservoirs, as was found in a novel study of 109 Swedish lakes (Kellerman et al., 2015). Using ultrahigh resolution mass spectrometry, it was found that degradation processes preferentially removed the oxidised aromatic compounds, whereas aliphatic compounds rich in N were more resistant to degradation, described as a gradient of decomposition from a high to low oxidation state of carbon. Anoxia in lakes also suppresses the mineralization of allochthonous OC, stimulating sediment storage and methanogenesis (Tranvik et al., 2009). Therefore, intrinsic properties of lake systems dominate over the extrinsic factors in these cases, because constraints in the terrestrial ecosystem including light and mineral sorption are not factors.

Lakes and reservoirs are extremely sensitive to climate change; inland waters in arid regions are likely to decrease with increased drought events. In temperate regions, the total surface area of inland waters is likely to increase with the construction of farm ponds and man-made structures for water supply (Tranvik et al., 2009). Lakes have often been overlooked in many global climate models and are often viewed as a passive, single pool. To improve model constraints, further investigation is needed in the roles of freshwater molecular processing on nutrient cycling, and the impacts of climate change on these processes.

2.8 Quantifying DOC in freshwater systems

Increasing concentrations of DOC in inland waters (Monteith et al., 2007), are a cause for concern for the water treatment industry, as water elevated in DOC is expensive and difficult to treat, and can result in a tainted colour and taste of the drinking water supply (Nguyen et al., 2005). Further, algal blooms from the increased runoff of N and P can interfere with the water treatment process by reducing the filtering efficiency through clogging, and by the production of toxic by-products such as trihalomethanes during the chlorination procedure.

Catchments sensitive to these increases are particularly important, such as upland areas that are often used as gathering areas for water supply (Thacker et al., 2008). Thus, there is an increasing demand for intensive monitoring with a high turnover of data.

Optical components of the humic substances transported into inland freshwaters provide aquatic organisms protection from harmful ultraviolet radiation (Blough and Del Vecchio, 2002), and give the ability to optically measure dissolved organic

carbon. Despite the importance of humic substances in freshwaters, their origins on a molecular level are difficult to trace (Del Vecchio and Blough, 2004), though developments in optical measurements have significantly contributed towards greater qualitative understanding. Using laser-photobleaching, Del Vecchio and Blough (2004) proved that the absorption- emission spectra of the chromophore (the part of the molecule responsible for colour) arises from a continuum of intramolecular charge-transfer interactions within the material. This disproved the past theory of superposition, which speculated that the final spectra emitted was the result of numerous independent chromophores (Goldstone et al. 2004 and Coble 2000).

Traditionally, quantifying the concentration of DOC has been measured through the use of 'colour', such as the Hazen scale. Recently, analytical techniques within the laboratory have been using total carbon analysers, which involves the infra-red analysis of DOC through the combustion to CO₂ (Menzel and Vaccaro, 1964; Chen et al., 2002). Both techniques are however, bound to laboratory conditions, introducing complications around the transport of samples back into the laboratory, and time taken for results to be obtained. Alternatively, absorption spectroscopy involves the measure of an output based on the amount of light absorbed by the sample, from a specific light source. Absorption in the UV-Visible range (400-800 nm) can also give indicators of the molecular properties. For example, specific ultra violet absorbance (SUVA) (also defined as the extinction coefficient) provides a measure of aromaticity (Weishaar et al. 2003). Fluorescence spectroscopy differs from absorption in that it measures the amount of light absorbed by a sample as a function of the photon wavelength, and can provide temporal and spatial information of DOM (Chen et al., 2003). While these

techniques are popular, the difference in DOM properties across different environments means that calibration for each site is necessary, further making the current methods time consuming and laborious.

The nature of organic components produced within the water body differs from that of terrestrial organic matter on the molecular level. Laboratory simulations such as Henderson et al. (2008) have shown that autochthonous material comprised more than 57 % hydrophilic compounds and specific ultra violet absorbance (SUVA) values of less than $2.0 \text{ L m}^{-1} \text{ mg}^{-1}$. This indicates that all aquatic organic matter (AOM) was dominated by low absorbance at the 254 nm range, much lower than that of terrestrially derived organic matter, such as plant, soil and microbial detritus. Further, proteins aromatic in character were not detected by SUVA, showing that this specific wavelength is only indicative of aromatic humic and fulvic like substances (Henderson et al. 2008). In the natural environment, there are few published examples of DOM dominant from autochthonous sources. One interesting example is Lake Fryxell in Antarctica, where stream input is mostly glacial meltwater and catchment soil is $<0.1\%$ OC, meaning that inputs of terrestrial DOM is negligible (Aiken et al., 1996). Here, the analysis of fractionated DOC through ^{13}C NMR showed that the organic matter produced within the lake and stream originated from the leaching of algal and bacterial biomass. However, data from Lake Fryxell modelled by Gondar et al (2008) showed that material from this lake does absorb some light. Mash et al (2004) found that autochthonous DOM sources in Arizona reservoirs had the same characteristics. Therefore, measuring autochthonous material by optical methods could lead to underestimations when quantifying the organic matter present in natural freshwaters.

The combined issue of constant calibration and underestimation has been addressed by recent research involving the combination of two different wavelengths through a two component algorithm approach (Thacker et al., 2008; Tipping et al., 2009). First, Thacker et al. (2008) demonstrated a monotonic increase in 23 concentrated DOM samples, suggesting that the concentration of DOC can be calculated with only the absorption data, based on the ratio of the extinction coefficient (or specific absorptivity) and the absorbance at two wavelengths. Although the wavelengths 254 nm and 340 nm were chosen, the extinction coefficient can be calculated at any given wavelength using ‘component A’ and ‘component B’, where component A is referred to as easily absorbing material such as lignin and component B refers to poorly absorbing material which is assumed to be hydrophilic in nature (Figure 2.4). Further testing of this model by Carter et al (2012) introduced a third component, component C, which represents a small fraction of non-absorbing DOM at a constant concentration of 0.8 mg L^{-1} . Model testing using approximately 1700 freshwater samples collected internationally, resulted in good predictions of DOC concentrations ($r^2 = 0.98$), without the need of recalibration for each site.

Where the model failed to give accurate estimations included 32 individual points from samples in Lake Pitkjarv in Estonia (Selberg et al., 2011) and in shallow lakes in the Yangtze basin (Zhang et al., 2005). In the latter case, the model underestimated [DOC] by an average factor of 2.1. The reason behind this is inconclusive, although it is noted that DOM in these areas absorbed light extremely weakly (Carter et al., 2012). In systems that are highly eutrophic, it could be the case that high concentrations of material that originate from the decay of algae are not detected by the parameters set in the model, leading to the underestimation of

the DOC concentration. Thus, there is a good possibility that this model could be applied in intensive monitoring of freshwater systems both in situ and in the laboratory.

To summarise, the radiocarbon content of rivers is a powerful tracer of the origins of terrestrial C pools, and provides a quantitative analysis of OM turnover, allowing for integrated modelling of terrestrial-aquatic nutrient cycling. However, a recent global analysis of riverine PO^{14}C and DO^{14}C highlighted considerable bias in the current dataset. We considerably expand the current dataset by providing an analysis of riverine PO^{14}C in lowland UK catchments, presented in chapter 4. In chapter 5, we reassess the global dataset of DO^{14}C , and expand this by presenting new and previously unpublished data for rivers in the UK and Norway. Finally, we carry out further testing of a multi-component model for measuring DOC concentration using UV-Vis spectroscopy, focussing on areas that are dominant in DOM of algal origin, as shown in chapter 6.

2.9 Overview

Understanding soil organic matter processing and its linkages between the terrestrial, aquatic and atmospheric environments is important in global scale climate modelling. The global terrestrial and aquatic database is extensive, although fundamental questions have yet to be answered, including the processes involved in the selective degradation of SOM on the molecular level, and the transformations and origins of terrestrial OM on entry into the watercourse. Within this review, three topics can be identified as important areas to address in the progression towards conclusive research on the functioning of OM in aquatic and terrestrial ecosystems. These are discussed below.

2.9.1 Quantification

For molecular level processing to be included in large scale models, quantitative information on destabilization and transport is crucial (Rumpel and Kögel-Knabner, 2011). Early qualitative work on OM function included the mechanisms behind recalcitrance, while more recent research has disproven this to be the dominant function of SOM processing (Dungait et al. 2012; Schmidt et al. 2011; Simpson and Simpson 2012). As criticised in (Kleber and Johnson 2010), contradictory evidence can result in ambiguity in the definition OM decomposition, and continuing the qualitative classification of organic matter may in fact, adversely affect progress in carbon turnover modelling and soil management. Therefore, extensive research into the quantitative behaviour of different forms of OM may better contribute towards a more inclusive stance in wider scale modelling of carbon. All results presented in this thesis have been quantified for the purpose of providing necessary constraints in large scale, integrated modelling.

2.9.2 Spatial scale

Though the database available for terrestrial and aquatic OM mechanisms is extensive, there remains considerable gaps in terms of location, soil classification and land use. In soil fractionation studies, methods are typically developed using a very limited range of soil types, and the nature of the method used varies considerably. Kirkby et al (2011) provides a useful comparison between the commonly used methods of fractionation across an international dataset and highlights a surprising difference in the values found for some components of OM, including organic P. In the same study, an independent fractionation method based

on past literature was used to measure the light fraction in agricultural soils only. In Schrumpf et al (2013) and Zimmermann et al (2007), similar methods were used across different soil types including grassland and forested soils. While method development using multiple soils is beneficial, classification of the different samples into land use area also conflicts across studies. As an example, Zimmermann et al (2007) classifies agricultural land inclusive of pasture and arable, whereas Schrumpf et al (2013) categorizes grasslands of any sort as a single entity, whereas arable is a standalone category. This is not uncommon, making cross-comparison increasingly difficult. Therefore, a standardized method for processing and classifying soil is needed, coupled with a more diverse range of soil types studied.

In rivers, data on PO^{14}C and DO^{14}C is available for some of the world's largest catchments, and those with high erosion. In temperate regions with a moderate to low erosion rate, the data available is scarce. In Marwick et al (2015) approximately 1134 individual data points for both dissolved and particulate measurements were collated from around the globe. Much of these were focussed on some of the largest rivers in the world, including the Amazon. In the UK, riverine ^{14}C measurements are confined to small, upland catchments. There is surprisingly little data on lowland, larger catchments where industry and urbanisation may dominate. As found in Butman et al (2015), DO^{14}C in 135 watersheds was depleted, owing to the increased mobility of aged C through anthropogenic disturbance. This is contrary to the average enriched DO^{14}C values found in the meta-analysis by Marwick et al (2015) and evidently a wider range of conditions is necessary for a reliable global dataset of riverine ^{14}C . Significant

contributions to this global dataset have been demonstrated in chapters 4 and 5, across lowland, larger watersheds in the UK.

2.9.3 Technology

Advances in analytical technology have undoubtedly contributed significantly towards a wider understanding in molecular level SOM processing, and the changes involved during erosion into inland waters. In terrestrial research, advances in ^{13}C NMR aided the development of the molecular understanding of humic substances. The development of ^{14}C analysis by accelerator mass spectrometry has given the ability to simulate the turnover of terrestrial C across different timescales. In aquatic ecosystems, the analysis of the ^{14}C radioisotope has contributed towards the understanding of SOM sources and the time elapsed from entry into the water course. Despite the total area of lakes only covering a fraction of the Earth's land surface, significant research using ultra high resolution mass spectrometry found that intrinsic properties of these systems governed the selective degradation of allochthonous OM. Despite this, over half of the OM present in soils remains to be characterized (Hedges et al., 2000). In large scale climate predictions, quantifying the SOM using advanced analytical methods may prove to be more effective in the future preservation of terrestrial carbon stocks in response to global climate change.

In aquatic systems, the quantifiable difference between terrestrially derived OM and material that was produced within the water body, is still developing. In most cases, analysis of aquatic OC quantity has been carried out under laboratory conditions using total carbon analysers and through optical measures using the SUVA at the single wavelength of 254 nm. Organic matter that is largely the result

of algal production and degradation has weaker light absorbing properties than terrestrial material, which may lead to the underestimation of DOC using optical absorbance alone. The development of a two-wavelength approach by Tipping et al (2009) and the introduction of ‘component C’ by Carter et al (2012) has been successful in predicting concentrations of aquatic DOC in global rivers and lakes, without the need for repeated recalibration. However, the efficacy of the algorithm approach needs to be established in highly eutrophic freshwaters, and potential use in situ should be explored in the future. Further testing of the two component algorithm approach is explored in chapter 6.

Table 2.1: A summary of the main structural components of SOM, their sources and how they are detected. Information was sourced from Simpson and Simpson (2012) and Kögel-Knabner (2002).

SOM structural component	Sources	Detection
Lignin	Vascular plant tissue. Cell walls of wood and bark.	Solid state ^{13}C NMR: aromatic/phenolic compounds. Solution state NMR: aromatic compounds Biomarkers: lignin phenols, free phenols from suberin.
Black carbon	Incomplete combustion of biomass and biofuels.	Solid state ^{13}C NMR: Aromatics (120-150 ppm). Biomarkers: Levoglucosan, benzene polycarboxylic acids, free sugars.
Cutin	Waxy, forming outer cell walls of leaves, stems, flowers and seeds.	Biomarkers: Alkanedioic acids.
Suberin	Forms inner cell wall in woody plants, coarse grasses and cotton fibres.	Biomarkers: Di and trihydroxyalkanoic acids.
Microbially derived compounds	Decomposition by-products of soil microbes and fungi.	Solution state NMR: microbial peptides, peptidoglycan Biomarker: Amino sugars, Phospholipid fatty acids.
Peptides	Shorter chain amino acids compared to proteins, found within the cells of plants, roots, fungi, bacteria.	Solution state NMR: ratio of methyl groups CH_2 and CH_3 distinguishes between peptide and proteins. Biomarkers: Free amino acids and amino acids after acid hydrolysis.

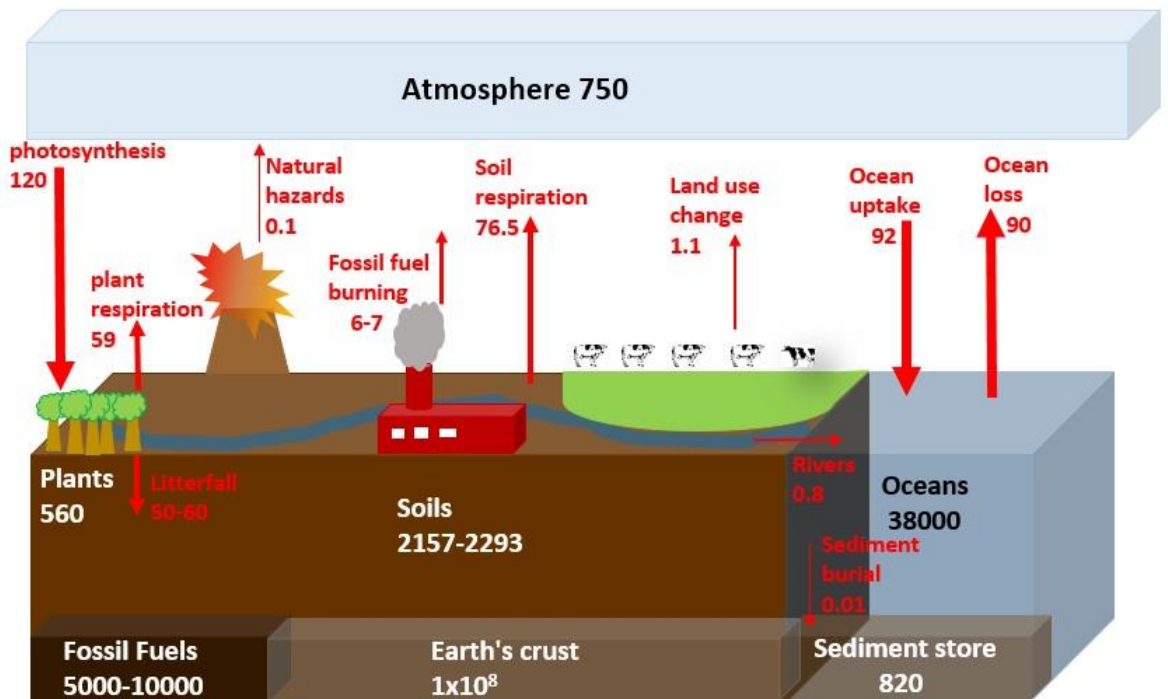


Figure 2.1: A simplified illustration of the global carbon cycle. Fluxes are shown by the red arrows and red values, all presented in Pg C a⁻¹ (10¹⁵ g C). Arrows are approximately proportional to the magnitude of the flux. Pools are either shown in the black or white writing, and are measured in Pg C (10¹⁵ g C). Values for land use change, fossil burning, litter fall, rivers, atmospheric pools and oceanic pools were quoted from Schlesinger and Andrews (2000). Soil pools and fluxes were quoted from Batjes (2014) and Raich and Potter (1995) respectively. Sediment storage was quoted from Cole et al. (2007).

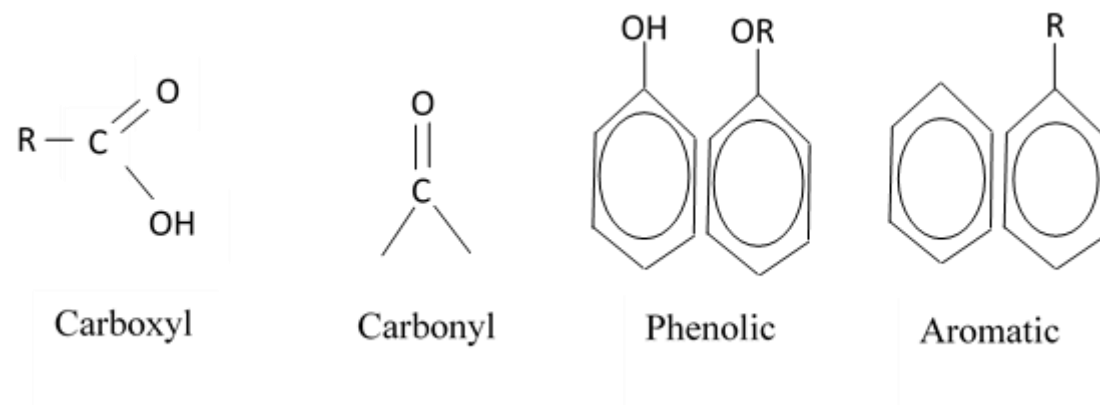


Figure 2.2: Examples of the carboxyl, carbonyl, aromatic and phenolic compounds present in SOM. Illustrations are redrawn from (Kögel-Knabner, 2002).

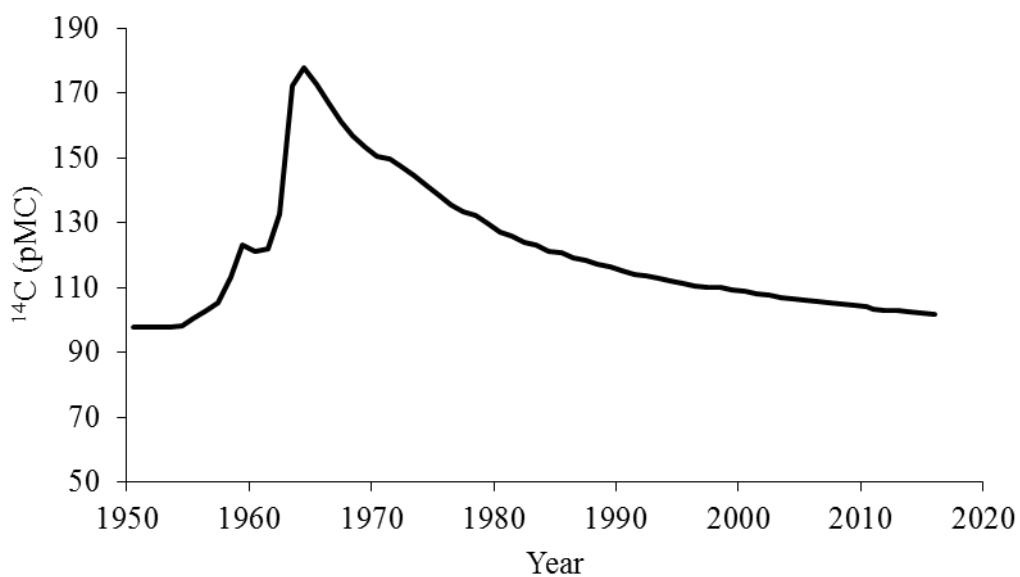


Figure 2.3: Example of the radiocarbon bomb peak as the result of atmospheric weapons testing. The figure has been redrawn based on (Hua, Barbetti and Rakowski, 2013), up to the year 2010. Data was extrapolated to extend the values to 2016.

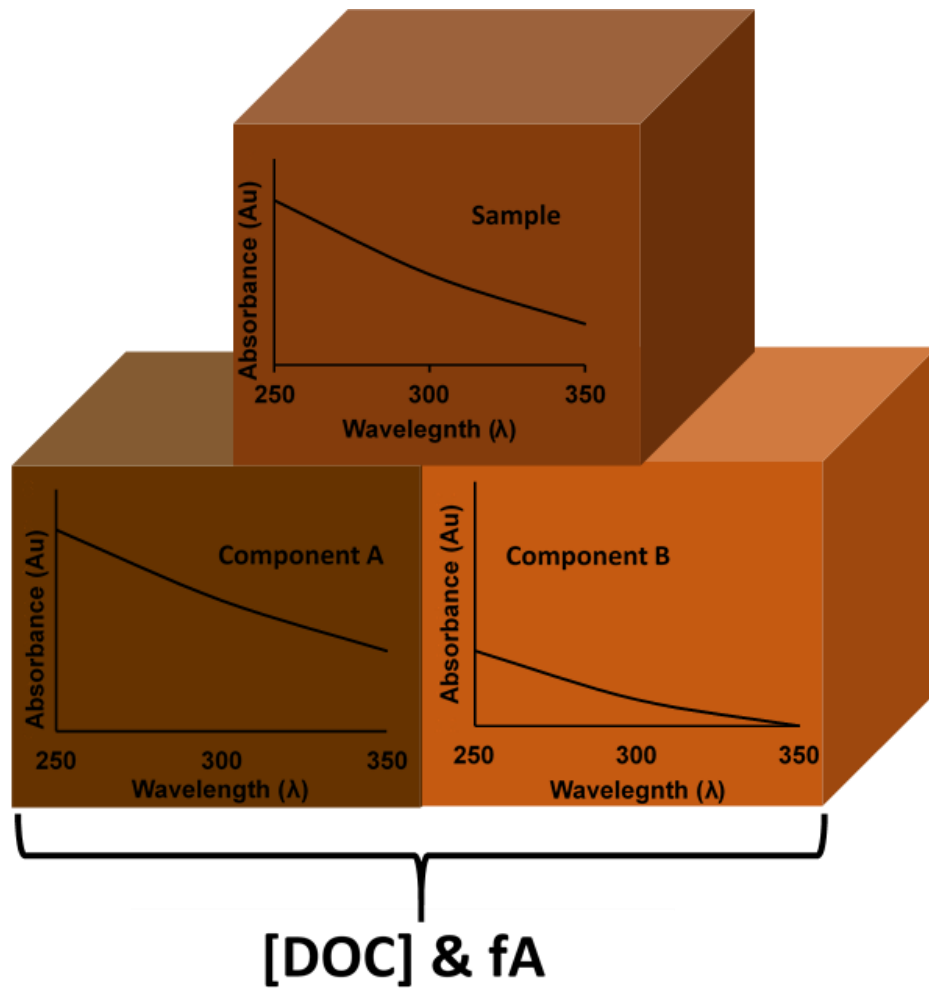


Figure 2.4: A schematic of the multi-component model of absorbance, redrawn and modified from Carter et al (2012). The top column represents the sample being analysed. The model apportions the sample into the two components. Component A (bottom left) accounts for strongly absorbing material, which results in higher extinction coefficients. Component B (bottom right) represents weakly absorbing material, which has lower extinction coefficients. The model can then find the total DOC concentration [DOC] of the sample, and the fraction of component A.

3. Density fractionation of soil organic phosphorus

JL Adams, E Tipping, A Lawlor and JN Quinton

Abstract

Organic phosphorus (oP) is a key nutrient element of soil organic matter (SOM), although its distribution with respect to SOM pools is lacking. Here, we used 20 soils from semi-natural and pasture ecosystems in the UK, to provide the first preliminary investigation of oP distribution between free and mineral associated SOM. A density fractionation procedure yielded 96% of the total mass. Mass concentrations (g/100g soil i.e. %) of C and N were greater in the light fraction, with very little variation between the different soils, while oP was slightly more concentrated in the heavy fraction. In contrast, in terms of the total soil mass, organic matter present in the heavy fraction was considerably more enriched in N and P at 82 % and 90 % of the total, respectively. The oP:C and N:C ratios we measured agreed with a new stoichiometric classification model, which demonstrates that the ratios increase with increasing mineral matter content. Our data considerably expands available information on oP in SOM pools, and is consistent with the concept that its molecular constituents strongly adsorb to mineral matter, even more so than N rich SOM components.

Keywords: Heavy fraction; light fraction; sodium polytungstate; stoichiometry; carbon; nitrogen

3.1. Introduction

Phosphorus (P) is the single major element in soil organic matter (SOM) that is almost entirely supplied by the parent material of (unfertilized) soils through weathering. Unlike the other macronutrient elements of SOM, including carbon (C), nitrogen (N) and sulphur (S), P is cycled mostly in geological timescales, which leads to P limitation in terrestrial ecosystems (Walker and Syers, 1976).

Organic phosphorus (oP) is a particularly important source for plants in both natural environments and in land managed for food production. It is a key component of plant cells including nucleic acids, phospholipids and adenosine triphosphate (ATP), controlling plant growth and metabolism (Schachtman, Reid and Ayling, 1998). Thus, P compounds play an integral role in intensive farming, which has led to a four-fold increase in P inputs to the biosphere, largely from the mining of P compounds (Falkowski et al., 2000; Elser and Bennett, 2011).

Understanding the behaviour of oP is therefore essential in understanding the wider nature of terrestrial biogeochemical cycling.

Analytical limitations have restricted the information available on the quantity and speciation of soil organic phosphorus. As an example, solid-state phosphorus-31 nuclear magnetic resonance (^{31}P NMR) cannot be used for detecting oP due to its low sensitivity (Turner et al., 2005). Thus, oP requires extraction from the soil into solution, which can have implications on the integrity of the P extract. Chemical sequential extraction procedures have been developed to partition organic phosphorus fractions into discrete pools based on solubility. Hedley and Stewart (1982) proposed a chemical fractionation method based on the idea that bioavailable material would be present in sodium bicarbonate, strongly bound oP

would be present in the sodium hydroxide extract and the most stable forms would remain in the residual fraction. The Hedley fractionation scheme has been used extensively, with considerable modifications for use in different soil types (Johnson et al. 2003). Using this technique, Yang and Post (2011) found that C and N were strongly correlated across different soils, while oP was not correlated to either, concluding that oP is decoupled from C and N. However, the physical fractionation of oP content, with regards to SOM pools has not been explored in its entirety. Kirkby et al., 2011 remains one of few studies to include oP, in a study of new and published density fractionated soil data, although their chosen methods do not reflect other commonly used protocols.

The physiochemical fractionation of SOM involves separation through flotation, sedimentation and aggregate disturbance. During fractionation, the organic debris including plant and animal material, referred to here as the light fraction, but sometimes referred to as particulate organic matter (Zimmermann et al., 2007), is separated from organic material bound to mineral matter, referred to as the heavy fraction (HF), using a dense solution. A range of fractionation methods are available (Sohi et al. 2001; Kirkby et al. 2011; Zimmermann et al. 2007), such that there is no standardised procedure, therefore research into the methodological aspects continue (Cerli et al, 2012). In well drained soils, the HF is generally regarded as the stable SOM pool, supported by stable isotope ($\delta^{13}\text{C}$) and radiocarbon (^{14}C) analyses, with the oldest organic carbon (OC) found within the HF (Trumbore, 1993; Swanston et al., 2005; Tan et al., 2007; Kögel-Knabner et al., 2008). Aggravation of the HF through ultrasound sonication releases intermediate material called the occluded fraction (OF), which is commonly

assumed to be more chemically degraded than the LF, and has smaller particle sizes (Golchin et al., 1994).

The distribution of the nutrient elements across SOM fractions has mostly been measured using the N content (through C:N ratio). Since C and N pools have been widely used to construct simple models of long term SOM turnover (Jenkinson et al. 1990; Sohi et al. 2001), information on the C and N content of SOM is abundant. Studies involving the C and N composition of fractionated soil frequently report correlations of varying strength in the C:N ratio within the heavy fraction, supporting the theory that C:N consistency is only associated with organic matter present in the heavy fraction (Kirkby et al., 2011). Almost all studies report a low C:N ratio within the HF, whereas the LF mostly has a high C:N ratio, although variation in the correlation strength is common (Kirkby et al., 2011). Clay content and soil texture has also been found to be a determinant of the persistence of OM in light and occluded soil fractions (Kölbl and Kögel-Knabner, 2004).

Available information of oP in fractionated soil is almost entirely restricted to the light fraction, and is very limited in comparison to fractionated C and N. In forested environments, analyses on the oP availability and enrichment with respects to land management change has been rigorously studied (O'Hara, Bauhus and Smethurst, 2006; Wick and Tiessen, 2008). Rodkey et al (1995) found extensive pools of phosphorus and nitrogen in the light fraction of forested soil in Indiana, the availability of which is related to the site productivity. In agricultural ecosystems, mobilization of oP and the effects of fertilizer application and crop rotation dominate the information available in the literature (Phiri et al., 2001; Curtin, McCallum and Williams, 2003; Wick and Tiessen, 2008). Salas et al (2003) also suggested the possible role of soil fungi in the oP immobilization in

agricultural, acidic soils. In more recent research, Kirkby et al., 2011 reports a variable relationship in the oP:C ratio, although this may arise from the variation in density separation methods used. To our knowledge, there have been no measurements yet of the distribution of oP between the LF and the HF and the range of soil types presented are lacking.

In bulk soils, stable SOM pools are known to contain more N, P and S per unit carbon, than its associated plant material, largely due to microbial reprocessing (Bol et al., 1999; Kramer et al., 2003), which could lead to near constant ratios of C:N:P:S (Kirkby et al., 2013). Kirkby et al. (2011) speculates that microbial biomass is the main precursor of the stable SOM pool. However, recent research by Tipping et al. (2016) proposed that the stable SOM fraction is more likely to be the result of selective adsorption by mineral matter, which could explain the enrichment of oP in mineral soils. Thus, a simple analysis of the distribution of oP across both SOM fractions is needed for further understanding, and improved modelling of SOM cycling for a range of ecosystems.

We aimed to investigate the distribution of oP between free and mineral associated SOM. To do so, we applied a physiochemical density fractionation method based on the procedure of Schrumpf et al. (2013), which in turn was derived from the methods of Golchin et al (1994) and Sohi et al (2001). Our sample set consisted of selected soils obtained in a survey of sites across the UK (Toberman et al, 2016), favouring soils with a relatively high %C content.

3.2. Methods

3.2.1. Sample selection

Soil samples were collected in a survey of the catchments of the rivers Avon (Hampshire), Conwy (N Wales), Dee (NE Scotland), and Ribble (NW England) carried out between 2013 and 2015 (Toberman et al, 2016). Samples included both topsoil (0-15 or 0-20 cm) and subsoil (15-40 or 20-40 cm). Twenty soil samples were chosen, covering a range of OM contents from 26.5% - 45.5% OC, and with sufficient light material to analyse, which precluded the analysis of arable soils. Samples were air dried and sieved to 2mm. Further information about the soil samples is shown in Table 3.1. Bulk analyses of the soils were reported by (Toberman et al. 2016).

3.2.2. Analysis of the bulk soil samples

Measurements of total C and N were performed using a Vario EL elemental analyser. Repeated determinations by this method on three representative UK soils over the period of this study gave relative standard deviations of between 2.1 and 3.6 % for TOC and between 1.7 and 3.1% for TN. Total P was measured using aqua-regia and microwave digestion based on EPA (2007). A 3:1 mixture of hydrochloric acid and nitric acid was heated to 175 °C in sealed Teflon vessels, which covered a period of 7 minutes, with the target temperature held for 4.5 minutes. Once cooled, the sample was filtered and diluted to volume using DI water. Total P was then measured by Inductively Coupled Plasma Optical Emission Spectrometry (ICP-OES) using an Optima 7300DV analyser. Inorganic P was extracted using a 25g subsample in 0.5 M sulfuric acid, which was shaken for 16 hours, centrifuged at 10000 rpm for 30

minutes and filtered using Whatman 1573 1/2 (12-25 μm) filters. These were then measured using a SEAL SQ2 discrete analyser. Organic P measurements were obtained through the calculated difference of the total and inorganic P results.

3.2.3. *Aggregate separation by density*

A schematic of the fractionation method is shown in Figure 3.1. We distinguish non-occluded and occluded light fractions (NLF, OLF) which were combined to make the light fraction (LF), and the heavy fraction (HF). One fractionation was performed for each soil. A 25 g subsample of each of the sieved soils were placed in 400 mL centrifuge bottles, with 250 mL sodium polytungstate (NaPT) (Sometu, Belgium) at a density of 1.6 g cm^{-3} (Cerli et al., 2012). The bottles were gently shaken by hand, then centrifuged at 5500 rpm for 30 minutes. If the quantity of floating material (NLF) was low, it was removed using a wide-tipped pipette and placed into 60 μm nylon mesh bags. For samples of heathland and forest soil with higher quantities of NLF, material was removed using a spatula and placed in 60 μm nylon mesh bags. The remaining suspension was brought back to its initial volume with fresh NaPT of the same density, re-centrifuged, and then residual light fraction was removed, this procedure being repeated until all NLF was accounted for. To minimise the loss of material during rinsing, deionised water was passed through the mesh bags, with all waste material collected in a plastic 1L beaker. The leachate was repeatedly measured for conductivity using a Jenway 4510 probe. Complete removal of excess NaPT was assumed when the conductivity fell below $50 \mu\text{s cm}^{-1}$, except that for calcareous soils, where $< 200 \mu\text{s cm}^{-1}$ was considered acceptable, because of dissolution of carbonates (Schrumpf et al., 2013). The rinsed samples were weighed, oven dried at $40 \text{ }^{\circ}\text{C}$, weighed again and once completely dried, were stored in a desiccator until further analysis.

Extraction of the OLF was carried out using ultrasound sonication (Sonics Vibracell CV18 probe). To avoid aggregate breakdown of the HF, a pilot test for each of the soil types, based on data for the bulk soil texture (Toberman et al, 2016) was carried out to find an optimal sonication frequency, following the procedure of Schrumpp et al. (2013). The samples were periodically checked for complete aggregate disruption using a 0.1 mL subsample observed under a microscope. Complete aggregate disruption was assumed when no further OLF material could be seen attached to minerals under the microscope. During sonication, the bottle was submerged in an ice bath and temperature measured and maintained at $< 40^{\circ}\text{C}$ (Schrumpp et al., 2013). Once fully sonicated, samples were left to stand for 1 hour and then centrifuged again at 5500 rpm for 30 minutes and the OLF extracted by pipette. The samples were repeatedly centrifuged to account for any leftover OLF if necessary. The OLF was added to the NLF in the $60\ \mu\text{m}$ mesh bags, the resulting LF was rinsed again until conductivity was < 50 or $< 200\ \mu\text{s}^{-1}$, dried at 40°C , weighed and ground to a fine powder using a Retsch MM400 mixer mill.

3.2.4. Extraction of the heavy fraction

The centrifuge bottles containing the remaining material (HF) were refilled with ultra-pure deionised water and centrifuged at 5500 rpm for 10 minutes. After each centrifugation, the supernatant was decanted into plastic beakers and measured for conductivity. This process was repeated until the waste water had a conductivity of < 50 or $< 200\ \mu\text{s}^{-1}$. The samples were then transferred into aluminium trays, oven dried at 40°C and weighed. The dried HFs were ground to a fine powder using a ceramic pestle and mortar.

3.3. Fractionated soil: Analyses.

3.3.1. C:N

Before analysis for C and N, any samples that might have contained inorganic carbonate (bulk soil pH > 5.5) were treated with 0.1 M HCL and observed under a microscope until all CO₂ release had occurred. These samples were then re-dried at 40 °C. Single determinations of total carbon (C) and nitrogen (N) in milled subsamples were made with a Vario EL elemental analyser, which was the same method as the bulk soils reported in (Toberman et al, 2016). Repeated determinations of three quality standards for the method over the period of this study gave relative standard deviations of between 2.1 and 3.6 % for C and between 1.7 and 3.1% for N.

3.3.2. P analysis

We used the same analyses as the bulk soils reported by (Toberman et al, 2016) for IP, but a different method was used for TP. Resource limitations meant that we were unable to determine soil TP by the same method for both bulk and fractionated soils. However, tests on a reference sample (ISE sample 921 from Wageningen University, Netherlands) and on several bulk soil samples showed that the two TP methods gave closely similar results (within 3% of each other on average). Our method for TP followed an ignition-extraction procedure as described in Watanabe and Olsen (1965). First, 0.5 g subsamples were ignited in a Pyrotherm muffle furnace at 550 °C for 1-2 hours, placed in 50 mL centrifuge bottles with 25 mL 0.5 mol sulphuric acid and shaken for 16 hours. These were then centrifuged at 10000 rpm for 30 minutes, filtered using Whatman 1573 1/2

(12-25 µm) filter papers and refrigerated at 4 °C until further analysis. The extracts were analysed for soluble reactive phosphorus using the molybdate method.

Organic P was obtained as the difference between TP and IP. These analyses were replicated four-fold.

Statistical analyses (t-tests and linear regressions) were performed with Microsoft Excel. Before conducting linear regression analyses, data were tested for normality using quantile–quantile plotting. For t-testing the D'Agostino-Pearson test was used to check for normality. Non-normal data were transformed using log transformations where necessary.

3.4. Results

3.4.1. Composition of C, N and P in the fractions

There was very little variation between the elemental concentrations of the light fraction, regardless of the different soil types and land uses. The heavy fractions varied appreciably between the sites, which can be seen from the summary of the elemental concentrations in Table 3.2. Overall, the concentration of C in the light fraction was much higher than that observed in the heavy fraction with an average of 36%, although it was expected to be ~ 50% (Tipping, Somerville and Luster, 2016). The heavy fraction was lower in C, with an average of 8.1 % (Table 3.2, Figure 3.2). The light fraction contained over double the N content compared to the heavy fraction, at 1.4% and 0.6% respectively (Figure 3.2). For most of the HF samples, the P is predominantly oP, at 0.04 %, compared to 0.03 % in the light fraction (Figure 3.2). Light fraction TP and IP were both slightly higher, at 0.06 % and 0.03 % respectively. Based on relative standard errors (Figure 3.3), the average

reproducibility was $\pm 14\%$ for the LF forms of P, and $\pm 6\%$ for the HF forms, which can be considered satisfactory, bearing in mind the several steps that are involved in the analytical procedure.

3.4.2. Element recovery and distribution

Recoveries were calculated by combining the mass data with measured element concentrations in bulk soil and in the two density-separated fractions (Table 3.3). The fractionation protocol resulted in an average recovery of $96 \pm 4\%$, with a range over the 20 soils of 90% - 105% measured by mass. Regression analyses indicated that mass recovery depended upon neither the amount of material in the heavy fraction, nor the carbon content of the bulk soil (data not shown). The small standard deviations show that recoveries were consistent across all of the samples. The method developed is therefore applicable to a range of different soil types and land uses, as long as the light fraction is in sufficient quantity to analyse (i.e 1g). Recoveries of OC and TN calculated as simple averages were each 91%, while the average recoveries of TP, IP and oP were 62%, 117% and 56% respectively. For all three P forms, the recoveries varied appreciably among the soils, more so than for OC and TN, although recoveries did tend to be higher in the semi natural (conifer, heathland and broadleaf woodland) sites.

To demonstrate the distribution of the nutrient elements, we calculated the fraction of each element across both light and heavy fractions (Figure 3.4, Table 3.4). The highest mass was always found in the heavy fraction, with an average of 93% (Figure 3.4). In 18 of the 20 soils, C, N and oP are predominantly in the HF, and the HF percentages are in the order $\text{oP} > \text{N} > \text{C}$. Organic carbon accounted for 75%

of C and 82% of N, while oP was 90%. The TP in the HF was 85%, while the fraction of inorganic P was 71%.

3.4.3. Stoichiometry

To explore the stoichiometric relationships, we assume the N in the samples to be entirely organic. According to Stevenson and Cole, (1999) inorganic N comprises 10% of TN on average, while Schulten and Schnitzer (1997) estimated 5%.

Inorganic contribution is higher in deeper soils, and soils with low OM content, whereas the soils studied here are relatively OM rich. We plotted N:C and oP:C against % C (Figure 3.5), as carried out by Tipping et al. (2016) in a global synthesis of > 2000 bulk soil data for C, N and oP. In the heavy fraction, increasing % C content corresponds to a decreasing ratio of both N:C and oP:C.

The light fractions both have even higher ratios, due to their enrichment of % C. For comparison, we plotted model fits of Tipping et al (2016) for the bulk soils

(Figure 3.5), with the data from the fractionated soils, which both agree. For our fractionated dataset, the light fraction showed average N:C and oP:C of 0.04 and 0.0008 respectively. The average N:C ratio of the HF (0.07) is significantly (p

<0.001) higher than that of the LF, the HF N:C ratio exceeding the LF ratio for 19 of the 20 soils. Such a difference also applies for HF oP:C ($p < 0.001$) (oP:C =

0.005), again with 19 of the 20 soils fitting the pattern. Significant relationships

were observed between C and N in the heavy fraction ($P = 6.8 \times 10^{-9}$). While oP and C were also significant ($P = 0.04$), they were considerably more scattered (Figure 3.5).

3.5. Discussion

The chosen soil fractionation method was successfully applied to the range of soil samples used, providing that there was enough light fraction to analyse. Only minor adaptations were necessary where the proportion of the light fraction was high, which included using a spatula to remove the light fraction, as opposed to using a pipette. There were many similarities to the method of Zimmermann et al (2007) which yielded fractions in agreement to the pools of the RothC model, although this only covered arable and agricultural soils. Our method resulted in an average sample recovery of 96% by mass. Recovery depended upon neither the amount of material in the heavy fraction, nor the carbon content of the bulk soil. The average recovery fell between the averages of 100% obtained by Swanston et al. (2002) for 7 soils, and 83% obtained by Schrumpf et al. (2013) for 48 samples; we used essentially the same method as these previous studies. The loss of some material in these types of methods is probably from some soluble compounds dissolving into the NaPT solution and even more likely that some material was lost during rinsing and collection of the separate fractions (Cerli et al., 2012). As in Cerli et al (2012), some samples had a recorded negative mass loss of soil, reflective of the difficulties in weighing small quantities of fractions. In our sample set, this included two rough grassland sites and one conifer plantation.

The concentration of C in the light fractions averaged 36%, indicating the preponderance of organic matter. There was only modest variation in the LF which was also observed in international soils synthesised by Kirkby et al (2011). The concentration is lower than the widely accepted value of 50% OC (Tipping, Somerville and Luster, 2016), indicating that the LF was predominantly but not

entirely OM, thus containing some mineral matter. Crow et al. (2007) reported values of 27% and 29% C in two soils and Swanston et al. (2002) obtained a mean of 25% C from 7 soils. Cerli et al (2012) observed decreasing C content in the light fraction with increasing sonication time and intensity, suggesting a higher content of mineral matter through aggregate breakdown. Thus the fractionation procedure certainly concentrates OM in the LF, but some mineral matter is retained. It is possible that sonication did not adequately disperse the two and was not observed in the sub-sample using a microscope. Pooling of the occluded fraction in with the light fraction could also add some mineral matter back into the light fraction.

By concentration, the light fraction was considerably more enriched in C and N, which is expected of organic matter absent of minerals. In contrast, the concentration of oP was slightly higher in the heavy fraction, and although the relationship between C and oP was significant, there was considerable scatter, which might reflect the generally small proportion of molecules containing oP, making it less strongly correlated to C and N. Similar patterns were also observed by Tipping et al. (2016) in bulk soil, although a variation in oP extraction methods may have contributed to the scattering in their dataset. The average concentration for IP (0.01%) seemed high, and a possible explanation is that the strong acid reagent used to extract IP caused hydrolysis of some of the LF OM, releasing IP. However, Turner et al. (2005) considered this to apply to only a small fraction of oP.

In contrast, in terms of the total soil mass, organic matter present in the heavy fraction was considerably more enriched in N and P at 82% and 90% of the total, respectively. This clearly shows an accumulation of N in fractions with high mineral matter content, and even more so with oP. As suggested in Tipping et al.

(2016) this could be due to adsorptive selection of individual molecules mobilized during decomposition of microbial and plant biomass, by minerals abundant in the heavy OM fraction.

There were definite losses of TP and oP, with recoveries of 62% and 56% respectively. The loss of oP probably occurs because it was obtained as the difference between TP and IP, because IP was a minor part of TP in the HF, and because IP losses were small. Greater losses of P forms in the grassland soils (rough grassland and improved grassland) could be the result of lower quantities of LF in these samples and lower masses of P forms (Table 3.3), which could increase the likelihood of material not being retained during the fractionation procedure. A possible general explanation for the losses of both TP and IP is the displacement by the NaPT of some OP adsorbed to mineral matter. It is known that monotungstate can displace inorganic phosphate from ferrihydrite (Gustafsson, 2003) and the same is likely to apply to polytungstate and organic phosphates. The concentration of NaPT used in the fractionation procedure is necessarily high, to achieve a high liquid density, and this would favour competition with OP adsorbed to mineral surfaces via ligand exchange with P ester groups. A smaller effect of polytungstate on IP recovery might indicate that most of the IP was not present as adsorbed inorganic phosphate. It is also possible that some of the oP in the fractionated samples was not captured during ignition, thereby underestimating it. In comparison to the procedure for measuring C and N, the steps involved in obtaining P values are greater and concentrations generally smaller, which inevitably leads to higher margins of (human) error involved during processing. Increasing the starting mass of the sample during the fractionation may alleviate this, although there would be cost and equipment implications involved with

increasing the volume of NaPT. It is therefore important to carefully consider the method, or combination of methods, used when determining the distribution of oP and associated constituents, as variations in analytical methods used can cause large variations in the results (Agbenin, Iwuafor and Ayuba, 1998; Kirkby et al., 2011).

The stoichiometric trends demonstrated in the Tipping et al (2016) model framework conform to two SOM end members, nutrient poor (≥ 50 % C) SOM (NPSOM) and nutrient rich (≤ 0.1 % C) SOM (NRSOM). Therefore, NRSOM dominates at low %C, which gradually decreases with increasing C content, and thus increasing NPSOM. The plots of N:C and oP:C against C (Figure 3.5) agree with the modelled outputs, confirming that the ratios change with decreasing C content, thus it cannot be possible to have constant ratios of C:N:oP (Tipping, Somerville and Luster, 2016). The LF P:C values are lower than predicted, and they mostly fall below the cloud of points in the bulk data analysed by Tipping et al (2016) (Figure 3.5), which were obtained predominantly from the organic horizons of forest soils. Tipping et al (2016) reasons that material derived from proteins is the likely source for mineralized N. This is supported by other research that shows material enriched in N extracted from soils is protein derived, and is an important determinant of SOM stabilization (Amelung, 2003; Rumpel, Eusterhues and Kögel-Knabner, 2004; Knicker, 2011). Here, the main source of oP seems to be independent of C and N. If, as suggested above, the low recovery of oP, compared to C and N in the fractionation procedure is due to competition with NaPT, then this would imply that adsorbed oP and N are in different molecules, with different chemical groupings involved in the adsorption process. The dominant source of oP is likely to be plant and microbially derived, in the form of

inositol phosphates, mostly myo-inositol hexakiphosphate, IP₆ (phytic acid) (Turner et al., 2002) although the variation of oP components across different soils is inconclusive (Turner et al., 2012; Jørgensen, 2015). The primary sources of oP in our dataset cannot be verified and applying the Hedley fractionation scheme to the different SOM fractions could provide a clearer indication of the distribution of specific oP compounds (Yang and Post, 2011).

The key result of this work is that the N:C and oP:C ratios of the HF are substantially lower than those of the LF. This is consistent with the preferential adsorption by mineral matter of N and P rich compounds, proposed by Tipping et al. (2016) as a principal mechanism by which NRSOM is formed. Thus, this work supports a new quantitative framework for SOM classification and characterisation, and provides important constraints to models of terrestrial nutrient cycling. However, there are aspects of the methodology that are a cause for concern, namely the loss of appreciable amounts of TP and oP. Further investigation is required, for more robust constraints in the modelling the distribution of all macronutrient elements across different SOM pools.

3.6. Conclusions

- The density fractionation method yielded good recoveries of soil mass, OC and TN for 20 semi-natural and pasture soils.
- Recoveries of TP and OP were relatively low, which might be explained by the displacement of adsorbed organic phosphates from mineral surface adsorption sites by the sodium polytungstate used to create the dense liquid for fractionation.

- For density separated soil organic matter, C and N were more concentrated in the light fraction, whereas oP was more concentrated in the heavy fraction.
- Mass balances showed that oP was highly enriched in the heavy fraction, containing 90 % of the total, followed by N and C, at 82% and 75% respectively.
- The variations with soil %C of stoichiometric ratios (P:C, N:C) in HF and LF agree approximately with the predictions of the two end-member mixing model of SOM advanced by Tipping et al. (2016) in which organic molecules rich in P and N preferentially accumulate on mineral matter surfaces through strong adsorption.

3.7. Acknowledgements

This work received National Capability funding from the UK Natural Environment Research Council (CEH project number NEC04841).

Table 3.1: Information about the soil samples.

Sample ID	Database ID	Sampling date	Lat (deg)	Long (deg)	MAP (mm)	MAT (°C)	Land use	Soil type	Upper depth (cm)	Lower depth (cm)
B1d	CW1d	05/08/13	53.19	-3.85	1391	9.9	Broadleaf woodland	Podzol	15	33
B1s	CW1s	05/08/13	53.19	-3.85	1391	9.9	Broadleaf woodland	Podzol	0	15
B2s	RW1s	25/04/13	54.00	-2.39	1614	7.9	Broadleaf woodland	Surface water gley	0	20
C1s	CC1s	06/08/13	53.03	-3.85	2309	7.3	Conifer plantation	Podzol	0	15
C2s	RC1s	01/05/13	54.01	-2.40	1614	7.9	Conifer plantation	Surface water gley	0	20
H1s	AH1s	23/07/13	50.83	-1.90	863	10.1	Heathland	Surface water gley	0	15
H2s	CH1s	06/08/13	53.26	-3.90	862	10.4	Heathland	Ranker	0	15
H3s	CM1s	29/10/13	53.15	-4.00	2707	5.3	Heathland	Surface water gley	15	26
H4d	RH1d	01/05/13	54.18	-2.29	1827	5.9	Heathland	Ranker	20	38
IG1s	AIG4s	24/07/13	51.13	-1.95	865	9.5	Improved grassland	Groundwater gley	0	15
IG2s	RIG4s	12/04/13	54.25	-2.32	2053	5.7	Improved grassland	Groundwater gley	0	20
IG3s	RIG5s	30/04/13	54.00	-2.70	1220	8.4	Improved grassland	Groundwater gley	0	20
R1s	ACG1s	22/07/13	51.13	-2.00	865	9.5	Rough grassland	Rendzina	0	15
R2s	ACG2s	23/07/13	51.38	-1.85	868	9.2	Rough grassland	Brown earth	0	15
R3d	CAG1d	06/08/13	53.08	-3.97	3105	6.1	Rough grassland	Surface water gley	20	44
R4s	CAG3s	29/10/13	53.14	-4.00	3105	6.1	Rough grassland	Ranker	0	15
R5s	RAG1s	01/05/13	54.25	-2.32	2053	5.7	Rough grassland	Groundwater gley	0	20
R6s	RAG2s	01/05/13	54.19	-2.35	1943	6.8	Rough grassland	Groundwater gley	0	20
R7s	RCG1s	22/02/13	54.14	-2.32	1491	6.8	Rough grassland	Ranker	0	15
R8s	RCG2s	25/04/13	54.20	-2.38	1943	6.8	Rough grassland	Ranker	0	20

MAP= mean annual precipitation. MAT = mean annual temperature.

Table 3.1 (continued).

Sample ID	Database ID	n ¹	Clay %	Silt %	Sand %	pH ²	Bulk density ³ g cm ⁻³	OC %
B1d	CW1d	10	10.2	50.3	39.5	5.64	0.28	4.52
B1s	CW1s	10	11.9	63.7	24.4	5.31	0.22	14.20
B2s	RW1s	10	9.9	49.6	40.5	6.09	0.57	4.51
C1s	CC1s	10	9.3	64.9	25.8	4.02	0.25	12.00
C2s	RC1s	10	9.7	46.2	44.0	4.03	0.45	8.16
H1s	AH1s	10	Nd	Nd	Nd	4.15	0.61	10.00
H2s	CH1s	10	Nd	Nd	Nd	4.32	0.50	11.60
H3s	CM1s	10	4.3	39.0	56.7	4.40	0.27	15.60
H4d	RH1d	10	8.3	61.3	30.4	3.68	0.55	11.30
IG1s	AIG4s	6	11.7	70.0	18.3	7.51	0.67	6.34
IG2s	RIG4s	10	10.7	52.5	37.3	5.42	0.40	13.80
IG3s	RIG5s	10	8.0	53.3	38.7	5.92	0.62	7.82
R1s	ACG1s	10	Nd	Nd	Nd	7.24	0.56	10.40
R2s	ACG2s	10	24.6	68.6	6.7	6.51	0.58	10.90
R3d	CAG1d	10	Nd	Nd	Nd	4.37	0.41	17.40
R4s	CAG3s	10	9.9	70.3	19.7	4.95	0.26	15.50
R5s	RAG1s	10	Nd	Nd	Nd	5.60	0.38	9.20
R6s	RAG2s	10	11.9	65.1	23.0	5.59	0.33	10.30
R7s	RCG1s	10	10.7	56.0	33.4	7.46	0.24	18.30
R8s	RCG2s	10	9.7	55.7	34.5	5.40	0.46	5.80

¹Number of cores (48mm diameter) that were combined to make a sample

²pH determined in H₂O

³Bulk density of the fine earth (<2mm)

Nd = not determined.

Improved grassland sites were the only ones to be periodically treated with fertilizer.

Table 3.2: Concentrations of the light fraction, heavy fraction and bulk soil for carbon (C) nitrogen (N), total P (TP) inorganic P (IP) and organic P (OP). S and D refer to shallow and deep respectively. Concentrations are presented as %. Data for TP IP and oP are mean values (n=4).

Sample ID	Light fraction					Heavy fraction				
	C	N	TP	IP	oP	C	N	TP	IP	OP
B1d	33.80	1.15	0.05	0.03	0.02	4.20	0.34	0.08	0.025	0.058
B1s	38.80	1.79	0.06	0.04	0.02	9.12	0.76	0.13	0.020	0.107
B2s	36.00	1.87	0.07	0.02	0.04	3.15	0.28	0.03	0.006	0.020
C1s	34.60	1.56	0.11	0.06	0.05	8.80	0.63	0.05	0.013	0.034
C2s	33.60	1.11	0.07	0.04	0.03	6.87	0.45	0.02	0.002	0.021
H1s	40.80	1.14	0.12	0.05	0.06	5.25	0.22	0.01	0.002	0.008
H2s	38.20	1.20	0.05	0.03	0.02	9.45	0.46	0.02	0.005	0.014
H3s	38.80	1.91	0.05	0.02	0.02	15.7	1.00	0.07	0.016	0.053
H4d	36.70	1.73	0.06	0.04	0.02	4.31	0.17	0.004	0.001	0.003
IG1s	34.00	1.16	0.07	0.03	0.04	7.87	0.54	0.08	0.036	0.046
IG2s	45.50	1.23	0.05	0.02	0.03	13.40	1.07	0.11	0.055	0.056
IG3s	39.40	1.61	0.05	0.02	0.03	5.28	0.35	0.04	0.014	0.030
R1s	26.50	1.26	0.07	0.02	0.05	9.06	0.71	0.06	0.003	0.053
R2s	34.30	0.96	0.03	0.01	0.01	7.74	0.78	0.02	0.005	0.020
R3d	35.50	1.93	0.05	0.02	0.03	8.28	0.54	0.04	0.003	0.036
R4s	30.80	1.52	0.04	0.03	0.02	12.40	0.96	0.03	0.005	0.025
R5s	43.60	1.93	0.06	0.03	0.03	4.79	0.40	0.05	0.012	0.039
R6s	31.30	1.23	0.04	0.03	0.01	7.10	0.59	0.02	0.006	0.017
R7s	33.00	1.11	0.07	0.03	0.03	15.6	1.34	0.08	0.003	0.080
R8s	35.80	1.32	0.05	0.03	0.03	4.25	0.45	0.03	0.004	0.026
Average	36.05	1.44	0.06	0.03	0.03	8.13	0.60	0.05	0.01	0.04
Std Dev	4.42	0.33	0.02	0.01	0.01	3.72	0.31	0.03	0.01	0.03

*Bulk soil TP values were obtained through aqua-regia, whereas the fractionated soils data was obtained through ignition-extraction.

Table 3.2 (continued)

Sample ID	Bulk soil				
	C	N	TP*	IP	OP
B1d	4.52	0.36	0.07	0.02	0.05
B1s	14.20	0.89	0.09	0.02	0.07
B2s	4.51	0.32	0.05	0.01	0.04
C1s	12.00	0.72	0.11	0.02	0.09
C2s	8.16	0.45	0.05	0.00	0.04
H1s	10.00	0.36	0.02	0.00	0.02
H2s	11.60	0.50	0.03	0.00	0.02
H3s	15.60	1.01	0.10	0.04	0.05
H4d	11.30	0.32	0.01	0.00	0.01
IG1s	6.34	0.70	0.20	0.08	0.12
IG2s	13.80	1.03	0.16	0.03	0.13
IG3s	7.82	0.47	0.08	0.01	0.07
R1s	10.40	1.03	0.16	0.01	0.15
R2s	10.90	0.95	0.13	0.01	0.12
R3d	17.40	0.84	0.06	0.01	0.06
R4s	15.50	1.14	0.07	0.01	0.06
R5s	9.20	0.60	0.09	0.01	0.08
R6s	10.30	0.67	0.07	0.02	0.05
R7s	18.30	1.53	0.16	0.01	0.15
R8s	5.80	0.54	0.09	0.01	0.08
Average	10.88	0.72	0.09	0.02	0.07
Std Dev	4.05	0.33	0.05	0.02	0.04

*Bulk soil TP values were obtained through aqua-regia, whereas the fractionated soils data was obtained through ignition-extraction

Table 3.3: Masses and recoveries of soil, C, N and TP for the bulk soil, light and heavy fractions. Mass is presented in grams. Recovery of the soil, C N, TP and corrected TP is presented in %. Shallow (s) and deep (d) are for depths of 0-15 cm and 15-40 cm respectively.

Sample ID	Bulk soil						Light fraction						Heavy fraction					
	Soil	C	N	TP	IP	OP	Soil	C	N	TP	IP	OP	Soil	C	N	TP	IP	OP
B1d	25.17	1.14	0.09	0.02	0.006	0.01	0.47	0.16	0.01	0.000	0.0001	0.0001	23.76	1.00	0.08	0.02	0.0059	0.014
B1s	25.03	3.55	0.22	0.02	0.005	0.02	4.64	1.80	0.08	0.003	0.0019	0.0007	18.88	1.72	0.14	0.02	0.0038	0.02
B2s	25.01	1.13	0.08	0.01	0.002	0.01	0.45	0.16	0.01	0.000	0.0001	0.0002	23.73	0.75	0.07	0.01	0.0013	0.005
C1s	25.00	3.00	0.18	0.03	0.005	0.02	2.88	0.10	0.05	0.003	0.0016	0.0014	23.35	2.06	0.15	0.01	0.0031	0.008
C2s	25.07	2.05	0.11	0.01	0.001	0.01	2.30	0.77	0.03	0.002	0.0010	0.0007	21.78	1.50	0.10	0.01	0.0005	0.005
H1s	25.06	2.51	0.09	0.01	0.001	0.005	4.53	1.85	0.05	0.005	0.0024	0.0029	18.29	0.96	0.04	0.002	0.0003	0.001
H2s	25.22	2.93	0.13	0.01	0.001	0.01	2.26	0.86	0.03	0.001	0.0007	0.0004	22.10	2.09	0.10	0.004	0.0011	0.003
H3s	25.09	3.91	0.25	0.02	0.01	0.01	0.77	0.30	0.02	0.000	0.0002	0.0002	22.64	3.55	0.23	0.01	0.0036	0.01
H4d	25.04	2.83	0.08	0.003	0.001	0.002	2.79	1.02	0.05	0.002	0.0011	0.0006	20.66	0.89	0.04	0.001	0.0001	0.001
IG1s	25.03	1.59	0.18	0.05	0.002	0.03	0.42	0.14	0.01	0.000	0.0001	0.0002	23.71	1.87	0.13	0.02	0.0086	0.01
IG2s	25.11	3.47	0.26	0.04	0.008	0.03	1.04	0.47	0.01	0.000	0.0002	0.0004	21.91	2.94	0.23	0.02	0.0121	0.01
IG3s	25.11	1.96	0.12	0.02	0.002	0.02	0.60	0.24	0.01	0.000	0.0001	0.0002	23.53	1.24	0.08	0.01	0.0033	0.007
R1s	25.09	2.61	0.26	0.04	0.004	0.04	1.51	0.40	0.02	0.001	0.0003	0.0008	22.83	2.07	0.16	0.01	0.0007	0.01
R2s	25.70	2.80	0.24	0.03	0.002	0.03	0.60	0.20	0.01	0.000	0.0001	0.0001	25.17	1.95	0.20	0.01	0.0010	0.005
R3d	25.03	4.36	0.21	0.02	0.002	0.01	5.12	1.82	0.01	0.002	0.0008	0.0015	18.81	1.56	0.10	0.01	0.0006	0.007
R4s	25.11	3.89	0.29	0.02	0.001	0.02	2.03	0.62	0.03	0.001	0.0006	0.0003	23.59	2.93	0.23	0.01	0.0012	0.006
R5s	50.02	4.60	0.30	0.05	0.007	0.04	1.12	0.49	0.02	0.001	0.0003	0.0003	48.02	2.30	0.19	0.02	0.0055	0.002
R6s	25.08	2.58	0.17	0.02	0.004	0.01	0.86	0.27	0.01	0.000	0.0003	0.0001	24.61	1.75	0.15	0.01	0.0016	0.004
R7s	25.06	4.59	0.38	0.04	0.002	0.04	1.89	0.63	0.02	0.001	0.0006	0.0006	20.62	3.22	0.28	0.02	0.0005	0.02
R8s	26.39	1.53	0.14	0.02	0.002	0.02	0.37	0.13	0.01	0.000	0.0001	0.0001	25.07	1.07	0.11	0.01	0.0010	0.007
Average	26.42	2.85	0.19	0.02	0.004	0.02	1.83	0.67	0.03	0.001	0.0006	0.0006	32.65	1.87	0.14	0.01	0.0028	0.009
Std Dev	5.56	1.09	0.09	0.01	0.005	0.01	1.50	0.57	0.03	0.001	0.0007	0.0007	6.08	0.81	0.07	0.01	0.0031	0.006

Table 3.3: continued

Sample ID	Recovery					
	soil	C	N	TP	IP	OP
B1d	96	102	95	116	109	120
B1s	94	99	102	122	116	124
B2s	97	81	94	56	81	51
C1s	105	102	107	50	94	41
C2s	96	111	110	59	237	49
H1s	91	112	102	131	486	90
H2s	97	101	102	80	220	60
H3s	93	98	95	65	34	90
H4d	94	68	104	78	110	63
IG1s	96	127	76	41	44	38
IG2s	91	98	96	61	144	39
IG3s	96	75	78	54	162	41
R1s	97	95	70	35	28	35
R2s	100	77	83	19	45	17
R3d	96	78	95	61	78	59
R4s	102	91	90	45	124	38
R5s	98	61	71	55	85	48
R6s	102	78	93	36	46	33
R7s	90	84	78	46	48	46
R8s	96	78	83	34	48	32
Average	96	91	91	62	117	56
Std Dev	4	17	12	30	105	29

Table 3.4. Distribution of the soil mass, C, N, oP, TP and IP measured across the light fraction and heavy fraction, measured by %.

Sample ID	Light fraction						Heavy fraction					
	Soil mass	C	N	OP	TP	IP	Soil mass	C	N	OP	TP	IP
B1d	2	14	6	1	1	2	98	86	94	99	99	98
B1s	20	51	37	3	10	33	80	49	63	97	90	67
B2s	2	18	11	3	5	5	98	82	89	97	95	95
C1s	11	33	23	15	22	34	89	67	77	85	78	66
C2s	10	34	21	13	25	67	90	66	79	87	75	33
H1s	20	66	56	67	75	88	80	34	44	33	25	12
H2s	9	29	21	12	21	38	91	71	79	88	79	62
H3s	3	8	6	1	2	5	97	92	94	99	98	95
H4d	12	53	58	46	68	94	88	47	42	54	32	6
IG1s	2	7	4	1	2	2	98	93	96	99	98	98
IG2s	5	14	5	3	2	2	95	86	95	97	98	98
IG3s	2	16	10	2	3	3	98	84	90	98	97	97
R1s	6	16	10	6	7	26	94	84	90	94	93	74
R2s	2	9	3	2	3	7	98	91	97	98	97	93
R3d	21	54	49	19	24	56	79	46	51	81	76	44
R4s	8	18	12	5	11	32	92	82	88	95	89	68
R5s	2	18	10	2	3	6	98	82	90	98	97	94
R6s	3	13	7	2	5	14	97	87	93	98	95	86
R7s	8	16	7	4	7	56	92	84	93	96	93	44
R8s	1	11	4	1	2	8	99	89	96	99	98	92
Average	8	25	18	10	15	29	92	75	82	90	85	71
Std Dev	6	18	18	17	21	29	6	18	18	17	21	29

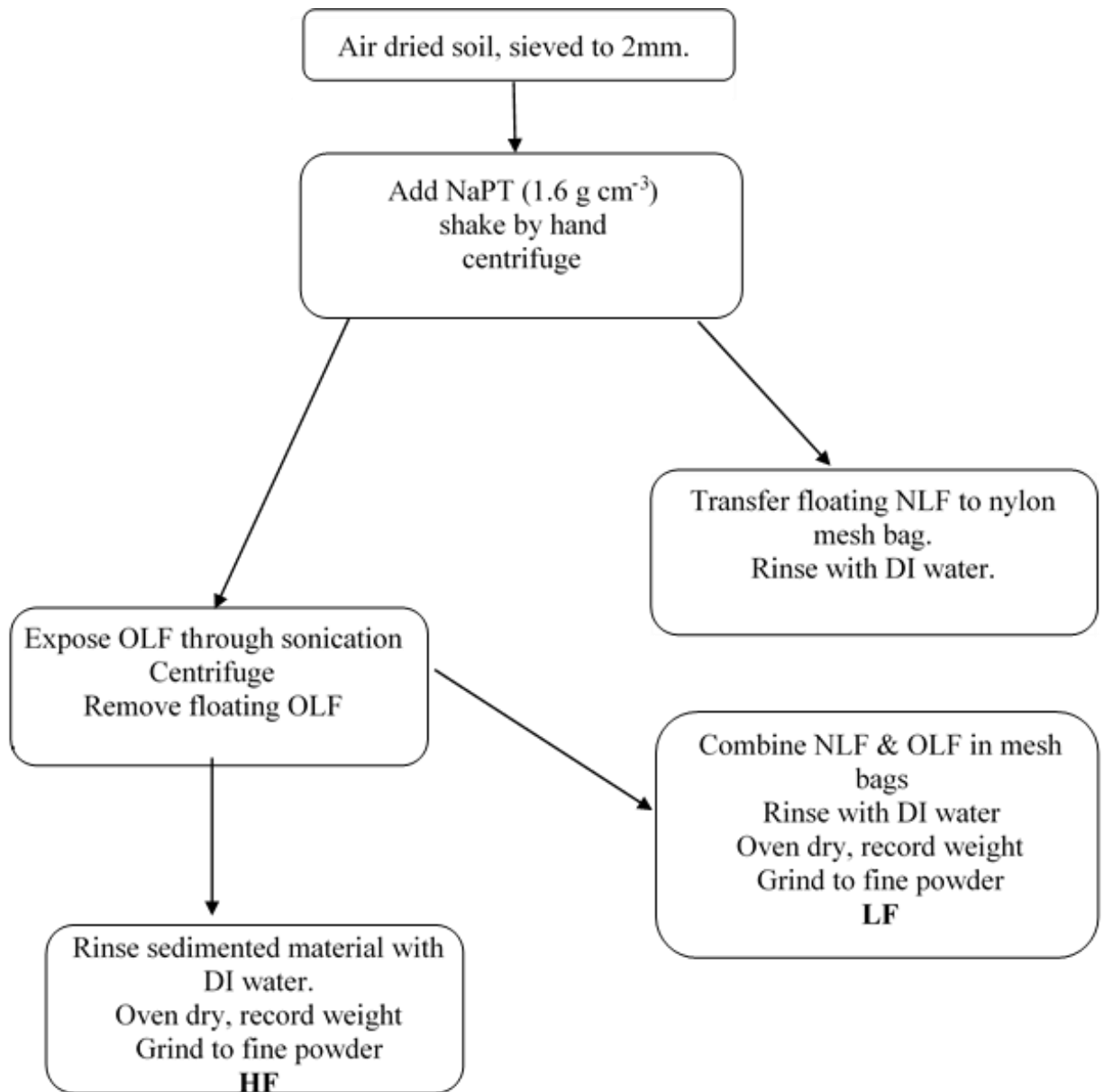


Figure 3.1 Schematic of the fractionation procedure. Abbreviations are as follows:

NaPT = sodium polytungstate, OLF = occluded light fraction, LF = light fraction,

HF = heavy fraction.

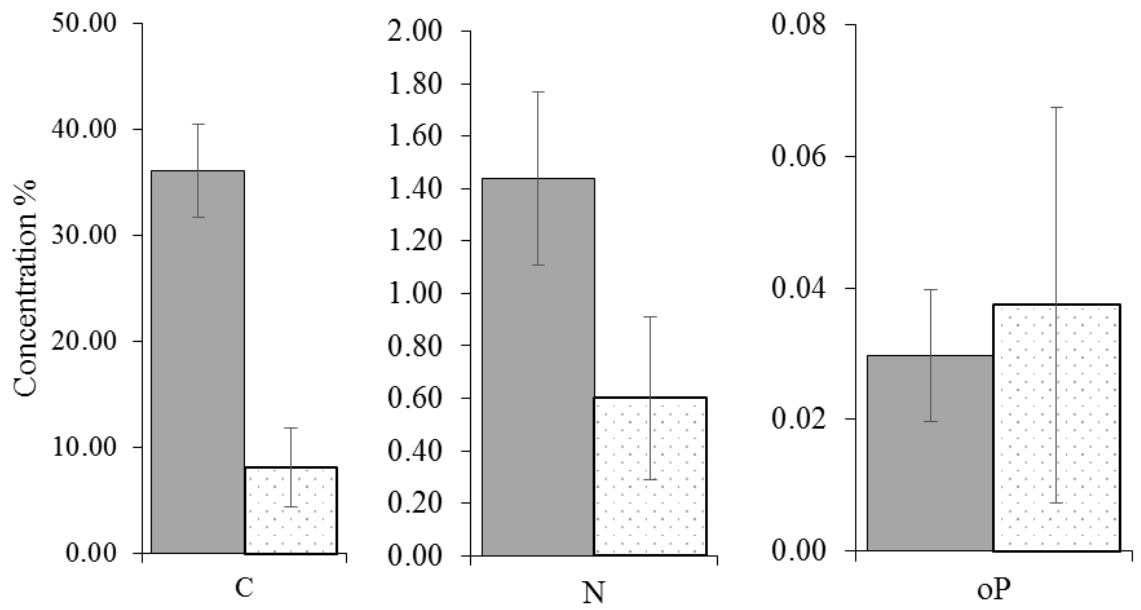


Figure 3.2: Average concentrations of the elements C, N, and oP, for the light and heavy fractions. The light fractionation is shown by the grey block and the heavy fraction by the dotted block. Standard deviations are shown by the error bars. Concentrations are shown in %.

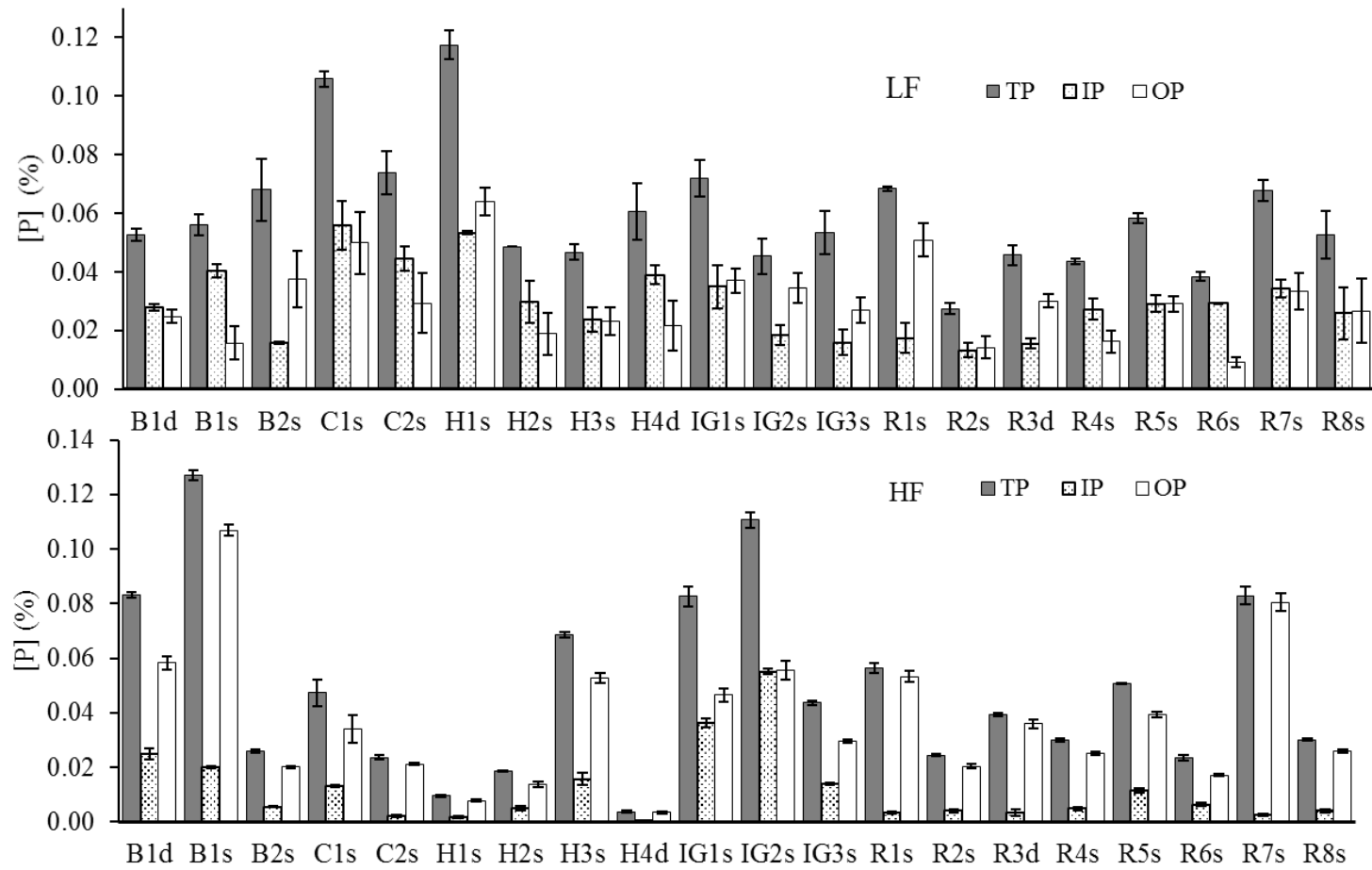


Figure 3.3. Concentrations of total P (TP), inorganic P (IP) and organic P (oP) for the light fraction (upper panel) and the heavy fraction (lower panel). Standard errors are shown by the error bars.

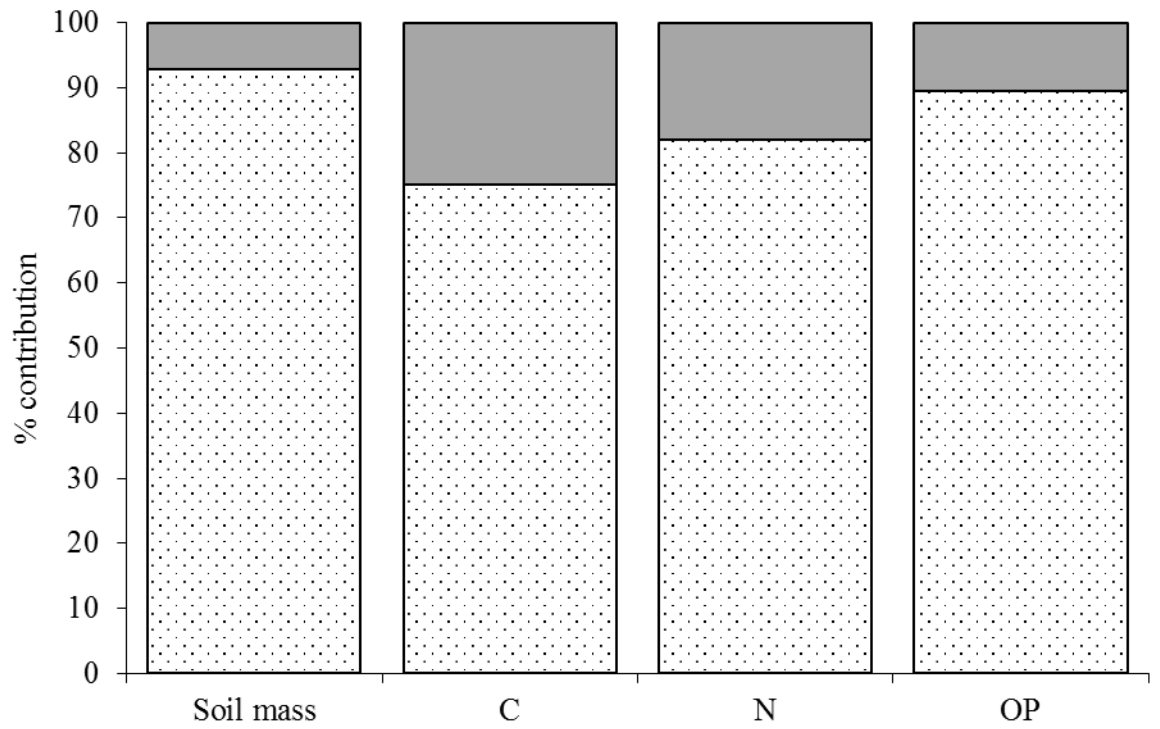


Figure 3.4: Soil mass and element distributions between the light and heavy fractions. The light fractionation is shown by the grey block and the heavy fraction by the dotted block.

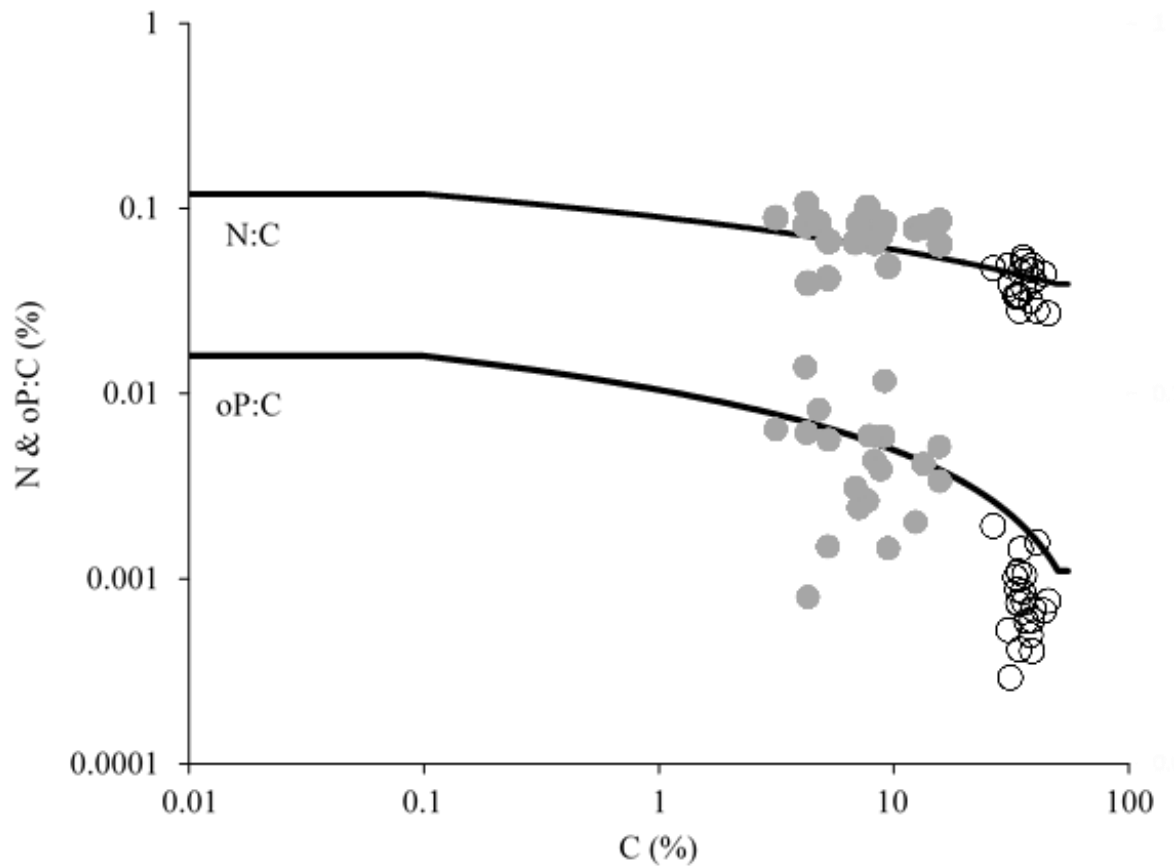


Figure 3.5: The N:C (upper plot) and oP:C (lower plot) against C for the light and heavy fractions. The black line shows the modelled values for the entire bulk dataset of the UK soil survey. Light fractions are shown by the hollow circles. Heavy fractions are shown by the grey circles.

4. Aged riverine particulate organic carbon in four UK catchments

JL Adams, E Tipping, CL. Bryant, RC. Helliwell, H Toberman, JN Quinton

Abstract

The riverine transport of particulate organic matter (POM) is a significant flux in the carbon cycle, and affects macronutrients and contaminants. We used radiocarbon to characterise POM in 9 rivers of four UK catchments (Avon, Conwy, Dee, Ribble) over a one-year period. High-discharge samples were collected on three or four occasions at each site. Suspended particulate matter (SPM) was obtained by centrifugation, and the samples were analysed for carbon isotopes. Concentrations of SPM and SPM organic carbon (OC) contents were also determined, and were found to have a significant negative correlation. For the 7 rivers draining predominantly rural catchments, PO^{14}C values, expressed as percent modern carbon absolute (pMC), varied little among samplings at each site, and there was no significant difference in the average values among the sites. The overall average PO^{14}C value for all 7 sites of 91.2 pMC corresponded to an average age of 680 ^{14}C years, but this value arises from the mixing of differently-aged components, and therefore significant amounts of organic matter older than the average value are present in the samples. Although topsoil erosion is probably the major source of the riverine POM, the average PO^{14}C value is appreciably lower than topsoil values (which are typically 100 pMC). This is most likely explained by inputs of older subsoil OC from bank erosion, or the preferential loss of high- ^{14}C topsoil organic matter by mineralisation during riverine transport. The significantly lower average PO^{14}C of samples from the River Calder (76.6 pMC),

can be ascribed to components containing little or no radiocarbon, derived either from industrial sources or historical coal mining, and this effect is also seen in the River Ribble, downstream of its confluence with the Calder. At the global scale, the results significantly expand available information for PO^{14}C in rivers draining catchments with low erosion rates.

Keywords: Particulate organic carbon, Radiocarbon, Rivers, Soils

4.1 Introduction

Particulate organic matter (POM) transported by rivers is defined as organic matter that does not pass a filter with sub-micron pore size, and mainly comprises allochthonous inputs from plant litter, soils and wastes, autochthonous phytoplankton and macrophyte debris, and in situ production from dissolved organic matter (Ittekkot and Laane, 1991). It plays a significant role in the carbon cycle, being a loss from the terrestrial environment, a source of C to the atmosphere due to decomposition during transit, and ultimately a gain to the marine environment (Raymond and Bauer, 2001; Rosenheim and Galy, 2012; Worrall, Burt and Howden, 2014). Particulate organic carbon (POC) accounts for approximately 50% of the riverine global organic carbon export of 0.4 Pg a^{-1} (Schlünz and Schneider, 2000; Aufdenkampe et al., 2011). Particulate organic matter also governs the transport of the macronutrients nitrogen and phosphorus (Meybeck, 1982; Walling, 2005), metals (Tipping et al., 1997) and organic contaminants (Foster et al., 2000). To understand and quantify these POM-associated processes, and thereby predict how they might respond to changes in land use, climate and other environmental drivers, we need to delineate the sources of POM in different systems.

Because POM is part of suspended particulate matter (SPM), information about sources can be obtained from more general investigations into SPM, which is known to comprise a mixture of terrestrial material derived from both surface and sub-surface materials including bedrock and mineral soil (Blair et al., 2003). The SPM entering the river systems is generally the result of physical weathering and physical disturbance through anthropogenic activity. Sediment sourcing techniques, including mineralogy (Klages and Hsieh 1975), chemistry (Gaillardet, Dupré and Allègre, 1999), magnetism (Gruszowski et al., 2003) and radionuclides (Estrany et al. 2010; Lu et al. 2014; Rosenheim and Galy 2012) identify sources of SPM as being primarily topsoil and sub-surface material including erosion of exposed banks. Walling (2013) summarized sediment source information on 84 UK rivers, and showed that on average topsoil was the largest contributor of SPM, with relative contributions from surface material and channel banks contributing between 50% to 99% and <50% respectively.

The organic matter components of SPM have been studied by a variety of analytical techniques and with stable isotopes and element ratios (da Cunha et al. 2000; Onstad et al. 2000; Kendall et al. 2001; Higuera et al. 2014), to obtain information on molecular structure and insight into the materials from which the POM is derived. Determination of the radiocarbon content of POM provides further information, not only on sources but also apparent age. Radiocarbon gives a measure of the time elapsed since C fixation into plants from the atmosphere, providing an understanding of the residence time of plant-derived C and losses of C through mechanisms including leaching and erosion (Trumbore, 2009). Naturally occurring atmospheric ^{14}C can be used for the measure of C turnover on the centennial and millennial timescale due to the natural radioactive decay

process, while “bomb carbon” originating from atmospheric weapons testing in the mid-20th century, which almost doubled the atmospheric ¹⁴C levels (Hua, Barbetti and Rakowski, 2013), provides information on decadal timescales. Radiocarbon has been used in studies of POM in rivers in North and South America (Raymond and Bauer 2001; Bouchez et al. 2014), Asia (Hilton et al., 2008; Rosenheim and Galy, 2012), Europe (Megens et al., 2001; Cathalot et al., 2013), and Africa (Marwick et al., 2015). Global PO¹⁴C (particulate organic radiocarbon) data documented by Marwick et al. (2015) shows that SPM in highly-eroding catchments is depleted in PO¹⁴C and low in OC (organic carbon).

The review of Marwick et al. (2015) shows that to date while there are many PO¹⁴C data for catchments with high sediment loads, there are relatively few for riverine PO¹⁴C in temperate, low-erosion European catchments and no known data for catchments of this kind in the UK. In the wider context, UK data may be of interest because UK soils tend to be rich in carbon, which may lead to differences from global averages. Therefore, understanding UK sources should improve our ability to model the terrestrial-freshwater C cycle, and its role in transferring carbon to the atmosphere and ocean. To this end, we aimed to determine the time elapsed between terrestrial fixation of C and entry into the watercourse, from four differing UK catchments. In doing so, we carried out a programme of sampling and analysis to determine the radiocarbon contents of the POM. Since SPM concentrations, and therefore POM transport, are elevated at high flow, we focused our sample collection on high-discharge events. To interpret the results, we made use of the extensive soil radiocarbon data available for the UK.

4.2 Methods

4.2.1 Field sites

Table 4.1 provides information on the individual rivers and their catchments, and their locations are shown in Figure 4.1. Data on discharge and rainfall were taken from the National River Flow Archive (NRFA) (<http://www.ceh.ac.uk/data/nrfa/> accessed January 2015) and Met Office (<http://www.metoffice.gov.uk/industry/data/commercial/rainfall> accessed March 2015) respectively. Catchment areas were obtained from the CEH River and Catchment Query and Extraction Layer (Racquel) (<http://wlwater.ceh.ac.uk/racquel/> accessed March 2015). Geological information was provided by the British Geological Society online map (<http://mapapps.bgs.ac.uk/geologyofbritain/home.html>, accessed March 2015). Soil types for England and Wales were obtained using soil maps (scale 1:250 000). For the Dee catchments, soil information was obtained from The James Hutton Institute online soils map (http://sifss.hutton.ac.uk/SSKIB_Stats.php accessed March 2015). Land use data were obtained from the website <http://digimap.edina.ac.uk/> (accessed March 2015).

The Ribble catchment is situated in north-west England and has a population density of 989 persons km⁻². Two major sub catchments, the Rivers Hodder and Calder drain from the north and south of the catchment respectively. Unlike other tributaries of the Ribble, the Calder catchment contains extensive conurbations including Burnley and Blackburn, with a history of industrial and mining activity. The upper parts of the catchment are responsive to rainfall, exhibiting a flashy flow regime.

The River Conwy is one of the major drainage systems in North Wales. The catchment has a population density of 49 persons km⁻². The topography is largely mountainous, giving a high river response during storm events.

Situated in the south of England, the Hampshire Avon catchment has a population density of 108 persons km⁻². The catchment is largely groundwater dominated due to the presence of chalk aquifers. Thus, the system at the tidal limit does not significantly respond during rainfall events.

The River Dee catchment is situated in the north-east of Scotland. The catchment is sparsely populated above the tidal limit, with a population density of 4 persons km⁻². The tributary of the River Gairn is situated in the upper western reaches of the catchment. The upper mountainous areas respond rapidly to rainfall and snowmelt, producing a flashy flow regime.

4.2.2 Sampling and analysis

To minimise risk of carbon contamination, all equipment used during sampling and processing was new or acid-washed and all samples were managed in a radiocarbon tracer-free laboratory. Water samples (5 L) were collected in high-density polyethylene containers from the tidal limit of the four main catchments, and additional upstream samples were taken in the Ribble and Dee catchments (Figure 4.1). For the Ribble, Conwy and Dee sites, samples were collected during high-flow events. For the Avon, which has a much less flashy flow regime, they were taken at regular intervals throughout one year. High flow events were identified from daily river levels measured at gauging stations near the sampling sites, and made available on-line by the Environment Agency of England and Wales and the Scottish Environment Protection Agency. During the period

October 2013 – October 2014, four samples were taken for most of the sites, but only three each at the Gairn and Dee A sites. Additional 500 or 1000 mL samples were collected for the determination of SPM concentration and the carbon content of the SPM.

The SPM was extracted from the water samples through repeated centrifugation (6 × 500 mL rotor spinning at 10000 rpm for 30 minutes), removal of supernatant and pooling, until approximately 100 mL of suspended sediment and water remained. To ensure the absence of inorganic carbonate, the concentrated suspended sediment was acidified by adding 400 mL of 1M HCl to the extracted sediment and left overnight. Samples were then twice rinsed and centrifuged with deionised water, and sub-sampled for radiocarbon analysis. Remaining sediment was frozen for further analysis.

Organic carbon content of the SPM was measured using two different techniques. Firstly a known volume of the additional water sample was filtered through a pre-weighed, pre-combusted (500 °C) Whatman GF/F filter paper. This was dried at 105°C overnight and reweighed to determine [SPM], then analysed for total carbon with a Vario EL elemental analyser at CEH Lancaster (Ribble, Conwy, Avon) and a Thermo Flash 2000 elemental analyser at the James Hutton Institute. The values obtained would include any inorganic carbon present in the samples. Secondly a sub-sample of the concentrated SPM was captured on a pre-weighed and combusted GF/F filter paper, and analysed. Results obtained by the two methods were in good agreement, suggesting that little or no inorganic carbonate had been present in the samples. Reported values are means from the two methods.

Graphite targets for ¹⁴C analysis by AMS were prepared by quantitative recovery of carbon in sealed quartz tubes followed by cryogenic separation of CO₂ (Boutton

et al., 1983). Aliquots of CO₂ were converted to an iron/graphite mix by iron/zinc reduction (Slota et al., 1987). A sub-sample of CO₂ was used to measure δ¹³C using a dual-inlet mass spectrometer with a multiple ion beam collection facility (Thermo Fisher Delta V) in order to correct ¹⁴C data to -25 ‰ δ¹³C_{VPDB}. The mass spectrometer was calibrated with international reference materials to a precision of ± 0.03 ‰. For five samples, difficulties were encountered in the measurement of ¹³C by mass spectrometry, and so instead values of δ¹³C were obtained during AMS analysis, and used to correct to δ¹³C = -25 ‰ vPDB. In these cases the δ¹³C values were not considered representative of the original combusted material.

In all but three cases ¹⁴C analysis was carried out at the Scottish Universities Environmental Research Centre AMS Laboratory, East Kilbride (Xu et al. 2004); these have publication codes starting SUERC. The other three measurements were on sample sizes of less than 500 µg carbon and were made at the Keck Carbon Cycle AMS Laboratory at the University of California Irvine (publication codes UCIAMS). Size matched process background materials and known age standards were prepared and analysed to check accuracy and precision. In keeping with international practice, the results are reported as absolute % modern (pMC) which involves a mathematical adjustment to account for ongoing radioactive decay of the international reference standard (oxalic acid, provided by the US National Bureau of Standards), since AD 1950 (Stuiver and Polach. 1997) with conventional radiocarbon ages (based on radioactive decay and relative to AD1950) provided where results are below 100 pMC. The ¹⁴C enrichment of a sample is measured as a percentage (or fraction) of the ¹⁴C activity relative to the modern standard of oxalic acid where 100% modern is defined as the value in AD 1950, in the absence of any anthropogenic influences. Radiocarbon contents can exceed 100 pMC if

they contain sufficient “bomb carbon”. Overall analytical precision is quoted at 1σ . Statistical analyses (t-tests, linear and power law regressions) were carried out using Microsoft Excel. Data were tested for normality and t-tests were first checked for equal or unequal variances. If data was not normally distributed, they were first log transformed.

4.2.3. Soil radiocarbon data

To aid the interpretation of the PO^{14}C data, we assembled soil radiocarbon data for UK sites under different land use. These comprised 70 data points for agricultural soils from Jenkinson et al. (2008), 132 values for semi-natural non-forested and forested soils from Mills et al. (2013), and 87 of our own unpublished data (H Toberman, JL Adams, E Tipping, CL Bryant) for semi-natural sites and improved grassland. The results are summarised in Appendix 5.1. We used values of ^{14}C (pMC) for samples taken over the time-period 1999 to 2013. Average values were calculated to simplify data presentation and provide an overall picture of radiocarbon with depth. Because ^{14}C is constantly changing, albeit slowly, the combination of data taken in different years involves approximation, but the time period for which data were taken was short in comparison to the turnover rate of bulk soil carbon as estimated by Mills et al. (2013). Therefore, the averages obtained will differ little from those that would apply had all the sampling been simultaneous.

4.3 Results

At a UK level, the study catchments vary with respect to size, altitude range, climate, soil type, and land use (Table 4.1). The Calder catchment stands out as the only one with a substantial urban area, and it is also industrialised. The Avon

catchment differs in that it lacks upland area and has more cultivated land. Furthermore, the River Avon discharge varies relatively little, owing to the dominant influence of groundwater. The other rivers display much more flashy flow regimes. In the Avon, Conwy and Ribble catchments, the main land use is livestock grazing, mainly on improved grassland in the Avon and Ribble, but mainly on unimproved grassland or heather moorland in the Conwy. Much of the Dee catchment is heather moorland and blanket bog, with significant but smaller areas of coniferous plantation woodland and improved grassland. None of the catchments contains extensive arable agriculture. In all cases, the dominant soil types have organic-rich surface horizons.

High flow water samples collected across the catchments varied considerably in average [SPM] and OC content (Table 4.2). The OC content (%) declines with increasing [SPM], the relationship following the power law, $OC(\%) = 26.7 [SPM]^{-0.22}$, which accounts for 75 % of the variance in OC content ($p < 0.005$). This is consistent with global-scale data collated by Marwick et al. (2015), and means that under conditions of high sediment delivery the SPM is relatively poor in OC.

The $\delta^{13}C$ values of the samples (Table 4.3) fall in the range -30 to -25 ‰, with all but one value < -27 ‰. These indicate that the carbon is derived almost exclusively from plants using the C_3 photosynthetic pathway, which is normal for northern temperate ecosystems like the UK (Still et al., 2003). The ^{14}C contents of the samples fell in the range 69-100 pMC, corresponding to conventional ^{14}C ages of 3000 years to modern (Table 4.3). The overall mean is 909 ^{14}C years with a standard deviation (SD) of 555 years. Comparison of the mean ^{14}C values for the individual rivers (Figure 4.2) shows that the only two rivers differing significantly from the others were the River Calder ($p < 0.01$) and Ribble B site ($p < 0.001$).

The markedly low ^{14}C for the Calder is probably related to its urban and industrial character, and the contribution of the Calder flow to that of the Ribble B is likely the reason for the moderately low PO^{14}C of the latter site. If the PO^{14}C data for the Calder and Ribble B are ignored, the overall average PO^{14}C value is 91.2 pMC (SD 3.0), and the average age of POC becomes 681 ^{14}C years (SD 246 years), which can be taken as a representative value for predominantly rural rivers.

To put the results into context, the radiocarbon content of catchment soils must be considered. A systematic survey of soil radiocarbon in proportion to land use or soil type is not available for each catchment, but a substantial body of radiocarbon data (Appendix 4.1) can be used to summarise land-use and depth variations for the UK (Figure 4.3). The results show that the highest ^{14}C contents are found for topsoils under forest, then for soils under non-forest semi-natural vegetation, then under agricultural land use. Sub-soil ^{14}C shows a fairly regular pattern of decline with depth (Figure 4.3). The average riverine PO^{14}C of 91.2 pMC is lower than the average soil organic ^{14}C values for forest and non-forest semi-natural topsoils, but only slightly less than the improved grassland average of 93.6 pMC, calculated from the two topsoil depths of 7 and 11 cm in Figure 4.3; note that none of our catchments included significant areas of arable soil.

Secondly, our results can be compared with a global dataset published by Marwick et al. (2015) (Figure 4.4). These authors identified [SPM] and the OC content (%) of SPM as useful variables against which to compare the ^{14}C values. In the global context, the UK [SPM] values are comparably low and the OC contents are comparatively high. The PO^{14}C values are high compared with data for high-SPM, low-OC systems, but lower than the previously reported data for the low-SPM, high-OC range.

4.4 Discussion

In attempting to interpret the PO¹⁴C data reported here, it must be borne in mind that all the measured values arise from the mixing of organic matter from different sources, and that any calculated ages are only apparent. Therefore, the mean of 680 ¹⁴C years must mean that both younger and older material is also present. An especially clear effect of mixing is seen within the present data, for the River Calder sub-catchment and Ribble B site (Table 4.3, Figure 4.2). The Calder PO¹⁴C values (68 – 82 pMC) are lower than at any of the other sites due to industrial and/or mining activity in the catchment; for example coal (¹⁴C ~ 0) may be present in the samples. Mixing of River Calder water with water from the other two Ribble tributaries (Figure 4.1) then leads to relatively low PO¹⁴C (84 – 89 pMC) in the samples from the Ribble B site.

For the 7 rivers other than the Calder and Ribble B, the average value of PO¹⁴C (91.2 pMC) could arise from the mixing of topsoil material with material from subsoils, exposed at the bank or via field drains (Chapman et al. 2001; Deasy et al. 2009). For example, if we assume that average subsoil has a ¹⁴C value of 75 pMC (from Figure 4.3, the value at a depth of about 50 cm), and adopt a mid-range value of 100 pMC for the topsoil (Figure 4.3), then the value of 91.2 pMC would arise from a mixture comprising 65% topsoil OC and 35% subsoil OC. But if a topsoil value of 95 pMC were chosen, which might arise if soil under improved grassland were the main source of riverine POM (Figure 4.3), the mixture would be 81% topsoil OC and 19 % subsoil OC. These results bracket the average contributions to riverine SPM of topsoil and subsoil (73%: 27%) obtained by Walling (2013)

from a collation of data for 84 UK rivers. However, the analysis is complicated by the fact that the OC content of soil decreases with depth, so that typically for UK soils, the subsoil OC concentration is only about one-fifth of the topsoil (Appendix 4.2). This would mean that to achieve the required amount of bulk subsoil OC to account for the PO^{14}C values, the SPM fractions would have to be weighted towards the subsoil, which would not agree with Walling's results. A possible explanation is that soil components that are rich in organic matter are preferentially mobilised from the subsoil.

Another process that might explain why the riverine PO^{14}C is depleted relative to topsoil (i.e. the average value of 91.2 pMC in the 7 rural catchments) is preferential mineralisation within the river channel of radiocarbon-rich topsoil organic matter (Marwick et al., 2015). This could arise because topsoil contains organic matter pools with different turnover rates, and therefore with different ^{14}C contents. On this basis, Mills et al. (2013) used a steady-state model with two main organic carbon pools having mean residence times of 20 and 1000 years to interpret observed topsoil ^{14}C data, and estimated that the pools were present in roughly equal proportions. At the present time, the faster turnover pool has a ^{14}C content greater than 100 pMC because of the presence of "bomb carbon", while the long-lived pool typically has a ^{14}C content of about 90 pMC. Furthermore, the topsoil contains plant litter deposited within the last few years, with a ^{14}C content slightly greater than 100 pMC. Both the litter and the 20-year major soil pool are mineralised in the terrestrial environment much faster than the 1000-year pool, and this difference would also be expected during riverine transport and temporary storage in the river bed. Loss of the more labile carbon would then reduce the PO^{14}C value compared to that of topsoil. From regression analysis of UK-wide

river data, Worrall et al. (2014) estimated that about 25% of POC is lost to the atmosphere as CO₂ during riverine transport. If so, then a substantial reduction in the radiocarbon content of riverine POC could occur during transit. However, comparisons of sediment storage and annual flux suggest that residence times of SPM in UK rivers with catchment areas comparable to those of the present study are short, rarely more than a year (Owens, Walling and Leeks, 1999; Collins and Walling, 2007) and so to achieve the 25 % mineralisation loss suggested by Worrall et al. (2014), rates of decomposition of POC in rivers would need to be appreciably higher than is generally accepted for their turnover in the soil. Dispersion of the material and exposure to light during riverine transport might accelerate the mineralisation process.

A possible explanatory factor with respect to our results is the effect of parent geology, the importance of which was highlighted by Longworth et al. (2007) to interpret PO¹⁴C results for rivers draining small rural catchments in the Hudson-Mohawk watershed in upper New York State. Like our catchments, this is a low-erosion system as evidenced by the 5-year average (2004-2008) [SPM] of 22 mg L⁻¹ for the Mohawk River at Cohoes (<http://waterdata.usgs.gov/nwis> accessed April 2015). Longworth et al. (2007) did not report [SPM] and OC content of SPM, and so their results are absent from the plotted values of Marwick et al. (2015) in Figure 4.4. Generally, their PO¹⁴C values are higher than ours, falling in the range 89 to 109 pMC, but mostly they exceed 100 pMC. They explained the geographical distribution of their data, i.e. spatial variations in PO¹⁴C values, in terms of contributions to POM from the physical weathering of shale (containing organic matter low in ¹⁴C). However, this is an unlikely explanation for the relatively depleted PO¹⁴C reported in the present work, because the 7 rivers that

provide the average of 91.2 pMC are in catchments free of rock types containing ancient organic matter (Table 4.1). Therefore it seems unlikely that the presence of ancient carbon sources provides a general explanation for depleted PO¹⁴C in low-erosion catchments.

The present results fit with and extend the data compiled by Marwick et al. (2015). The plots in Figure 4.4 show that the global data fall into two zones. One occurs at high [SPM] and low OC content, for which very low ¹⁴C values are observed, and the data encompass highly eroding, unstable systems (Smith et al., 2013). As noted by Marwick et al. (2015) this will reflect the strong dilution of topsoil-derived POC with eroded mineral matter low in OC but highly-aged, possibly with near-zero ¹⁴C. This zone occurs for [SPM] greater than about 100 mg L⁻¹ and for OC contents less than about 2%. The other zone is for lower [SPM] and higher OC content and there appears to be no true trend in the PO¹⁴C values with either [SPM] or OC content in this range, especially after the addition of the new data presented here (Figure 4.4). Thus we find a range of PO¹⁴C between about 80 and 110 pMC in the low-SPM, high-OC zone. Based on the present study and the conclusions of Marwick et al. (2015), variations in PO¹⁴C in low-erosion rivers can be attributed to variations in a number of factors. In approximate order of general importance these are (i) topsoil O¹⁴C variations across different land uses, (ii) catchment size and bank erosion, (iii) decomposition of POM during riverine transport, (iv) inputs of organic matter highly depleted in ¹⁴C (from coal, shale or industry) and (v) in-river carbon fixation. Different combinations of these factors between rivers, or in the same rivers at different times, could generate the observed range of PO¹⁴C values. Progress towards the precise attribution of POC sources will require all these factors to be considered when designing field surveys and experiments. The

fractionation of POM, e.g. by density or particle size, may also be a useful tool in characterising the $PO^{14}C$. In the meantime, modelling and forecasting future change in POC fluxes will only be approximate. However, it seems certain that the riverine transport of carbon fixed many centuries ago, arising from both topsoil and subsoil, is contributing appreciably to carbon budgets in the UK and other low-erosion locations, and will continue to do so.

The high degree of consistency among the rivers (Figure 4.2) means that the results presented here are probably representative of pasture and upland catchments of similar size or greater across the UK and represents the first such samples to be recorded. This significantly contributes to our understanding of aquatic carbon cycling and nutrient dynamics, for the UK and globally. Catchments dominated by arable agriculture are missing from this study and should be considered in future research. We would expect that their rivers would have lower $PO^{14}C$, in view of the available data on arable topsoils showing them to be relatively low in ^{14}C (Figure 4.3). The likely lower $PO^{14}C$ values in arable-dominated catchments, together with contributions of POC from catchments with coal mining and industry, will tend to make the average age of POC entering the sea from the whole UK, somewhat greater than the average value of 680 ^{14}C years derived for the rural catchments of the present study.

4.5 Conclusions

- Particulate organic matter transported at high flow by 7 UK rivers draining pastoral rural landscapes had an average ^{14}C content of 91.2 pMC, corresponding to an apparent average age of 681 ^{14}C years. These rivers show no significant difference ($p > 0.05$) in their average ^{14}C values.

- Owing to industrial and mining activity in its catchment, the River Calder's POM was significantly more depleted in ^{14}C (average 76.6 pMC). The Ribble B site, of which the River Calder is a tributary, also showed depleted PO^{14}C as a result of the contribution from the Calder catchment.
- Erosion of topsoil is an obvious major source of riverine POM. The most likely explanations for the relatively low PO^{14}C in the 7 rural rivers compared to topsoil O^{14}C (range 94 – 109 pMC depending upon land-use) are firstly, inputs of older subsoil OC due to bank erosion and secondly, preferential mineralisation of ^{14}C -rich organic matter during riverine transport.
- The present results are probably typical of other UK rivers with similar catchment soils and land uses. We expect that catchments dominated by arable soils would have lower PO^{14}C values because of lower topsoil radiocarbon levels.

4.6. Acknowledgements

The research was funded by the UK Natural Environment Research Council Macronutrient Cycles Programme (LTLS project, Grant No. NE/J011533/1), and the Scottish Government. We are grateful to A Panton (National Oceanography Centre, University of Southampton), EC Rowe (CEH Bangor) and C Somerville for assistance with sampling, P Scholefield (CEH Lancaster) for providing catchment area values, the analytical chemistry teams at CEH Lancaster and the James Hutton Institute (Rural and Environment Science and Analytical Services Division of the Scottish Government) for organic carbon measurements, and K Howarth (Environment Agency, North-West England) for facilitating access to sampling sites in the Ribble catchment. Thanks are

due to the staff at the SUERC AMS Laboratory, East Kilbride for carbon isotope measurements, and to Dr Xiaomei Xu at the Keck Carbon Cycle AMS Laboratory, University of California, Irvine for analysis of three of the samples (Table 4.3).

Table 4.1. Catchment information. Discharge data are from records of between 35 and 50 years up to the present. Geology, soil type and land use are presented in order of importance.

	Calder	Hodder	Ribble A	Ribble B	Conwy	Avon	Gairn	Dee A	Dee B
Catchment drainage area (km ²)	317	258	446	1144	365	1713	146	2039	2080
Altitude range (masl)	50-560	40-480	20-420	15-560	10-1060	4-240	220-1100	30-1220	20-1220
Mean annual rainfall (m)	1.1	1.5	1.2	1.2	2.1	0.8	1.1	0.9	0.8
Mean annual air temperature (°C)	8.9	7.7	8.8	8.6	8.4	9.6	5.1	7.6	7.7
River discharge (m ³ s ⁻¹)									
mean	8.6	8.8	13.5	33.2	18.9	20.2	3.9	47.0	no data
95% exceedance	1.9	1.1	1.1	4.6	1.4	6.2	0.8	8.7	no data
10% exceedance	19.5	22.0	34.4	81.2	45.8	39.0	7.4	94.6	no data
Principal bedrock geology ^a	CM MG	MG SSM L	MG CM SSM	MG CM SSM	SSM SC	Ch SSC	Ig VS	VS Ig	VS Ig N
Principal soil types ^b	CS U A	CS SP BE	Sg CS A	Sg CS A	Pz SHG SG	Rz SG SP	P Gs BE	BE Rz A	BE Rz A
Principal land cover ^c	IG U	B HG IG	IG B HG	IG U B	IG B AG	IG W SU	MH H B	H HG MH	MH H HG

^a Key to geology: Ch chalk, CM coal measures, Ig igneous intrusion, L limestone, MG millstone grit, N Neogene rocks – gravel sand silt and clay, SC sandstone and conglomerate, SSC sand silt and clay, SSM sandstone siltstone mudstone, VS volcanic and sedimentary rock.

^b Key to soil type: A alluvisol, BE brown earth, CS cambic stagnogley, Gs gleysol, P peat, Pz podzol, Rz rendzina, SG stagnogley, SHG stagnohumic gley, SP stagnopodzol, U urban, ^c Key to land cover: AG acid grassland, B bog, H heathland, HG heather grassland, IG improved grassland, MH, montane heathland, SU suburban, U urban, W woodland

Table 4.2. Mean concentrations of SPM and OC contents of SPM. Values in brackets are standard deviations, and reflect both natural variation and the averaging of results obtained by different methods (Section 3.2.2).

River	[SPM] mg L ⁻¹	OC content %
Calder	52.8 (±63.2)	8.8 (±4.7)
Hodder	13.4 (±6.8)	15.0 (±8.0)
Ribble A	13.8 (±7.6)	14.3 (±5.7)
Ribble B	21.3 (±19.0)	16.1 (±10.3)
Conwy	2.7 (±1.0)	24.6 (±10.3)
Avon	8.1 (±5.4)	19.1 (±6.3)
Gairn	0.8 (±0.2)	35.9 (±19.2)
Dee A	0.8 (±0.5)	14.4 (±14.2)
Dee B	0.9 (±0.5)	35.0 (±17.7)

Table 4.3. Isotope data for POM in high-flow samples. Values are given of ^{14}C (pMC), $\delta^{13}\text{C}$ (‰ vPDB) and conventional radiocarbon age (years BP). The errors in ^{14}C are expressed as $\pm 1\sigma$ (pMC) where σ is the overall analytical uncertainty. Bracketed values of $\delta^{13}\text{C}$ are not necessarily representative of the original combusted material (see Section 4.2.2).

River	Date	$\delta^{13}\text{C}$	^{14}C	$\pm 1\sigma$	Age	Publication No.
Calder	4/10/13	-28.2	75.06	0.35	2243	SUERC-52256
	22/10/13	-27.5	68.86	0.30	2935	SUERC-52262
	2/1/14	-28.2	81.80	0.36	1552	SUERC-52267
	7/1/14	-28.5	80.58	0.37	1672	SUERC-52274
Hodder	4/10/13	-28.6	89.89	0.39	794	SUERC-52257
	22/10/13	-28.6	91.09	0.42	687	SUERC-52263
	2/1/14	-28.8	91.25	0.40	673	SUERC-52268
	7/1/14	(-28.6)	89.92	0.39	792	SUERC-52275
Ribble A	4/10/13	-25.2	88.95	0.41	878	SUERC-52258
	22/10/13	-28.6	87.67	0.40	995	SUERC-52264
	2/1/14	-29.1	89.55	0.41	825	SUERC-52272
	7/1/14	-29.3	89.26	0.41	850	SUERC-52276
Ribble B	4/10/13	-28.6	84.68	0.39	1274	SUERC-52261
	22/10/13	-28.6	84.68	0.39	1273	SUERC-52265
	2/1/14	-28.7	88.15	0.41	951	SUERC-52273
	7/1/14	-28.8	84.34	0.39	1306	SUERC-52277
Conwy	7/1/14	-28.5	90.52	0.42	737	SUERC-52278
	27/1/14	(-23.0)	90.09	0.28	775	UCIAMS-144595
	14/2/14	-29.2	97.90	0.49	108	SUERC-53199
	22/10/14	-28.3	100.07	0.47	Modern	SUERC-58254
Avon	22/10/13	-28.2	90.60	0.40	731	SUERC-52266
	6/2/14	(-28.4)	88.78	0.28	895	UCIAMS-144596
	23/4/14	-29.9	92.63	0.48	553	SUERC-54377
	28/8/14	-30.1	92.62	0.41	554	SUERC-57317
Gairn	7/1/14	-28.5	90.58	0.42	732	SUERC-52283
	26/2/14	(-25.9)	90.92	0.31	700	UCIAMS-144597
	16/3/14	-27.0	95.84	0.45	279	SUERC-54379
Dee A	7/1/14	-27.9	93.74	0.41	457	SUERC-52282
	26/2/14	-28.2	89.52	0.45	827	SUERC-53201
	21/3/14	-27.2	88.09	0.46	957	SUERC-54382
Dee B	7/1/14	-27.9	93.04	0.41	517	SUERC-52281
	26/2/14	(-28.6)	88.88	0.45	885	SUERC-53200
	16/3/14	-27.7	88.95	0.44	878	SUERC-54378
	21/3/14	-27.6	91.76	0.44	628	SUERC-54383

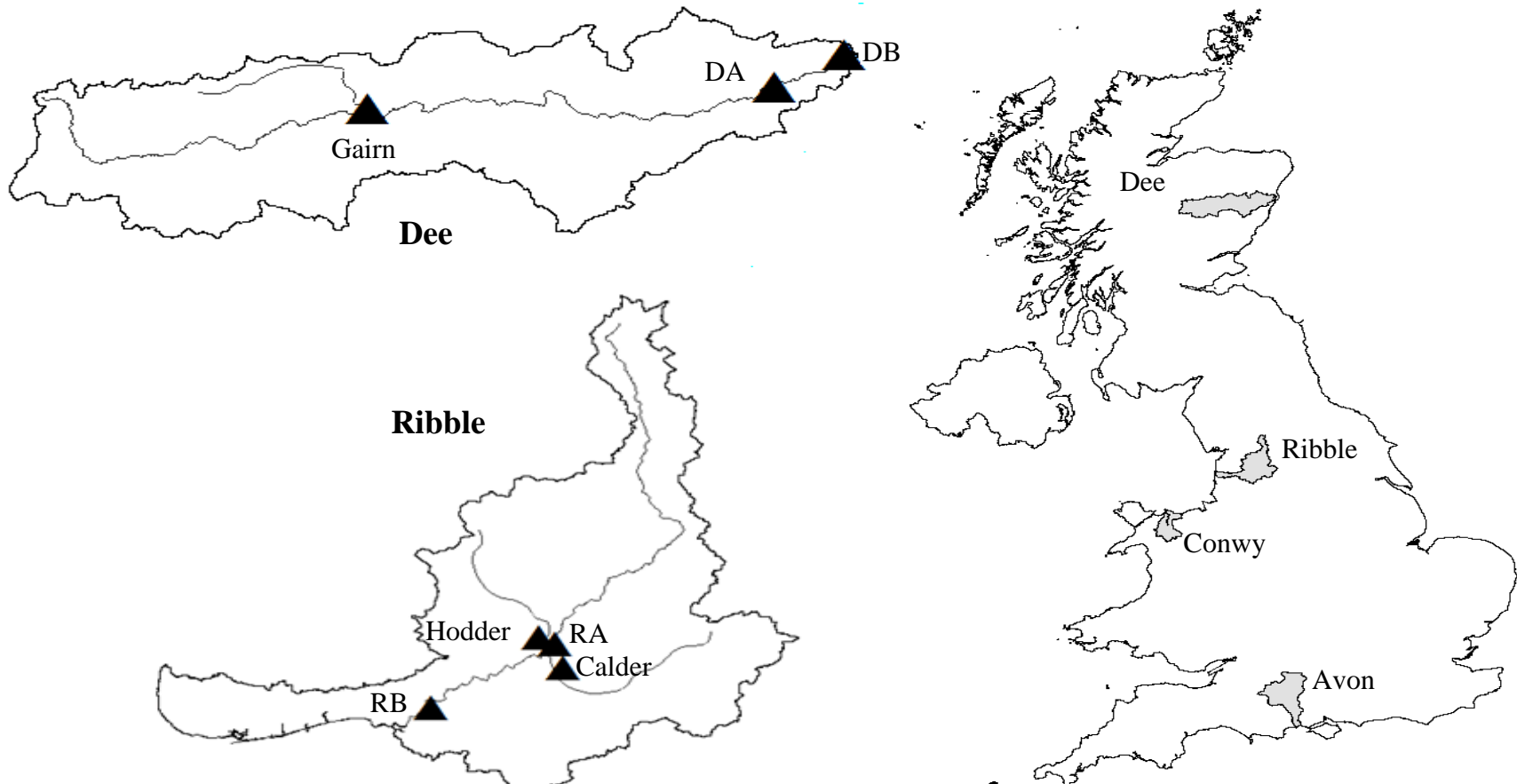


Figure 4.1. Location map showing the study catchments. For the Dee and Ribble, black triangles indicate sampling sites. The Avon and Conwy sampling sites were at the tidal limit.

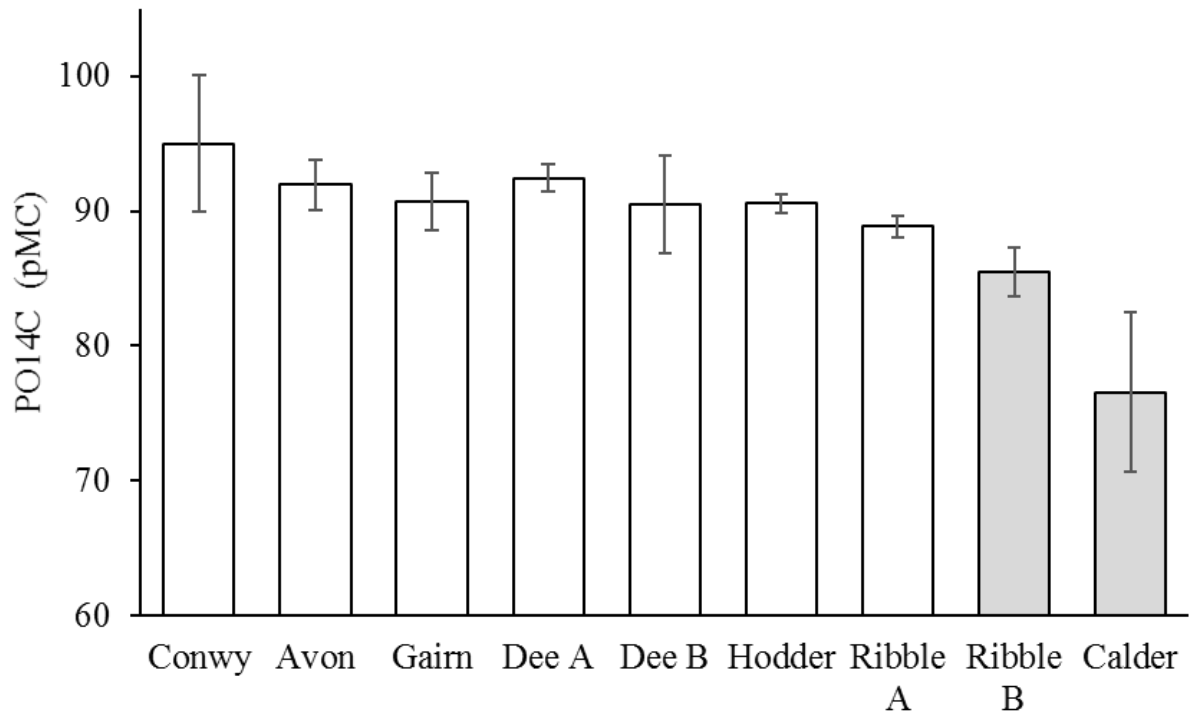


Figure 4.2. Average PO¹⁴C (pMC) for suspended sediment collected at high flow at the 9 sampling sites. Error bars represent standard deviations. Greyed bars show the two sites for which the PO¹⁴C values differ significantly from the others.

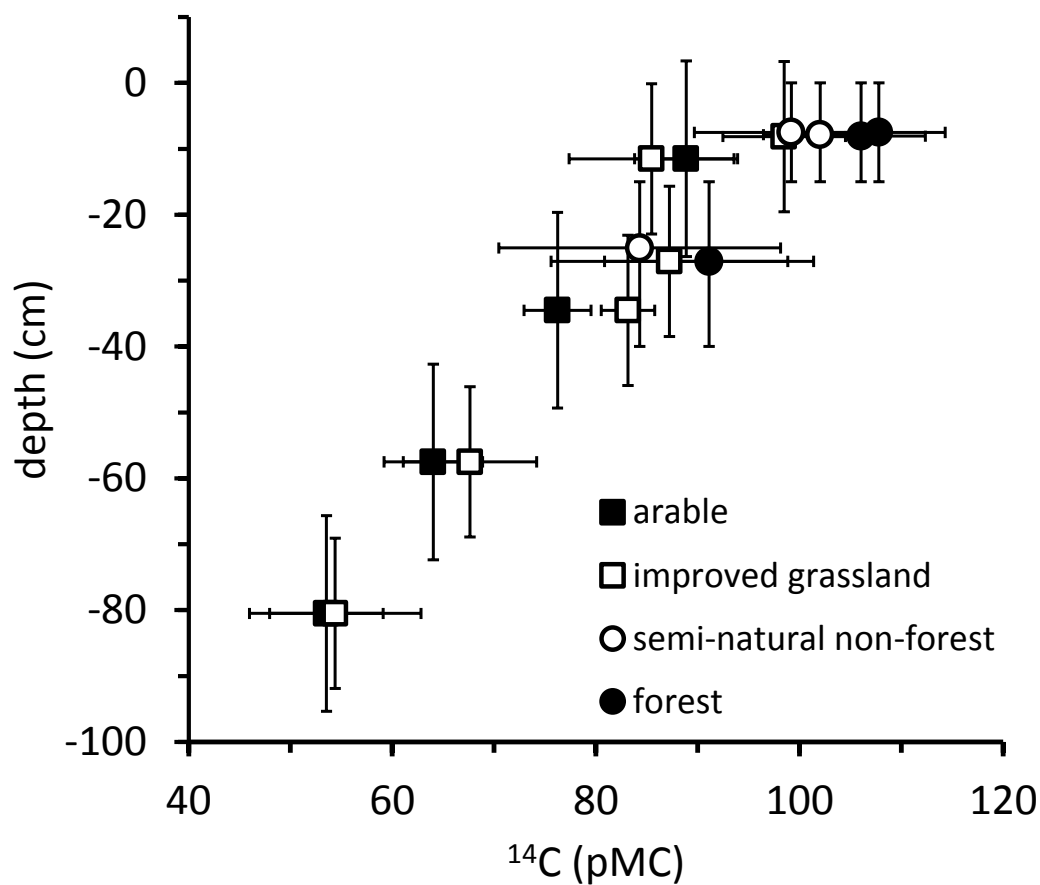


Figure 4.3. Soil radiocarbon plotted against soil depth for 296 samples of UK soils.

Depths are plotted as the weighted average of sampling depths. The horizontal bars are standard deviations in ^{14}C , the vertical bars are ranges of sampling depth. See Appendix 5.1 for details.

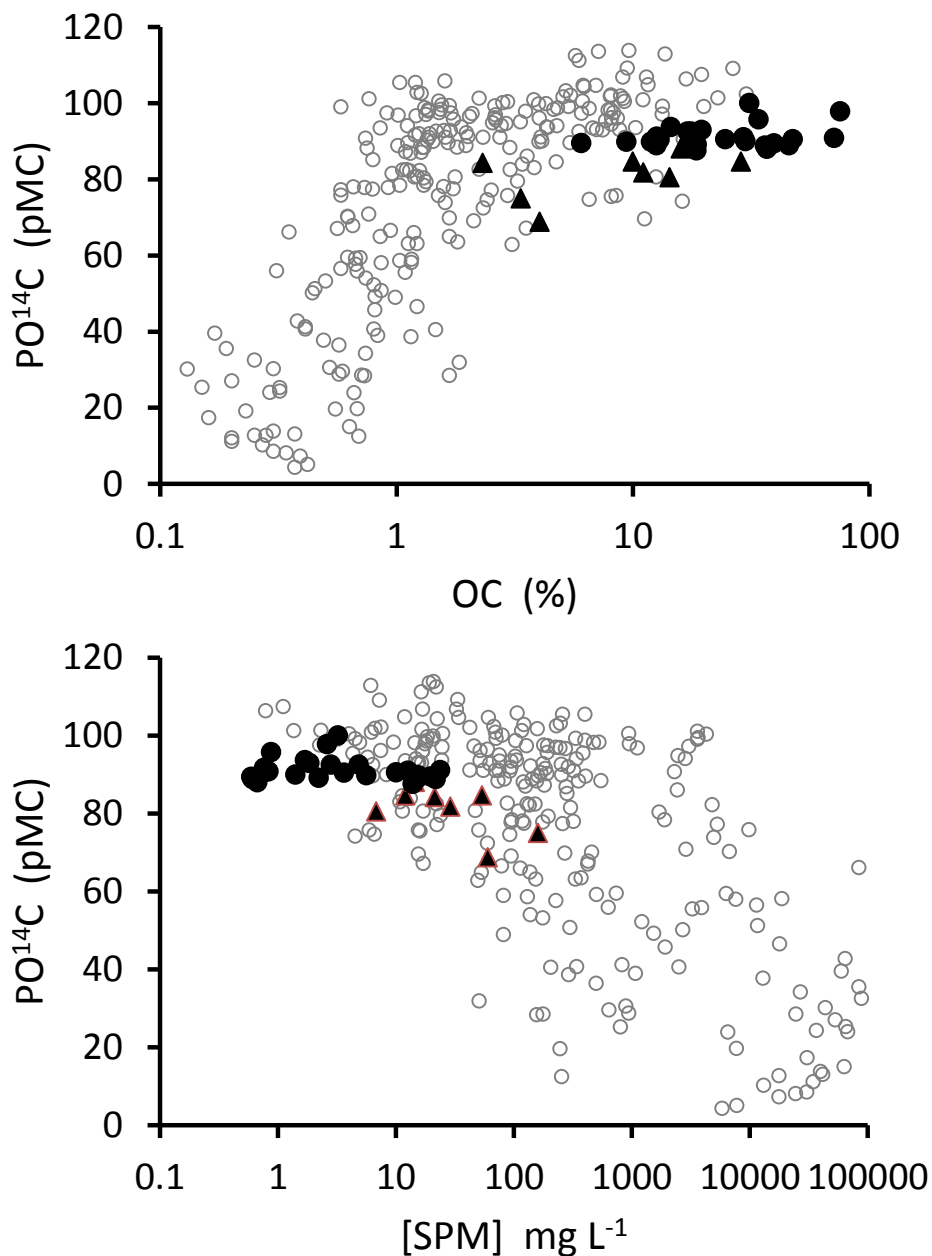


Figure 4.4. Radiocarbon contents of POM, i.e. PO¹⁴C, plotted the against OC content of SPM (%) and [SPM]. Global data collated by Marwick et al. (2015) are represented by the open circles. Data for the 7 rurally-dominated UK sites are shown by filled circles. Values for the Rivers Calder and Ribble B are shown by filled triangles.

5. Quantifying sources of dissolved organic radiocarbon in rivers

JL Adams, E Tipping, R Helliwell, N Pedentchouk, R Cooper, S Buckingham E Gjessing, P Ascough, CL Bryant, M Garnett

Abstract

Radiocarbon measurements of riverine dissolved organic matter (DOM) provide powerful modelling constraints on transport from terrestrial ecosystems, to freshwater and the oceans. Currently, the global database of DO^{14}C spans five continents, although recent assessment of the dataset identified a paucity of information for lowland catchments and those dominated by urban landscapes and arable agriculture. We collated new and previously unpublished data for rural, urban and arable catchments in the UK, with the urban and arable catchments significantly more depleted in ^{14}C than the rest of the UK data. The new UK data fitted within the trends of the global data, which contained ~800 individual values, categorised by the dominant land use of the catchments, although the urban UK samples were appreciably higher in DOC concentration. To provide a temporal view of the DOC sources, we applied a variable soil organic matter (SOM) turnover model with fast (~1 year) slow (~20 year) and passive (~2000 year) pools, which allowed for estimations of the fractions of the pools to the riverine DO^{14}C values. The model successfully estimated the sources of 88% of the dataset, and provides a reasonable comparison of data collected decades apart, using the most complete and up to date synthesis of global riverine DO^{14}C .

Keywords: Dissolved organic carbon, soil organic matter, turnover, sources, subsoil, topsoil.

5.1 Introduction

Riverine transport of dissolved organic carbon (DOC) is a considerable source of atmospheric and oceanic C, with an export of 0.4 Pg C a^{-1} , which is influenced by complex in stream processing such as mineralization by microbial communities (Aufdenkampe et al., 2011). Radiocarbon (^{14}C) analysis of riverine DOC is a powerful tracer of the origins of C pools and provides a quantitative analysis of organic matter (OM) turnover. The long half – life of naturally occurring ^{14}C (5730 years) can be used to quantify the turnover of C on the centennial and millennial timescales, while the ^{14}C bomb spike of the atmospheric weapons testing period provides estimates of turnover on the decadal timescale.

Since the development of accelerator mass spectrometry (AMS) and improvements in sample size and cost, the database of aquatic ^{14}C has increased considerably.

However, the interpretation of the dataset is complicated by the constantly changing atmospheric ^{14}C signal. While ^{14}C sources are influenced by natural radioactive decay, the “bomb peak” has decreased through time, largely due to assimilation into the oceans (Heinze et al., 2015). Therefore, the constantly changing atmospheric ^{14}C signal means that samples taken decades apart would comprise different ^{14}C contents, such that they are not directly comparable. Thus, long term modelling of terrestrial-aquatic C cycles must not consider individual measured values as ‘fixed’, and there has been little attempt to synthesise this global dataset from a temporal perspective.

The most recent, comprehensive review of global riverine DO^{14}C (Marwick et al., 2015) reported an average of $\Delta^{14}\text{C}$ 24‰ (102.4 pMC) for data between the period of 1990-2015, indicating some influences of ^{14}C originating from the atmospheric weapons testing period of the 1950s and 60s. The review highlighted a

disproportionate number of studies focussed on either headwaters (Schiff et al. 1997; Evans et al. 2007; Moore et al. 2013; Moyer et al. 2013; Tittel et al. 2013) or at the basin outlet only (Raymond et al., 2007; Hood et al., 2009; Sickman et al., 2009; Butman et al., 2012; Hossler and Bauer, 2012; Wang et al., 2012). In the UK, the majority of the dataset represents small upland, peat dominated watersheds (Billett et al. 2007; Palmer et al. 2001; Evans et al. 2007; M. F. Billett et al. 2012a). Further, international data of riverine DO^{14}C were assessed by Butman et al. (2015), who found that the apparent age of riverine DOC increased with population density and the proportion of human dominated landscapes in the basin area. From this, Butman et al. (2015) estimated that 3-9% of riverine DOC is aged C mobilised by human disturbance. It is therefore important to consider both lowland catchments and those heavily influenced by arable agriculture and urbanisation, which may deviate from the global averages. Understanding the processes involved in these systems should therefore improve the ability to model the transport of C from terrestrial to freshwater ecosystems.

However, the review of Marwick et al. (2015) did not consider the temporal changes involved in the terrestrial ^{14}C sources, and thus the composition of the bulk riverine data. There were also publications on riverine DO^{14}C not included in the dataset of Marwick et al. (2015) and data from the pre-1990s is not considered. Therefore, we aimed to estimate sources of DOC of global rivers over a changing timescale. In doing so, we collated a revised global dataset and presented original and previously unpublished data for the UK and Norway, some of which date back to the early 1960s. We applied the dataset against soil organic matter (SOM) pools constrained by radiocarbon data, as shown in Mills et al. (2013), and the models of Tipping et al.

(2012) and Davies et al. (2016), providing a time dependent interpretation of DOC sources.

5.2 Methods

5.2.1 Original data for the UK and Norway

The previously unpublished UK data includes small streams that were sampled between 1995 and 2007, which were all situated in upland areas of Northern England. Nine samples were collected from two sites on Great Dun Fell (GDFa and GDFb), situated in the north Pennines of England. These samples were collected at regular intervals between 1995 and 1996. Gais Gill drains a catchment area of 1 km² and is situated in the west of the Yorkshire Dales National Park, draining into the upper River Lune catchment. These samples were collected between 2005 and 2007. Doe House Gill was sampled in 2006, which drains a small catchment area of 0.3 km², and is a tributary of the River Duddon (Tipping et al., 2007).

The next riverine DO¹⁴C survey ran between October 2013 and October 2014 and included four large, lowland catchments of contrasting characteristics. The Ribble catchment, situated in the North West of England drains an area of 1144 km², mostly dominated by improved grassland for pasture. Two major sub-catchments of the Ribble catchment were included in the survey; the River Calder and the River Hodder drain from the south and the north of the catchment respectively, with the Calder catchment containing extensive conurbations and historical mining activity. In contrast, the Hodder catchment is rural and drains mostly upland moorland areas. The Conwy catchment, situated in North Wales has a high river response during storm events, owing to the largely mountainous landscape. The Avon catchment in the south of the UK is largely groundwater fed from the presence of chalk aquifers. Finally, the

Dee catchment in the north-east of Scotland is sparsely populated above the tidal limit, and contains extensive heathlands and conifer plantations. The River Gairn sub-catchment of the Dee is situated in upper mountainous areas of the Cairngorm National Park and responds rapidly to rainfall and snowmelt. More detailed descriptions of these catchments are included in Adams et al. (2015) (chapter 4). We collected between four and five surface water samples, in parallel with samples collected for riverine PO¹⁴C (Adams et al., 2015) (chapter 4). These were collected at high flows, identified by daily river level measurements by the Environment Agency of England and Wales and the Scottish Environment Protection Agency which are freely available on-line. The Avon catchment, which does not exhibit much variation in flow regime, was instead taken at regular intervals throughout the sampling period. We took an additional four low flow samples, collected from the River Hodder sub-catchment.

Two catchments situated in North Yorkshire were sampled between March and October 2015, both of which contained extensive arable and/or urban landscapes. The River Aire serves several towns and cities including Leeds, which was upstream of the sampling site. The River Derwent and three small tributaries – Barlam Beck, Spital Beck and Throwmires Beck drain extensive arable landscapes. Additionally, we obtained unpublished data from the University of East Anglia on two catchments. The River Wensum, situated in the east of England, drains ~80% arable land, while the Lymington River flows through the New Forest National Park and into the Solent estuary on the south coast of the UK. Table 5.1 provides additional information on the catchment characteristics, including drainage area, geology and land use.

In 1962, three samples were collected from three forested catchments in southern Norway. One sample was taken from a small catchment, east of the town Sarpsborg.

The other two samples were taken from catchments situated approximately 30km north-west of Oslo, and 90km north of Oslo. Six samples were collected in the 0.4 km² (Mulder et al., 1990) Birkenes catchment of southern Norway, between 2006 and 2007 (S. Buckingham, unpublished). This catchment is mostly undisturbed and is dominated by spruce forests. The catchment lies on granitic bedrock, with the soils dominated by shallow podzolised acidic brown earths.

5.2.2 Collection and analysis

Prior to collection, and to minimise risk of carbon contamination, all equipment used was either new or acid washed and all samples were processed in a radiocarbon tracer free laboratory. We carried out precautionary leak tests on high density polyethylene bottles, using samples from the Hodder sub-catchment stored over a period of three months, to determine whether artefacts from the plastic would leach into the sample. No influences from the bottles were observed, thus we believe the measured DO¹⁴C values to be true. Two litre surface samples were collected from each of the sites, which were all situated above the tidal limit. The samples were filtered using pre-combusted (500⁰C for at least four hours) and pre-rinsed Whatman GF/F (0.7 µm) filter papers. The supernatant was decanted into acid washed 2 L glass Schott bottles and sent to the Scottish Universities Environmental Research Centre (SUERC) accelerator mass spectrometry laboratory, East Kilbride, UK (Xu et al. 2004).

All water samples were purged to remove any inorganic carbon, followed by quantitative recovery of C in sealed quartz tubes and cryogenic separation of CO₂ for the preparation of the graphite targets (Boutton et al., 1983). Subsamples of the CO₂ were used to measure δ¹³C by dual-inlet mass spectrometry with a multi ion beam collection facility (Thermo Fisher Delta V) for correction of the ¹⁴C data to -25‰

$\delta^{13}\text{C}_{\text{VPBD}}$. The mass spectrometer was calibrated with the international reference materials to a precision of $\pm 0.03\text{‰}$. There were three cases where purging did not sufficiently remove all of the carbonate, reflected by the higher $\delta^{13}\text{C}$ values. These were re-analysed, purging down to pH 2, rather than 4. On some occasions there was not sufficient material to re-analyse; these samples have been omitted from the following data analysis, but are included in Appendix 5.1 for reference. We also omitted samples that showed $\delta^{13}\text{C}$ values higher than -24‰ (Marwick et al., 2015), as these suggest the presence of residual carbonate, possibly not completely removed during purging and acidification, which will deplete the overall ^{14}C signal. Results for the DO^{14}C are reported as absolute % modern (pMC), with conventional radiocarbon ages provided where results were below 100 pMC and ‘modern’ stated where samples contain sufficient “bomb carbon”. Analytical precision is quoted at 1σ . Preparation of samples for the analysis of ^{14}C is detailed further in Adams et al. (2015) (chapter 4).

For the Ribble, Conwy, Avon, Dee, Aire and Derwent catchments, additional 500 mL samples were collected for analysis of the DOC concentration, which were measured using a Vario EL elemental analyser at CEH Lancaster, and a Thermo Flash 2000 elemental analyser at the James Hutton Institute for samples from the Dee catchment. All statistical analyses (t-tests and linear regressions) were carried out using Microsoft Excel. Data was first checked for normality and equal variances and log transformed if necessary.

5.2.3 Collation of the dataset

We first assessed the entire dataset reported in Marwick et al. (2015). Where data were initially reported as either $\Delta^{14}\text{C}$ ‰ or fraction of modern carbon (fMC), we converted to percent modern carbon (pMC), in line with international practice and to

aid comparison with our new dataset, using equation 1 and 2 in chapter 2. We re-reviewed the dataset of Marwick et al. (2015), making necessary corrections (Benner 2004; Billett et al. 2012b; Butman et al. 2012; Masiello and Druffel, 2001; Wang et al. 2012; Evans et al. 2007). Additional screening of available literature was conducted through web searches and citations. The NERC radiocarbon facility (NRCF) also conducted screening of their dataset, which includes all data analysed at the facility, from the point of recording. From these searches, we found an extra 78 data points from 13 studies. Two of these were published in the same year or after the publication of Marwick et al. (2015). Our unpublished dataset added an extra 114 data points, spread over 25 different sites in the UK and Norway.

The literature was restricted to bulk ^{14}C values, except measurements made on Suwannee River fulvic acid (SRFA) reference standards, which are highlighted in Appendix 5.1. We did not include data that were obtained directly from the outlets or processing stage of water treatment works. Samples collected below the tidal limit were restricted to recorded salinities of < 1 , in line with Marwick et al. (2015). The study of riverine DO^{14}C in the Chernobyl exclusion zone (Nagao et al. 2004) was not included in our dataset, as the recorded DO^{14}C was significantly influenced by the nuclear accident, and is not considered representative in the global DO^{14}C dataset.

5.2.4 Land classifications

To interpret the data, we categorised the dataset based on surface soil ^{14}C and the single dominant land use, which would have considerable influences on the ^{14}C signal. For example, Mills et al (2013) found global forested soils to be more ^{14}C enriched than semi natural landscapes. We accepted the dominant land use as described by the authors, though if the publication referred to another study for

catchment information, we collated the data from there. For studies that did not include sufficient information, we accessed open source data freely available online (<http://www.waterandclimatechange.eu/land-cover>: accessed March 2017).

Our classifications comprise wetlands (W), which includes upland peatlands, bogs, fens and glacial tundra. Arable (A), is defined as farming of crops, with regular fertilizer application and managed drainage. Forests (F) includes broadleaf woodland, conifer plantation, boreal and tropical. Some catchments were not dominant in any land use, which are categorised as not arable, forest or peatland (NWFA), which comprised half of the UK catchments (Figure 5.2). The final category is the same as the latter, but with considerable urban influence (NWFAU).

The year that the sample was collected was also important for our analysis. Where studies only provided a range of years, for example 1990-1997 (Schiff et al., 1997), we used the median year for the data analysis.

5.2.5 Application of modelled SOM pools

Radiocarbon data of soil organic matter provides powerful constraints when determining soil carbon dynamics, with ages reflecting soil carbon stability and depth (Trumbore, 2000). On entry into the watercourse, DOM from the different soil organic matter (SOM) profiles will reflect these turnovers (Butman et al., 2015). On this principle, we applied modelled ^{14}C values for SOM based on three pools, as identified by the database of Mills et al. (2013). Turnover rates of these pools are quantified by the atmospheric ^{14}C values up to 2010 (Hua, Barbetti and Rakowski, 2013); we extrapolated the dataset to extend the data to the year 2016 (Figure 5.1, black line). Steady state input of C was chosen, which was multiplied by the given

atmospheric ^{14}C value to obtain the input of ^{14}C to the soil, which is calculated on an annual basis.

Litter C is assumed to enter a pool of rapid turnover of 1 year, defined as the fast pool, while the slow pool reflects a turnover of 20 years. The fast and slow pools together make the topsoil that produces DOM. The passive pool comprises approximately half of the topsoil, though its turnover results in insignificant proportions of DOM. Here, the fast and slow pools are assumed to be 50:50, to provide a simple way of constraining the two topsoil sources. This is represented by the upper blue line in Figure 5.1. The lower blue line represents the modelled OM pool for deep soil, which has a mean residence time of 2000 years, with a ^{14}C value of between 80 and 81 pMC, depending on the year, and assuming steady state conditions. From these, we can estimate the fractions of these pools to the sample collected for any given year, by:

$$f_d = (pMC - pMC_s)/(pMC_d - pMC_s) \quad (1)$$

$$f_s = 1 - f_d \quad (2)$$

Where pMC is the bulk ^{14}C content of the sample, pMC_s is the average ^{14}C content of the fast and slow pools for any given year and pMC_d is the ^{14}C content of the subsoil pool. The fractions of the sub-soil and topsoil are given by f_d and f_s respectively.

For our interpretations, we assume the turnover of different land classes to be the same. The modelled OM turnovers are applied to the global dataset to obtain an overall insight, but not to provide a precise interpretation of each data point.

5.3 Results

5.3.1 Original data for the UK and Norway

We first consider the original dataset for the UK, which contained catchments that were variable with respect to land use, catchment size, altitude and geology. The samples collected varied considerably in DOC concentration, although only six data points exceeded 10 mg L⁻¹. The highest recorded DOC concentrations were all situated in upland catchments, notably GDF A (22.3 mg L⁻¹) and Gais Gill (14.8 mg L⁻¹) (Table 5.1). The values for $\delta^{13}\text{C}$ mostly fell between a range of -25‰ to -31‰, indicating a presence of carbon derived from plants with the C₃ metabolic pathway, which is typical of vegetation in the UK and the northern hemisphere (Still et al., 2003).

When interpreting the ¹⁴C data, it is important to consider that the measured values arise from the mixing of different sources of DOC. Highly enriched DO¹⁴C will correspond to recently assimilated OC through either terrestrial or aquatic photosynthesis, while depleted DO¹⁴C will likely arise from sub-surface soil and parent material. In addition, rivers draining urban catchments will contain sources of industrial effluent which often contain highly depleted ¹⁴C from household products and fossil derived fuels. Thus, the reported ages are only apparent. Radiocarbon contents of the UK samples fell in the range of 78-110 pMC (Table 5.2), which corresponds to conventional ¹⁴C ages of 1855 years B.P to modern. The mean values in Figure 5.2 show that nine sites were significantly ($p = 1.9 \times 10^{-5}$) more ¹⁴C depleted, seven of which were categorised as arable and urban. Depleted DO¹⁴C in the Wensum catchment and the Derwent including its tributaries – Throwmires Beck, Barlam Beck and Spital beck - is probably the result of extensive arable activity.

Managed drainage of arable sites encourages infiltration of water down to deeper soil, rather than overland flow, which results in the mobilization of aged ^{14}C . Arable topsoils also tend to be slightly more ^{14}C depleted than semi natural and forested soils (Jenkinson, Poulton and Bryant, 2008; Adams et al., 2015) (chapter 4). The Calder and Aire catchments contain extensive conurbations, meaning that the depleted signal is likely from industrial effluent. The samples collected from the Calder may also contain waste from coal mining, and the mixing of this river water with water from the Hodder and the main River Ribble will lead to depleted ^{14}C at the downstream Ribble B site (categorised as NWFA). In the Avon catchment, the depleted DO^{14}C reflects passage through deeper soil. Chalk aquifers in the Avon catchment may further deplete the DOC due to the longer residence times of the river water.

Figure 5.3 shows the DO^{14}C content against DOC concentration for the UK data, including the new results reported here. The majority of the data already published for the UK include upland wetland areas, which tend to be more concentrated in DOC (17.3 mg DOC L⁻¹ average) and more enriched in DO^{14}C on average (107.4 pMC), suggesting the release of enriched OC from the surface of the basin profile. The most concentrated DOC was found in a degraded bog (61.8 mg DOC L⁻¹, 54.8 mg DOC L⁻¹) (Evans et al., 2014) and an upland wetland site (43.0 mg DOC L⁻¹) (Tipping et al., 2010). Higher average DOC concentrations were also observed in the upland catchments of GDFa (10.7 mg L⁻¹) and GDFB (8.7 mg L⁻¹), which were also categorised as wetlands. Elevated DOC concentrations in the River Calder sub-catchment (8.3 mg L⁻¹) suggests some urban influences, possibly from the outlets of several water treatment works present in the catchment. The lowest DOC concentrations included arable catchments in the UK (data reported here), and sites with mixed land uses in the Conwy catchment (Evans et al., 2007). These also

contained the most depleted DO^{14}C , and can be attributed to the release of aged sub-surface sources, which are lower in OC content (Jobbágy and Jackson, 2000). The most enriched DO^{14}C found in our dataset was in the river Lymington (109.4 pMC average), which mostly drains forested land. Our original dataset considerably expands the information available for riverine DO^{14}C in the UK, and provides new information on lowland catchments of contrasting land uses.

5.3.2 Applying the UK data to the international data

The international dataset is dominated by catchments with mixed land uses, described here as NWFA (Figure 5.4). Catchments disturbed by anthropogenic activity including arable and urban systems are less well represented globally (n= 38 and 28 respectively). Both of these systems do not considerably vary in DOC concentration and the UK sites tend to be lower than the international sites on average, with the arable sites at 2.6 mg DOC L⁻¹ and the urban dominant systems at 4.4 mg DOC L⁻¹. In contrast, DOC drained from wetlands is appreciably more variable, with concentrations as low as 0.8 mg DOC L⁻¹ from a catchment in Northern Alaska (Guo, Ping and Macdonald, 2007) to 95 mg DOC L⁻¹ found in a peatland catchment in Finland (Evans et al., 2014). On average, DOC draining from wetlands was the most concentrated at 28.4 mg DOC L⁻¹, followed by forested catchments at 6.0 mg DOC L⁻¹.

The distribution of DO^{14}C is appreciably skewed towards modern contemporary sources, with 65% of the samples greater than 100 pMC. The most depleted values were found in catchments in Northern Alaska (Guo, Ping and Macdonald, 2007), in the Yukon basin (Aiken et al 2014), and in the Kimberly region of North Western Australia (Fellman et al., 2014). From our land use classifications, it seems that

forested catchments drain more enriched DO^{14}C , with an average of 108.2 pMC. In contrast, both urban and arable dominated catchments drain more depleted DO^{14}C sources on average, at 92.5 pMC 84.5 pMC respectively. Generally, lower DOC concentrations correspond to more depleted DO^{14}C , though some wetland catchments do not conform to this pattern, which is possibly the result of human modifications (Evans et al., 2014). Our original dataset mostly fits with the general trend of the global data, as sorted by land use. However, UK catchments dominated by urban landscapes seem to be more concentrated in DOC than the global data points, though this is based on only five separate samples.

5.3.3 Temporal analysis of riverine DO^{14}C

We plotted the global dataset in terms of the land classification and the year that the samples were collected, to indicate the scale that the data spans through time. The collated data covers over five decades, from forested catchments collected in 1962 (data reported here) to the new UK data collected in 2015. ^{14}C values that constrain turnover of the fast, slow and passive pools used in the $\text{N}^{14}\text{C}(\text{P})$ models of Tipping et al. (2012) and Davies et al. (2016) were used to give a broad perspective on the DO^{14}C sources. Overall, 88% ($n = 963$) of the samples fell within the two modelled pools (Table 5.3). Arable samples were situated closer to the subsoil pool, with 18% ($n=38$) of the samples falling below this boundary, indicating the average depleted ^{14}C in relation to the global dataset (Table 5.3, Figure 5.5). Catchments dominant in urban systems (NWFAU) were similarly closer to the subsoil boundary. In contrast, forested samples were much closer to the boundary of the topsoil pool, indicating average enriched DO^{14}C . Wetlands were much more spread in terms of the DO^{14}C and 4% ($n = 200$) of the values fell below the 2000 year pool, possibly due to drainage and

management, and climatic variations (temperate and tropical) (Evans et al., 2014).

Overall, 71 data points were more enriched than the modelled topsoil OM pool. In the forested category, this was the case for 38 of the 201 samples. The wetland class had 15 samples above the topsoil OM pool, and one sample for the NWFA class. Since the topsoil OM pool represents the most recently fixed atmospheric ^{14}C , the riverine DO^{14}C should not exceed this, suggesting that the model does not acceptably fit these points.

We estimated the sources of DOC by calculating the proportions of topsoil (upper line, Figure 5.5) and subsoil (bottom line, Figure 5.5), such that any sample is a mixture of the two pools. Examples of these estimations are listed below, though this was carried out for the entire dataset (Appendix 5.1). Samples that were below the 2000 year pool contained a subsoil fraction of 1.0, showing that material was exclusively from this pool. Samples that were on the boundary of the topsoil pool contained a topsoil fraction of 1.0, including samples from pristine tropical forest in the Congo basin (Spencer, Butler and Aiken, 2012) and blanket peatlands in the UK (Billett, Garnett and Harvey, 2007). The Aire catchment, which contains extensive conurbations had a calculated subsoil fraction of 0.8 for both DO^{14}C measurements (85.8 pMC, 84.9 pMC), compared to 0.4 for the other urban catchment in the UK dataset (Calder). The samples collected in Norwegian forested catchments from 1962, with ^{14}C contents of 97.1 pMC, 99.7 pMC and 98.8 pMC contained subsoil fractions of 0.6, 0.5 and 0.5 respectively. A forested sample collected in 2009, with a similar ^{14}C value (97.9 pMC) (Tittel et al., 2013) contained a subsoil fraction of 0.4. Similarly, a sample collected in 2010, with an enrichment of 96.7 pMC (Tittel et al., 2013) contained the same subsoil fraction. Thus, samples with similar measured ^{14}C

values, but sampled decades apart, may not contain the same fractions of topsoil and sub-soil.

5.4 Discussion

The original data collected for lowland catchments considerably expands the information available for the UK, and captures a far wider range of land cover. The new data included measurements from urban dominated catchments and arable, with the arable samples appreciably more depleted in DO^{14}C . These data agree with the global urban and arable dataset and suggest the release of aged ^{14}C by human disturbance. This was also suggested in Butman et al. (2015), though differences in the type of human activity were not addressed. It is likely that the aged urban sources will originate from the effluent of water treatment works (Griffith, Barnes and Raymond, 2009b), while arable catchments are well drained, thus leaching older ^{14}C sources, rather than enriched sources through overland flow. Arable catchments may also have more depleted topsoil ^{14}C values, as crop cultivation removes the input of litter to the fast pool (Adams et al., 2015), though this would be a minor effect compared to deep soil drainage. Overall, the UK data fit within the scope of the global data and do not considerably deviate from global measurements of the same land use category. The urban samples collected in the UK had higher DOC concentrations than the global data, which could indicate larger inputs of water treatment effluent from densely populated areas in the catchments. The Calder sub-catchment accounts for a large percentage of the population density of the Ribble catchment (989 persons km^{-2} (Adams et al., 2015)) while the Aire drains a major city with a population density of 4066 persons km^{-2} . However, the available dataset for urban catchments is lacking,

and further investigation into these may provide a clearer indication of any deviations from the global dataset.

The modelled turnover of the SOM pools of Mills et al. (2013), Tipping et al. (2012) and Davies et al. (2016) fitted well with the global dataset and although they are not precise for any particular sample, the pools allow to scale the data in terms of its sources. By quantifying the fractions of the pools to the samples for a given year, we estimated the sources contributing to similar ^{14}C values collected at different times. This was the case for the forested values collected in 1962, compared with similar ^{14}C values collected for forests in 2009 and 2010 (Tittel et al., 2013), which showed slight variations in the estimated ^{14}C sources. However, 71 samples were above the topsoil boundary and 47 for the subsoil boundary (Table 5.3). For the topsoil boundary, the samples should not be more enriched, as the pool is based on the turnover of the most recently assimilated C. The calculated average of the two topsoil pools (1 year and 20 year turnovers) is possibly an oversimplification. Better model constraints may be achieved if riverine DO^{14}C data from the 1960s, 70s and 80s were made available.

An important factor to consider when interpreting the data is the flow of the river at the time of sampling. Though the flow is not frequently quoted in the literature, the modelled fractions provide an indication of the conditions at the time of sampling. It is known that the age of OC increases with increasing soil depth. At lower flows, greater proportions of riverine DOC will be sourced from the interaction with parent material and older OC from sub-surface soil horizons, resulting in an overall aged bulk ^{14}C sample and a higher modelled fraction of sub-soil (2000 year pool). The global dataset shows that both small and large basins measured at baseflow tend to give more depleted ^{14}C signatures (Schiff et al., 1997; Neff et al., 2006; Raymond et al., 2007). Higher flows, including storm runoff, will mobilize more enriched OC

from the soil profile, which in turn dampens the depleted ^{14}C signal, resulting in enriched riverine DOC during these conditions (Schiff et al., 1997) and higher fractions of the modelled topsoil pool. However, catchments draining glacial meltwaters (Aiken et al. 2014; Hood et al. 2009) and those dominated by groundwater sources (Fellman et al., 2014) do not conform to this pattern due to the abundance of ancient OC sources and natural decay through storage.

Estimating the fractions by this means is further complicated by in river processing that may lead to overestimations of the sub-surface (i.e 2000 year pool) soil input. It is known that more enriched, labile C that would originate from the 1 and 20 year pools can be preferentially mineralized, and was demonstrated experimentally by Raymond and Bauer (2001). This process was also considered the dominant driver for CO_2 outgassing in rivers of the humid tropics, though only for particulate OC (POC) (Hilton, Galy and Hovius, 2008). Marwick et al. (2015) and Mayorga et al. (2005) both suggested a link between preferential mineralisation of labile ^{14}C and depletion downstream, in large passive basins with extensive longitudinal gradient. Thus, mineralisation will likely influence the measured DO^{14}C in rivers, though this is highly dependent on basin characteristics (Marwick et al., 2015).

The most recent global synthesis of riverine DO^{14}C by Marwick et al. (2015) highlighted important gaps in the dataset, though several studies were not included. Our study therefore provides the most extensive and up to date analysis of global riverine DO^{14}C , categorised by different land uses, and considerably expands the data available for the UK. Globally, the new data reported here considerably increases that available for arable and urban systems, and thus will improve models of terrestrial – aquatic carbon cycling and nutrient dynamics. Further, land disturbance by anthropogenic activity has been identified as a potential driver of aged riverine DOC

(Raymond and Bauer, 2001; Sickman, Zanolli and Mann, 2007; Moore et al., 2013).

Arable and urban dominated catchments are lacking in the global dataset and should therefore be considered in future studies.

5.5 Conclusions

- The new data reported here considerably expand the current dataset available for both the UK and globally. DOC from catchments dominated by arable and urban land uses was significantly more depleted in DO^{14}C than the rest of the new UK data.
- Terrestrial sources of DO^{14}C can be reasonably well estimated by the mean residence time of the different SOM pools used in the models of Tipping et al. (2012) and Davies et al. (2016), with 88% of the dataset falling between the two modelled pools. Arable and urban land classes were mostly situated towards the subsoil pool, while DO^{14}C in the forested ecosystems were dominated by the topsoil pool.
- Catchments that are considerably influenced by anthropogenic activity are not well represented by the global dataset and should be considered in future research.

5.6 Acknowledgements

This research was funded by the UK Natural Environment Research Council Macronutrient Cycles programme (LTLS project, Grant No. NE/ J011533/1) and the Scottish Government. We are grateful to A Panton (National Oceanography Centre, University of Southampton), EC Rowe (CEH Bangor) and C Somerville for assistance with sampling the Avon, Conwy and Ribble catchments respectively. We thank the

analytical chemistry teams at CEH Lancaster and the James Hutton Institute and to K Howarth of the Environment Agency, North West England, for access to the sites in the Ribble catchment.

Table 5.1. Catchment information. Discharge data are from records between 35 and 50 years up to the present. Geology, soil type and land use are arranged in order of dominance. Information for Doe House Gill was obtained from Tipping et al. (2007).

	Aire	Derwent	Wensum	Lymington	G DFA GDFB	Gais Gill	Doe House Gill
Catchment drainage area (km ²)	282	1586	162	99	0.0004	1	0.3
Altitude range (masl)	87-582	10-452	34-93	6-118	480-848	321-587	240-730
Mean annual rainfall (m)	1.2	0.8	7.0	0.9	1271	1714	3250
Mean annual air temperature (°C)	9	9	10	11	6	7	6
River discharge (m ³ s ⁻¹)							
Mean	6.5	16.7	0.9	1.1	N.D	N.D	4.8
95% exceedance	0.6	4.4	0.2	0.05	N.D	N.D	-
10% exceedance	17.0	35	1.7	2.8	N.D	N.D	-
Principal bedrock geology	LS	Cl	CH	S	LS	SS	SS
	SS	MS	SS	SI	SS	LS	MS
	CM	LS		Cl	MS	SIS	SIS
Principal soil types	Gley	Gley	Brown earth	Gley	Blanket peat	Brown earth	Gley
	Brown earth	Brown earth	Brown sand	Brown earth	Gley	Gley	Podzol
	-	-	Gley	Rendzina	Brown earth	Podzol	Ranker
Principal land cover	U	A	A	F	B	IG	RG
	A	IG	IG	H	H	RG	IG
	IG	F	F	IG	RG	H	B

Catchment information for the Ribble, Dee, Avon and Conwy catchments can be found in Adams et al. (2015) (chapter 4).

Table 5.2: Isotopic data for the original and unpublished UK dataset. Values are given of ^{14}C (pMC), $\delta^{13}\text{C}$ (‰ vPDB) and conventional radiocarbon age (years B.P). Errors of the ^{14}C are expressed as $\pm 1\sigma$ (pMC) where σ is the analytical uncertainty.

River	Date	$\delta^{13}\text{C}$	^{14}C	+/-1 σ	Age	Publication No.
Calder	04/10/13	-27.90	97.62	0.43	131	SUERC-51573
	22/10/13	-29.10	94.95	0.44	354	SUERC-50020
	02/01/14	-29.50	96.79	0.45	200	SUERC-51860
	07/01/14	-29.70	97.29	0.45	159	SUERC-51866
Hodder	22/10/13	-29.70	103.66	0.48	Modern	SUERC-50021
	02/01/14	-29.70	101.52	0.47	Modern	SUERC-51861
	01/07/14	-29.18	94.58	0.44	385	SUERC-57325
	01/07/14	-29.25	94.56	0.45	387	SUERC-57327
	10/07/14	-28.98	98.21	0.43	83	SUERC-57321
	10/07/14	-29.05	95.22	0.44	331	SUERC-57322
Ribble A	04/10/13	-30.10	103.19	0.47	Modern	SUERC-51574
	22/10/13	-29.90	104.32	0.48	Modern	SUERC-50022
Ribble B	02/01/14	-24.50	97.64	0.43	130	SUERC-51862
	04/10/13	-29.60	99.63	0.44	N.D	SUERC-51575
	22/10/13	-29.60	101.19	0.44	Modern	SUERC-50023
	02/01/14	-28.60	99.99	0.47	N.D	SUERC-51865
Conwy	07/01/14	-25.00	96.34	0.45	238	SUERC-51869
	07/01/14	-29.30	99.74	0.47	N.D	SUERC-51870
	27/01/14	-28.80	102.61	0.49	Modern	SUERC-53193
	14/02/14	-29.40	98.07	0.46	95	SUERC-53195
Avon	22/10/14	-28.20	104.87	0.49	Modern	SUERC-58255
	22/10/13	-28.94	97.34	0.45	154	SUERC-50024
	23/04/14	-31.06	80.79	0.35	1650	SUERC-59410
Gairn	27/08/14	-29.60	83.27	0.37	1407	SUERC-61782
	07/01/14	-29.48	104.71	0.46	Modern	SUERC-52638
	26/02/14	-26.51	105.76	0.51	Modern	SUERC-53179
Dee A	07/03/14	-26.77	104.40	0.52	Modern	SUERC-53183
	07/01/14	-29.00	103.22	0.48	Modern	SUERC-52639
	26/02/14	-28.63	103.08	0.52	Modern	SUERC-53180
	07/03/14	-28.63	102.46	0.51	Modern	SUERC-53184
Dee B	16/03/14	-28.70	100.14	0.50	Modern	SUERC-53190
	07/01/14	-29.18	103.66	0.48	Modern	SUERC-52640
	26/02/14	-28.62	102.50	0.51	Modern	SUERC-53181
	07/03/14	-29.00	102.03	0.51	Modern	SUERC-53185
Aire	16/03/14	-28.79	99.31	0.50	N.D	SUERC-53191
	21/03/04	-28.50	97.67	0.45	37	SUERC-53203
	29/06/15	-28.68	85.76	0.40	1170	SUERC-68181
	27/10/15	-28.57	84.89	0.37	1252	SUERC-68183

Table 5.2. (Continued)

River	Date	$\delta^{13}\text{C}$	^{14}C	+/-1 σ	Age	Publication No.
Derwent	04/03/15	-24.40	95.17	0.44	335	SUERC-63913
	29/06/15	-28.07	78.75	0.70	1855	SUERC-69559
	27/10/15	-28.25	94.40	0.44	399	SUERC-68187
Barlam Beck	29/06/15	-29.34	93.56	0.43	471	SUERC-68856
	27/10/15	-29.50	96.82	0.45	196	SUERC-68188
Spital Beck	04/03/15	-24.13	101.21	0.47	Modern	SUERC-63915
	29/06/15	-28.55	84.77	0.39	1263	SUERC-68857
	27/10/15	-29.45	89.12	0.39	861	SUERC-68189
Throwmires Beck	04/03/15	-26.97	95.91	0.43	272	SUERC-63914
	29/06/15	-28.80	91.91	0.38	1549	SUERC-68855
	27/10/15	-28.79	93.21	0.41	500	SUERC-68861
Wensum	24/08/15	-25.00	88.28	0.40	1002	SUERC-68178
	24/08/15	-23.90	87.87	0.40	1039	SUERC-68179
	24/08/15	-25.80	85.91	0.40	1220	SUERC-68180
Lymington	25/08/15	-28.9	108.98	0.50	Modern	SUERC-63903
	25/08/15	-29.3	109.63	0.48	Modern	SUERC-63904
	25/08/15	-28.9	109.61	~0.50	Modern	SUERC-63905
Great Dun Fell A	12/09/95	-25.60	108.86	~0.50	Modern	AA-22644
	09/10/95	-25.30	100.66	~0.50	Modern	CAMS-38815
	06/11/95	-25.20	106.94	~0.50	Modern	AA-22645
	04/12/95	-26.70	94.96	~0.50	N.D	CAMS-38817
	03/01/96	-26.70	106.89	~0.50	Modern	AA-22647
	19/02/96	-26.40	106.03	~0.50	Modern	CAMS-38819
	25/03/96	-26.40	106.62	~0.50	Modern	AA-22648
	29/04/96	-25.40	91.85	~0.50	N.D	CAMS-38821
	28/05/96	-27.20	106.59	~0.50	Modern	CAMS-38823
	09/10/95	-26.90	104.52	~0.50	Modern	CAMS-38816
Great Dun Fell B	06/11/95	-25.20	103.65	~0.50	Modern	AA-22646
	04/12/95	-28.40	103.79	~0.50	Modern	CAMS-38818
	03/01/96	-28.20	104.35	~0.50	Modern	AA-22652
	19/02/96	-27.10	99.38	~0.50	N.D	CAMS-38820
	25/03/96	-25.00	105.65	~0.50	Modern	AA-22649
	29/04/96	-26.90	83.89	~0.50	N.D	CAMS-38822
	28/05/96	-26.40	103.42	~0.50	Modern	CAMS-38824
	10/10/05	-29.10	102.49	0.31	Modern	SUERC-8832
Gais Gill	24/10/05	-29.20	106.92	0.32	Modern	SUERC-8833
	07/11/05	-29.10	109.63	0.48	Modern	SUERC-9572
	21/05/06	-29.00	107.80	0.47	Modern	SUERC-11385
	15/11/06	-28.30	107.26	0.47	Modern	SUERC-12984
	3/12/06	-28.10	106.49	0.47	Modern	SUERC-14147
	01/02/07	-27.80	103.25	0.45	Modern	SUERC-14148
	14/02/07	-27.90	105.68	0.49	Modern	SUERC-14149
	18/02/07	-28.50	103.27	0.45	Modern	SUERC-14150
Doe House Gill	2006	-27.20	105.44	0.49	Modern	SUERC-14151

Table 5.3. Number of samples in each of the land categories that fall above the 50:50 fast pool (1 year and 20 years) or fall below the 2000 year pool.

Land category	Number of samples above topsoil pool	Number of samples below subsoil pool	Number of samples within the boundary	Total number of samples	% of samples within the boundary
A	1	7	30	38	79
F	38	2	161	201	80
NWFA	17	26	452	495	91
NWFAU	0	3	25	28	89
W	15	9	177	201	88

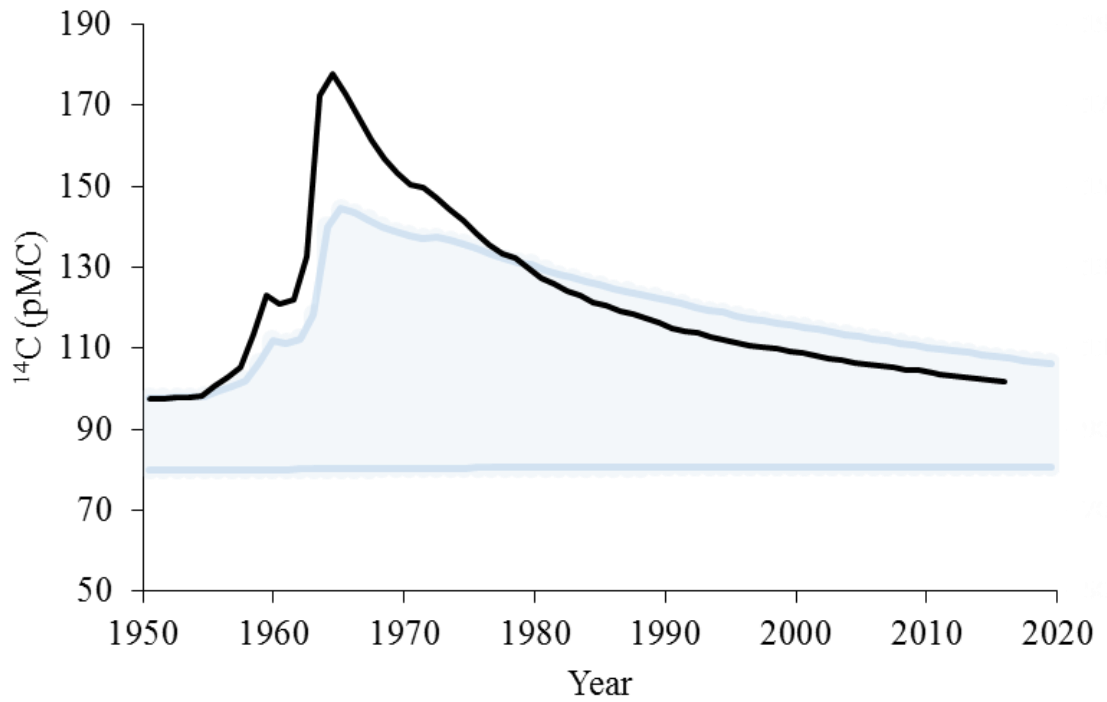


Figure 5.1 Atmospheric ^{14}C content (black line) (Hua, Barbetti and Rakowski, 2013), extrapolated to 2016 and the two modelled SOM pools. The upper blue line represents the average of the 1 year and 20 year pool. The lower line is the 2000 year SOM pool assuming steady state conditions.

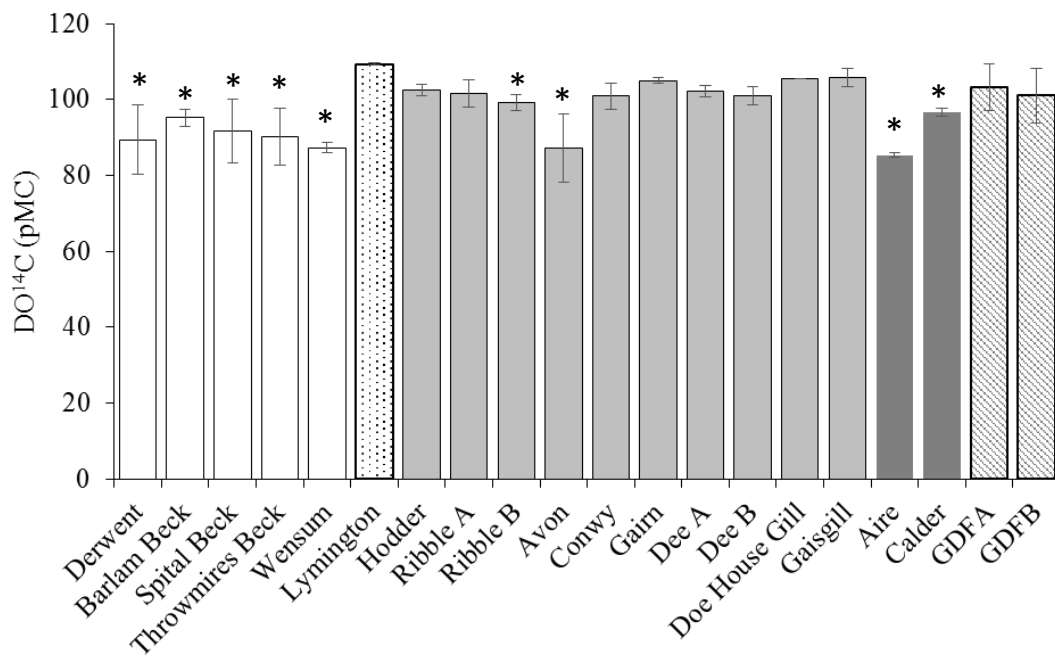


Figure 5.2 Average DO¹⁴C content of the original and previously unpublished data for rivers in the UK. The white blocks are arable sites (A), the dotted blocks are forested sites (F), light grey blocks are not wetland, forest or arable sites (NWF), dark grey blocks are mixed sites with urban influence (NWF AU) and diagonally lined blocks are wetland sites (W). Standard deviations are shown by the error bars. Starred bars show the nine sites that were significantly different.

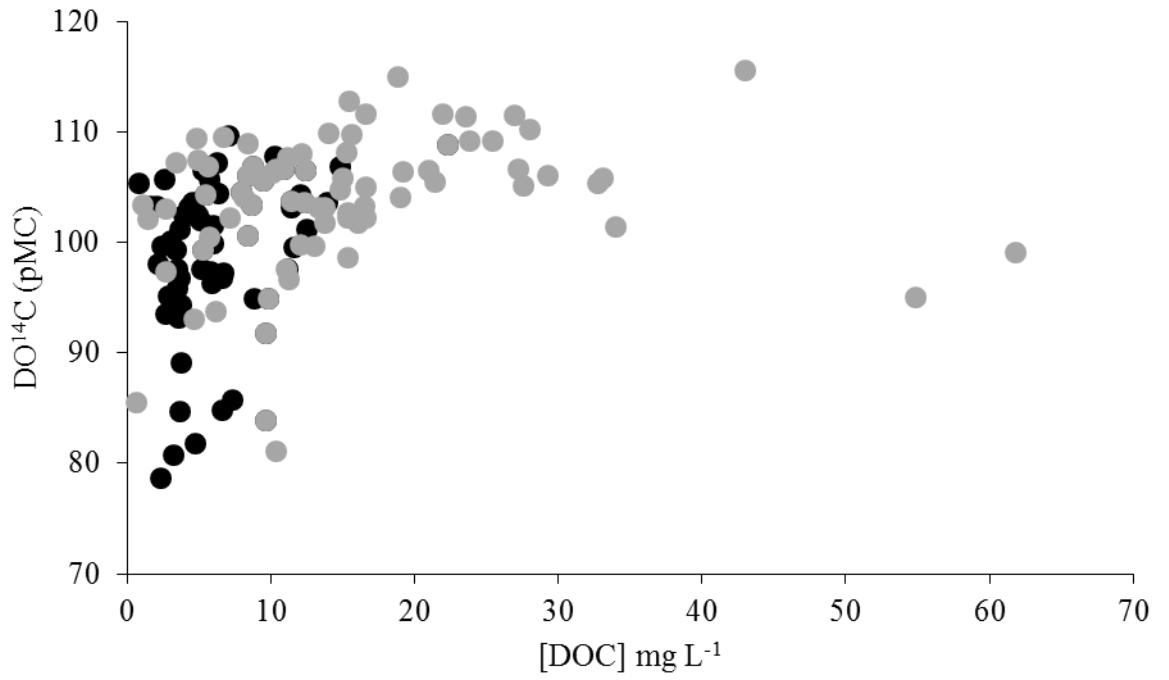


Figure 5.3. DO ^{14}C and DOC concentration for all data available for the UK. The black markers show the original dataset presented in this study. The grey markers show data available in the literature.

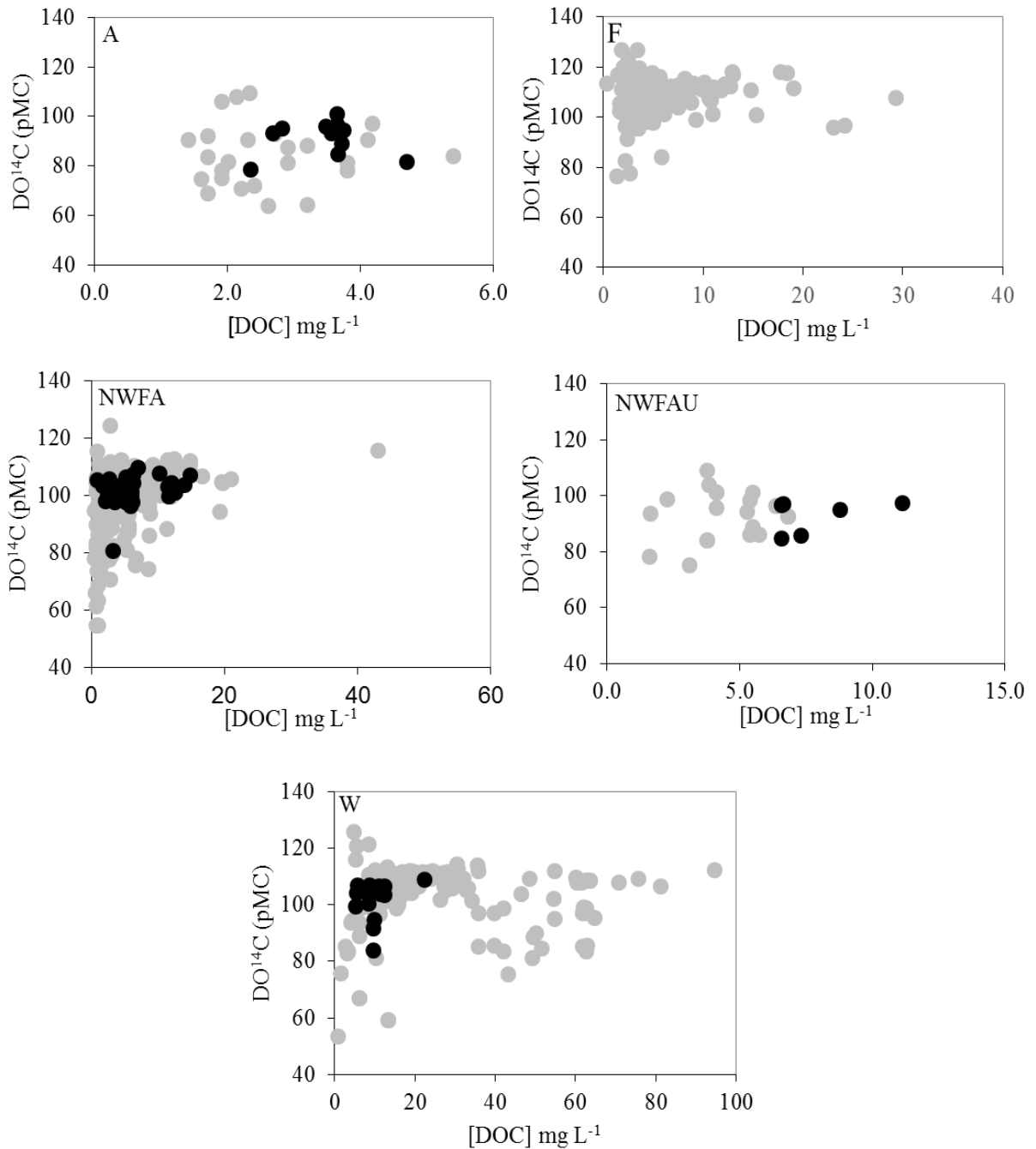


Figure 5.4 DO¹⁴C and DOC concentration for the global dataset, classified by land use. A is arable, F is forested ecosystems, NWFA is catchments not dominated by wetland, forest or arable, NWFAU is the latter but with considerable urban influences, and W is wetland ecosystems. The black markers show the original UK dataset presented in this study. The grey markers show the global data available in the literature. New data on the forested UK catchment is not shown as DOC concentration was not available.

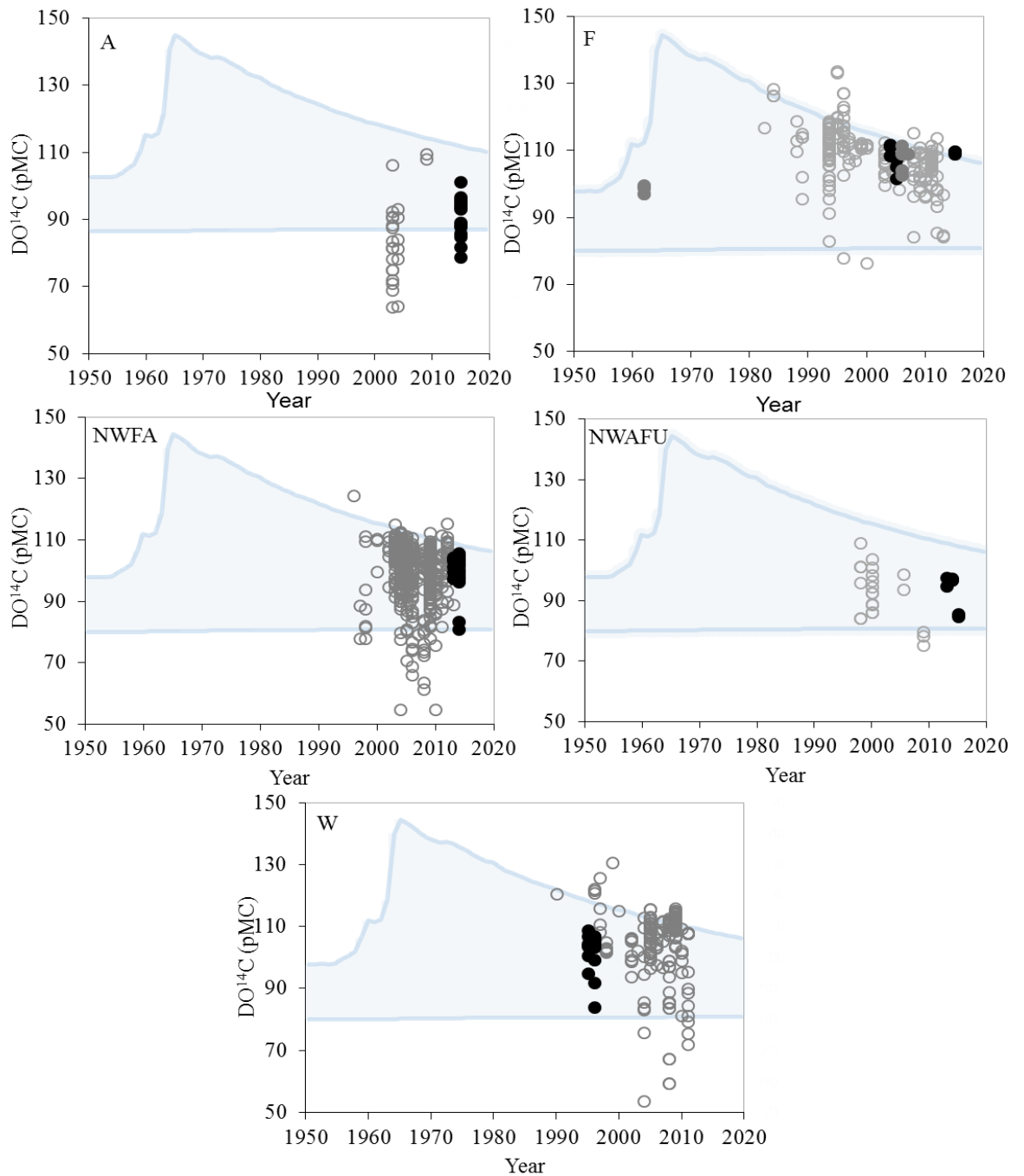


Figure 5.5. DO¹⁴C values for the global dataset, plotted by year and classified by land use. The upper blue line represents the average of the 1 year and 20 year pool. The lower line is the 2000 year SOM pool assuming steady state conditions. The black markers show the original dataset presented in this study. The hollow grey markers show data available in the literature. The filled grey markers show the previously unpublished Norwegian forested data.

6. The contribution of algae to freshwater dissolved organic matter:

Implications for UV spectroscopic analysis.

JL Adams, E Tipping, H Feuchtmayr, H Carter, P Keenan

Abstract

Dissolved organic matter (DOM) is an important constituent of freshwater. It controls aquatic ecological and biochemical cycling, and can be problematic in the water treatment process. Thus, the demand for rapid and reliable monitoring is growing, and spectroscopic methods are potentially useful. A model with three components, two absorbing in the ultraviolet (UV) range and one non-absorbing and present at a constant concentration, was previously found to give good predictions of dissolved organic carbon concentration, [DOC], across 1700 freshwaters ($R^2=0.98$). However, the model underestimated [DOC] in shallow, eutrophic lakes in the Yangtze Basin, China, raising the possibility that DOM derived from algae might be poorly estimated, and this is supported by new data for eutrophic British lakes. We estimated the extinction coefficients in the UV range of algae-derived DOM, from published data on algal cultures and new data from outdoor mesocosm experiments, in which high concentrations of DOC were generated under conditions similar to those in natural waters. The results demonstrate the weak UV absorbance of DOM from algae compared to terrestrial sources. Introduction of the new extinction coefficients into the three-component model allowed the contribution of algae-derived DOM to DOC in surface water samples to be estimated. Concentrations of DOC due to algae ranged from zero to 8.3 mg DOC L⁻¹, and the fraction of algae-derived DOC ranged from zero to 97%. Further work is required, using data from a wide range of contrasting

waters, to determine whether a generally-applicable model can be established to predict [DOC] from spectroscopic data.

Keywords: Absorption spectroscopy, algae, autochthonous, dissolved organic carbon

6.1. Introduction

Dissolved organic matter (DOM) is ubiquitous in surface, soil and ground waters, and chiefly comprises partially decomposed plant and animal material. It provides a source of energy for microbes, controls absorption of light and photochemical activity, sorption of metals and other organic pollutants, and pH buffering. Reactions of DOM with chlorine during drinking water treatment produce by-products including trihalomethanes and haloacetic acids, which are a risk to human health (Nguyen et al., 2005). The need to monitor the quality and quantity of DOM has increased considerably in recent years, partly because of the widespread observed increases in concentrations and fluxes of dissolved organic carbon (DOC) (Monteith et al., 2007), which has implications for ecology and the costs of water treatment.

Dissolved organic matter is routinely quantified by the DOC concentration, [DOC], for example by infra-red detection of CO₂ after combustion. Significant correlations between optical absorbance and [DOC] mean that approximate quantification can be achieved from UV-visible absorption spectroscopy at a single wavelength. However, temporal and spatial variation in the spectroscopic properties of DOM, exploited for example in the use of specific ultra-violet absorbance (SUVA) as an indicator of DOM quality (Weishaar et al. 2003), means that the single wavelength approach cannot generally provide an accurate measure of [DOC] (Tipping et al., 2009). Therefore, Tipping et al. (2009) developed a two-component model employing UV

absorbance data at two wavelengths, and showed that it could provide precise estimates of [DOC] in a variety of surface water samples.

The two-component model adopted the linear sum of the concentrations of component A (DOC_A) and component B (DOC_B), representing strongly and weakly UV-absorbing material respectively. Further development of this modelling approach by Carter et al. (2012) introduced a third component – ‘component C’ which represents non UV-absorbing DOC assumed to be present at the same concentration in all samples. Thus, the [DOC] was further represented by the linear sum of the concentrations of the three components in the following equation:

$$[\text{DOC}] = [\text{DOC}_A] + [\text{DOC}_B] + [\text{DOC}_C] \quad (1)$$

Testing the adapted model over 1700 surface water samples resulted in good, unbiased predictions of [DOC] ($r^2 = 0.98$) with fixed spectral characteristics of the end members A and B, combined with a small constant concentration of component C at 0.8 mg L^{-1} . Thus, the dual wavelength approach may give the ability to measure [DOC] rapidly and cheaply, without the need for laboratory processing and measurement.

However, for eutrophic shallow lakes of the Yangtze basin (Zhang et al., 2005), the model underestimated [DOC] by an average factor of 2.1 (Carter et al., 2012). The average extinction coefficient of $6.5 \text{ L g}^{-1} \text{ cm}^{-1}$ at 280 nm in these samples suggests the presence of material that absorbs UV light more weakly than either component A or B. Further, Zhang et al. (2005) found a positive relationship between DOM fluorescence and eutrophication in the Yangtze basin lakes, which indicated possible influences from phytoplankton production. Therefore, it appears that the three-component, dual wavelength (Carter) model may be effective only when the DOM

under consideration is predominantly terrestrial in origin, and further investigation of the optical properties of algae-derived DOM, and how they affect the performance of the model is necessary.

UV spectroscopic data for DOM derived from different algal species have been reported by Nguyen et al. (2005), who worked with axenic cultures, and by (Henderson et al., 2008), who worked with non-sterilised cultures, both under laboratory conditions. Nguyen et al. (2005) reported that the DOM produced comprised labile carbohydrates and proteins, with low SUVA values compared to those of terrestrially-sourced DOM. Henderson et al. (2008) also found the DOM to absorb UV light weakly. De Haan and De Boer, (1987) concluded from field observations of [DOC] and UV absorbance of the humic lake Tjeukemeer that water entering from the neighbouring eutrophic lake Ijsselmeer brought weakly UV-absorbing DOM. Osburn et al., (2011) studied saline waters of the prairie lakes region of the USA, which were rich in DOM of autochthonous (i.e. algal) origin, created by bacterial processing of primary production, and reported optical absorption at 350 nm. Their values were appreciably lower than those commonly observed for waters with comparable [DOC] but with terrestrial sources of DOM (Carter et al., 2012).

These laboratory and field observations suggest that DOM derived from algae has different absorption characteristics from terrestrially sourced material, but they do not permit a general quantitative assignment of spectroscopic parameters. Therefore, we aimed to quantify the contribution of algae-derived DOM to freshwater [DOC], and to UV absorbance, in order to evaluate how the presence of such DOM in water samples would affect estimation of [DOC] by UV spectroscopy. By this means, we made new measurements on algal derived DOM, using outdoor mesocosms, which offer conditions arguably more realistic than those in algal cultures. From the available

data, we then derived representative extinction coefficients for algae-derived DOM. The absorbance parameters were used to analyse the data for a new freshwater sample set, biased towards eutrophic water bodies, to estimate concentrations of algae-derived DOM and the fraction of total [DOC] that they account for.

6.2. Methods

6.2.1. Model explanation

The measure of optical properties used here is defined by the extinction coefficient of the sample (E ; also known as specific absorbance), which is the ratio of the absorbance at a given wavelength to [DOC] and with units $L\ g^{-1}\ cm^{-1}$ (Tipping et al., 2009). The basis of the model of Carter et al. (2012) is that the DOM that absorbs UV light can be represented as a mixture of two components, A and B, each with a defined UV spectrum. The fraction of component A (f_A) is derived from the extinction coefficients of components A and B as given by:

$$f_A = \frac{E_{B,\lambda_1} - R E_{B,\lambda_2}}{R(E_{A,\lambda_2} - E_{B,\lambda_2}) + (E_{B,\lambda_1} - E_{A,\lambda_1})} \quad (2)$$

where E_A and E_B are the extinction coefficients of components A and B at two given wavelengths (λ_1 and λ_2) and R is the measured ratio of absorbance at the same two wavelengths. The value of f_A can then be substituted into the following equation to obtain a single extinction coefficient for the sample being measured:

$$\begin{aligned} E_{AB,\lambda} &= f_A E_{A,\lambda} + f_B E_{B,\lambda} \\ &= f_A E_{A,\lambda} + (1 - f_A) E_{B,\lambda} \end{aligned} \quad (3)$$

where $E_{AB,\lambda}$ is the extinction coefficient of the sample at either of the two chosen wavelengths and f_A and f_B are the fractions of components A and B ($f_A + f_B = 1$).

To calculate the total [DOC], the measured absorbance at the chosen wavelength is divided by $E_{AB, \lambda}$ from equation 3, with the constant [DOC_C] (0.8 mg L⁻¹) added.

$$[DOC] = \frac{A_{\lambda}}{E_{AB, \lambda}} + [DOC_C] \quad (4)$$

The choice of wavelengths for the calculation is flexible, as long as they differ sufficiently. Carter et al. (2012) reported extinction coefficients for a number of wavelengths in the range 254 – 355 nm, and used various combinations to analyse published data. The model is best-applied to filtered samples (as used in the present work) and is assumed to apply to all freshwaters irrespective of pH or ionic composition. Henceforth, we shall refer to the three component model with fixed [DOC_C] as the Carter model.

6.2.2. Sample collection and processing

The mesocosms are part of the CEH aquatic mesocosm facility (CAMF) (<http://www.ceh.ac.uk/our-science/research-facility/aquatic-mesocosm-facility>, accessed May 2016). The facility contains 35 mesocosms, each of 2 metre diameter and 1 metre depth, simulating shallow lakes. Of the 35 mesocosms used for a stressor experiment, four were selected (mesocosms 4,7,15 and 20) to generate a range of chlorophyll concentrations, [Chl_a]. As part of the stressor experiment, each of the mesocosms had various climatic simulations implemented, including heating and nutrient addition (DOM free). Mesocosms 4 and 20 were both unheated with intermittent nutrient addition, 7 was heated with intermittent nutrient addition and 15 was heated without intermittent nutrient addition. Sampling took place on seven occasions between February and August 2015. The dominant phytoplankton classes for each of the four mesocosms were Chlorophyceae and Cyanophyceae, with a

bloom of Euglenid in mesocosm 7 in the early summer. A 500 ml sample was collected from the four mesocosms in pre-rinsed vessels. A 125 ml sub-sample was filtered using a Whatman GF/F (0.7 μm) filter paper. Analysis of [DOC] and [Chla] were performed as described in the analyses section below.

Surface water samples representative of different states of eutrophication and DOM source were collected from catchments in the North of England (Figure 6.1, Table 6.1, Appendix 6.1). The sample sites included the Shropshire – Cheshire meres region, which are situated in the north-west midland outwash plains, and drain predominantly small catchments of agricultural, urban and parkland catchments (Reynolds, 1979; Moss et al. 2005). Fisher et al. (2009) showed a range of [Chla], from 2-68 $\mu\text{g L}^{-1}$ across the meres region (Appendix 6.1). Ten of the samples taken were from sites situated in the outer reaches of the Lake District national park and four samples were from reservoirs in west Yorkshire, all of which drain predominantly upland moorland. Ten further sites included small farm ponds in the Fylde area of Lancashire, and rivers and small streams draining lowland arable farmland and urban areas in Yorkshire. One 500 ml sample was collected from each site, after rinsing the vessel with the surface water. The samples were taken back to the laboratory where they were filtered using a Whatman GF/F (0.7 μm) filter, which was subsequently used for [Chla] analysis. The filtered sample was then analysed for [DOC]. All samples were processed within three days after collection.

6.2.3. Analyses

The determination of phytoplankton [Chla] followed closely with the method of Maberly et al. (2002). A known volume of the sample was filtered through a Whatman GF/F (0.7 μm) filter paper and immediately submerged in 10 mL of industrial methylated spirit (96% ethanol, 4% methanol). This was left overnight, in the dark at 4 °C. Following centrifugation at 4500 rpm, absorbance was read using an Agilent 8453 diode spectrophotometer with a 1 cm quartz cuvette. Absorbance readings from 665 and 750 nm were used to calculate [Chla] following Marker et al. (1978). The mesocosm samples were analysed for [Chla] by the CAMF team using a Whatman GF/C (1.2 μm) filter paper, which was submerged in 10 mL 96% ethanol and left overnight at 4 °C. Though different extraction methods were used, a comparison between ethanol and methanol mix were found to be equally efficient (Jespersen and Christoffersen, 1987). Mesocosm samples collected on the 12th August 2015 were analysed in situ using an AlgaeTorch (bbe moldaenke, Germany). The AlgaeTorch was used for all 32 mesocosms during eight months of the prior experiment alongside the above extraction method. The regression of all data was used to calculate [Chla] for the 12th August 2015 ($r^2 = 0.67$, $p < 0.0001$).

The filtered water from the field samples were analysed for pH and conductivity using a glass probe with a Radiometer instrument and a Jenway 4510 probe respectively. The pH electrode and conductivity meter were calibrated at the beginning of each sample set. For the mesocosm experiment, pH and conductivity were measured in situ, using a Hydrolab DS5X multiparameter data sonde (OTT Hydromet). For samples collected on 12/8/2015 and 26/8/2015, pH and conductivity were measured

using an EXO2 multiparameter data sonde (Exowater). Both multiparameter sondes were calibrated in the laboratory before sampling the mesocosms.

A 3 mL sample was measured for absorbance in the UV-Vis range (200 nm – 900 nm) using an Agilent 8453 diode spectrophotometer with a 1 cm path length quartz cuvette. Prior to each sample batch, measurements were made on a blank using Milli-Q water, which the spectrum of the samples are corrected against. A 10 mg L⁻¹ solution of naphthoic acid was used as a quality control. Absorbance values at 270 nm, 350 nm and 700 nm were selected for [DOC] calculation following the model described in Tipping et al. (2009) and Carter et al. (2012).

The remaining sample was acidified with 3 M hydrochloric acid and purged with zero grade air for 4 minutes to remove any inorganic carbon. The sample was then combusted at 905 °C with cobalt chromium and cerium oxide catalysts, which converts all leftover carbon to CO₂. The CO₂ was measured for [DOC] through infra-red detection using a Skalar Formacs CA16 analyser.

Calculations of standard deviations, t-tests, and regression analyses were carried out using Microsoft Excel. The Solver function in Microsoft Excel was used to perform minimisations in the apportionment calculations.

6.3. Results

6.3.1 Estimating extinction coefficients for DOM derived from freshwater algae

The four selected mesocosms were repeatedly sampled and represent enclosed systems where allochthonous inputs are negligible. They therefore simulate conditions where the dominant DOM component is algae-derived and includes subsequent microbial processing. Measured and modelled [DOC], and absorbance data for the

four mesocosms are shown in Figure 6.2. At 270 nm and 350 nm, the absorbance increased slightly through time. The modelled [DOC] also slightly increased, but the measured [DOC] increased considerably, from 8.2 mg L⁻¹ to 48.2 mg L⁻¹ in mesocosm 4 for example. The same pattern can also be seen in the mesocosms with lower [DOC] such as mesocosm 15, which increased from 4.5 mg L⁻¹ to 14.1 mg L⁻¹. The [DOC] and absorbance results presented in Figure 6.2 were plotted in terms of their extinction coefficients over time (Figure 6.3). Here, it can be seen that the optical properties of the DOM progressively declines over both wavelengths. Furthermore, there was a significant relationship ($P < 0.005$) between measured [DOC] and [Chla] for the mesocosm samples (see Appendix 6.2). The average pH for the mesocosms was 9.7, and there was no significant relationship observed between measured [DOC] and pH.

By considering the changes involved in the mesocosms during the sample period, the extinction coefficients of the additional DOC produced were estimated. The increase in [DOC] was firstly calculated for each of the mesocosms by finding the differences between the first data point, and the last four. Then, the average between the four mesocosms was determined. The same was done for the absorbance values at both wavelengths. The ratio of the average absorbance and [DOC] increase was calculated to provide average extinction coefficients, which were 4.90 L g⁻¹ cm⁻¹ at 270 nm and 1.09 L g⁻¹ cm⁻¹ at 350 nm. Average extinction coefficients of the laboratory simulations of green algae, cyanobacteria and diatom cultures were also calculated from the SUVA (254nm) values presented in Henderson et al. (2008) and Nguyen et al. (2005), which gave similar values to the mesocosm experiments, at 4.2 L g⁻¹ cm⁻¹ and 4.8 L g⁻¹ cm⁻¹ respectively. Direct quantification of the optical properties of oceanic DOM are not commonly quoted. Therefore, in view of the fact that DOM in

the open ocean is also largely phytoplankton derived (Biddanda and Benner, 1997; Jiao et al., 2010), we estimated extinction coefficients for marine DOM, for the Mid-Atlantic Bight region. This was calculated by combining absorbance data (Helms et al., 2008), with a measured [DOC] of 0.9 mg L^{-1} (Guo, Santschi and Warnken, 1995). The extinction coefficients at 270 nm and 350 nm for the open ocean were 6.4 L g cm^{-1} and 1.0 L g cm^{-1} respectively, which are similar to the values obtained for the mesocosms, lab cultures and Yangtze basin samples (Table 6.2). All of these values are compared with the model parameters derived by Carter et al. (2012) (Table 6.2), and show that all of the calculated values fall considerably below the modelled parameters for components A and B.

6.3.2 *Natural water samples*

The field sites included arable farm ponds, small lakes, reservoirs and small streams, with different extents of eutrophication, as indicated by the averages and ranges of [Chla] (see Appendix 6.1). A range of [DOC], pH and conductivity was measured across all of the field samples, and are summarised in Table 6.1.

Samples collected from the field sites showed the widest range of [DOC], from 1.7 mg L^{-1} in a soft water lake to 63.5 mg L^{-1} in a peat dominated lake (Figure 6.4, Appendix 6.1). Overall, the field samples gave a relatively good fit, with an average modelled:measured ratio of 0.96. However, model predictions for seven sites were too low (average modelled:measured ratio = 0.7) and these were all situated in the Shropshire-Cheshire meres region. In our judgement, the results from these seven sites cannot be satisfactorily explained by the model. Combining the data from all of the Shropshire - Cheshire meres sites with the Yangtze Basin samples identified in

Carter et al. (2012) shows that the model fails with eutrophic lakes and this is worse in samples with lower [DOC] (Figure 6.5).

6.3.3 Modification of the three-component model of UV absorption

We modified the three-component model of Carter et al. (2012) by replacing the non-UV-absorbing component C (equations 1 and 3), present at the same fixed concentration in all samples, with a component, C2, that represents DOM originating from algae, and has the extinction coefficients (Table 6.2) derived as described above. First, we examined whether this affected application of the model to data from 426 UK surface water samples previously used by Carter et al. (2012) to derive model parameters. This was done by re-optimization, assuming component C2, rather than C, to be present at a fixed concentration. The derived parameters using component C2 were almost the same as the original values; the new fitted extinction coefficients for components A and B differed by less than 0.5% from the original ones, and the fixed concentration of C2 was greater by only 0.06 mg L⁻¹. Therefore we concluded that the substitution of the weakly UV-absorbing component C2 for the non-absorbing C does not affect the model parameters when applying the model to samples with, on average, little algae-derived DOM.

We next used the modified model to quantify the contribution of algae-derived DOM to freshwater samples. In this application, the model is not being used to estimate [DOC], but rather uses the measured value to estimate the fractions of components A, B and C2 in the sample. The observed absorbance at a given wavelength is given by:

$$A_{\lambda} = [\text{DOC}] \{f_A E_{\lambda A} + f_B E_{\lambda B} + f_{C2} E_{\lambda C2}\} \quad (4)$$

Since f_A , f_B and f_{C2} must total unity, only two need to be specified, and therefore all three values can be estimated from absorbance values at two appropriately-separated wavelengths, for a known (measured) value of [DOC]. This was done for each sample by minimizing the sum of the squared residuals between the measured and calculated absorbance values. For the new data reported here, we used wavelengths of 270 nm and 350 nm, while for the Yangtze basin samples (Zhang et al., 2005) the wavelengths were 280 nm and 355 nm (Table 6.2). The calculation procedure yields values of f_A , f_B and f_{C2} , together with [DOC_A], [DOC_B] and [DOC_{C2}]. For comparison, we also set the modified C2 parameters with the assumption that C2 did not absorb at all in the UV, by setting the C2 parameters to zero.

6.3.4 DOM derived from algae in freshwater samples

The results of the modified model showed that the proportion of [DOC_{C2}] increased with increasing f_{C2} (Figure 6.6), with over half of the sites showing high proportions of f_{C2} (Table 6.3), which included the Shropshire – Cheshire meres sites and the Yangtze Basin samples. Typically, the Shropshire – Cheshire meres sites were low in f_A , with the majority of the [DOC] made up of f_A and f_B . The exception is SCM7(a) (Hanmer 1), which was almost entirely f_A , despite being poorly predicted by the model. The f_{C2} value shows that the contribution of algae-derived DOC can be as high as 0.97 (97%). This was observed in one of the Yangtze basin samples (YB15), which equated to 4.1 mg L⁻¹ DOC out of 4.3 mg L⁻¹. There was a wide range of f_{C2} values across the sample set, from 0.7 - ≤ 0, but the average contribution of algal DOC observed was 0.41 (41%), which equated to an average [DOC_{C2}] contribution of 2.7 mg L⁻¹. The results further suggested that the model will underestimate overall [DOC] with f_{C2} values from as little as 0.35 (35%), which was observed in SCM7(b) (Hanmer

2) (Table 6.3). The sites that had negligible f_{C2} values consisted of mainly the river and tributary sites and sites from the Lake District, all of which were predicted well originally and tended to have higher proportions of f_A . In comparison, the average contribution of algal DOC when the C2 parameters were set to zero, was 0.36 (36%), with a $[DOC_{C2}]$ contribution of 2.3 mg L^{-1} , making a difference of 0.05 and 0.38 mg L^{-1} respectively. This therefore demonstrated that the small C2 values make little difference to the outcome of the $[DOC_{C2}]$ and the f_{C2} values (Appendix 6.3).

6.4. Discussion

The mesocosm experiments provided a valuable simulation of a shallow lake system, and our assumption is that the DOM produced during the observation period results from the fixation of atmospheric CO_2 by algae and its subsequent release. Although some allochthonous sources could influence the mesocosm DOC, these can be discounted for the following reasons. (1) The climatic simulation experiment conducted by the CAMF team commenced in 2013, when sediment from a natural lake was added to the mesocosms, and therefore there has been enough time for DOC in the water column to come to equilibrium with the sediment. (2) An increase in pH could provide a mechanism for releasing DOC from sediment (Tipping 2002), but during our observation period there were no systematic changes in pH, and thus is reasonable to assume that there was no net DOC release from the sediment during this time. (3) Addition of allochthonous DOM into the mesocosms may have occurred through rainfall, but rainwater $[DOC]$ is typically low, around 0.6 mg L^{-1} for parts of the UK (Wilkinson et al., 1997) and $< 2 \text{ mg L}^{-1}$ globally (Willey et al., 2000), insufficient to generate the large observed increases in $[DOC]$ - and would not drastically affect the results. (4) There was a significant relationship ($P < 0.005$)

between [DOC] and [Chla] for all of the observed mesocosms, supporting the fact that DOC not explained by the model must be derived from phytoplankton sources.

However, this relationship is weak, as the measure of [Chla] is related to phytoplankton production, which is not necessarily equal to the rate of decay, and thus release of the algae-derived DOC.

When the mesocosm data are plotted in time series, the absorbances at 270 nm and 350 nm and the modelled [DOC] increased slightly (Figure 6.4). In contrast, the measured [DOC] through time increased considerably, suggesting that the extra material produced within the mesocosms can be detected in the UV-Vis range, but are poorly absorbing. The Carter model therefore failed to accurately predict [DOC] in the mesocosms because the DOM produced is below the lower limit set for component B. The observed increase in absorbance values suggested that the material is not completely invisible, thus would not be accounted for in component C either. The production of weakly absorbing material is also reflected in the decrease in extinction coefficients across both wavelengths through time (Figure 6.5). Since DOM present in the open ocean is also largely phytoplankton derived, the calculated extinction coefficients were compared and were found to be in strong agreement (Table 6.2). At 254 nm, the extinction coefficients for the laboratory cultures of green algae, cyanobacteria and diatoms were also compared and were found to be in agreement. We therefore assume that a single representative set of extinction coefficients for algae derived DOM for analysing freshwaters is reasonable.

The extinction coefficients of algae-derived DOM, calculated for the new component C2 parameters (Table 6.2), represent very low light absorbing properties. This therefore suggests that the constituent molecules lack conjugated or aromatic moieties commonly associated with fulvic acids derived from lignin phenols (Del Vecchio and

Blough, 2004), and thus terrestrially derived material. When the contribution of algae-derived DOC was small, the model worked by assuming the low absorbing values were zero and with constant concentration (0.8 mg L^{-1}). However, this was not the case when a substantial portion of the overall [DOC] was derived from $[\text{DOC}_{C2}]$. Nevertheless, the similarities between the new C2 parameters and the zero values demonstrate that the absorbance by C2 is considerably low.

By substituting the fixed component C parameter (0.8 mg L^{-1}), to the algae-derived DOM values, we were able to reasonably quantify the contribution of algae-derived DOM to the overall [DOC] of the samples. By far the highest $[\text{DOC}_{C2}]$ concentration was 8.27 mg L^{-1} , which was observed in SCM2 (Blakemere Moss) (Table 6.3).

However, the f_{C2} value for this site was much lower in comparison to the rest of the sites, reflective of the outstandingly large overall [DOC] (63.5 mg L^{-1}). While the overall concentration of algae-derived DOC may not be high, large fractions of f_{C2} were observed in samples with lower overall [DOC]. These also included the sites that were unsatisfactorily predicted by the original model. Therefore, algae-derived DOM does have the potential to account for large proportions of DOC in some freshwaters, and it is particularly important in eutrophic waters with smaller overall concentrations of DOC. This could have considerable effects on the direct monitoring of freshwater [DOC] through absorbance spectroscopy and could lead to underestimations in highly eutrophic freshwaters.

Thus, the current state of the model is that [DOC] is predicted well across a range of optical properties, including material transformed through photodegradation (reflected by f_B in Table 6.3), which considerably reduces the absorbance (Donahue et al. 1998; Waiser et al. 2000). For example, satisfactory model predictions were still achieved

despite the longer residence time of DOM and high proportions of component B in a series of lake samples from Ontario, Canada (Carter et al., 2012). This further supports the fact that allochthonous material in any state can be managed by the model, but when a significant fraction of algae-derived DOM is present, the model will fail. However, the capability of the model cannot be solely determined by the [Chla] as eutrophic and hypereutrophic systems can still be successfully modelled, if the dominant source of DOC is allochthonous.

The quantification of algae-derived DOM through the new component C2 parameters suggests that the non-absorbing fixed value of component C (0.8mg L^{-1}) can be replaced. In principle, this can be done to estimate the total [DOC] if the absorbance at three wavelengths is used. However, the low light absorbance of the C2 parameters will have implications on the prediction of [DOC] if high precision monitoring is not used. What cannot be clear from the analyses is whether the algae-derived DOM produced within the samples is homogenous. Realistically, the material produced is likely to comprise a range of optical properties, such that the calculated extinction coefficients are not absolute. However, the similarity between the extinction coefficients for the mesocosms, the open ocean example, and the laboratory cultures of Henderson et al. (2008) and Nguyen et al. (2005), suggest that assuming homogenous spectral properties for algae-derived DOM is reasonable. For a validated quantification of algae-derived DOM, further investigation into the material produced from different species would be necessary.

Moreover, other instances where the Carter model have failed to predict DOC need to be considered. Pereira et al. (2014) found that streams of tropical rainforests in Guyana contained between 4.1% and 89% optically invisible DOM in response to rainfall events. Here, the modelled [DOC] was also considerably less than the

measured [DOC]. Therefore, large concentrations of natural DOM components not detectable by UV-Vis are also possible, although the source of this material is likely to differ from that observed in our sample set.

Intensive monitoring of DOC is becoming increasingly important, particularly for water treatment purposes. This work considerably increases our understanding of analysing multiple components of freshwater DOC and thus their origins and behaviour, and demonstrates that accurate in situ monitoring could be a viable commercial option. When applied to natural systems where terrestrial DOM is likely to dominate, the Carter model in its current state provides a useful and reliable means of measuring [DOC]. However, users of the current model should consider its efficacy under circumstances where phytoplankton derived DOM is dominant and in these situations, confirmatory direct DOC measurements are advised.

6.5. Conclusions

- A previously developed 3-component model gave good predictions of [DOC] for natural water samples containing terrestrially dominant DOM sources. In shallow, eutrophic lake samples, the model gave unsatisfactory predictions of [DOC].
- The contribution of algal DOC to the overall concentration can be quantified, by using the extinction coefficients derived from the mesocosm time series experiments, to use as new parameters for a variable model component C (C2).
- The variable component C2 showed that algal DOC can account for up to 97% of the overall [DOC] of highly eutrophic freshwaters, which could have

considerable implications on the direct prediction of freshwater [DOC] using UV-Vis.

- The optical properties of algae-derived DOM in freshwaters are therefore reasonably quantifiable, and consideration for a replacement, variable third model component should be considered.

6.6. Acknowledgements

This research was funded by the UK Natural Environment Research Council CLASPDOG project (Grant No: ST/K00672X/1). The mesocosm experiment was part of the MARS project, funded under the 7th EU Framework Programme (contract no. 603378). We are grateful to Jessica Richardson, Mitzi De Ville and other team members of the CEH aquatic mesocosm facility (CAMF) for collecting samples and providing data, to Stephen Maberly for providing guidance and to Pamela Tipping for help with field sampling.

Table 6.1. Summary of [DOC], pH, conductivity and [Chla] for the field sites.

Sample type	Number of samples collected	Average [DOC] measured mg L ⁻¹	Average [DOC] modelled mg L ⁻¹	Average pH	Average Conductivity μs cm ⁻¹	Average [Chla] μg L ⁻¹
SCM	21	14.1	11.7	8.2	358.0	14.3
LD	10	2.9	2.9	7.6	86.0	14.1
RES	4	8.9	10.4	7.2	96.0	16.7
FY	5	21.7	22.6	8.0	311.0	91.5
RIV	6	4.6	4.4	7.8	598.0	16.1
RTB	9	3.5	3.7	7.9	647.0	13.6

* SCM= Shropshire Cheshire meres, LD = Lake District, RES = Reservoirs, FY = Fylde farm ponds, RIV = River, RTB= Tributary/small stream

Table 6.2. Calculated extinction coefficients for phytoplankton derived material in the mesocosms and the open ocean. Model extinction coefficients for components A and B are parameters obtained from Carter et al. (2012). Mesocosm extinction coefficients were derived from data in Figure 6.2. Open ocean extinction coefficients were derived from data provided in Helms et al. (2008) and Guo et al. (1995). The Yangtze basin samples were obtained from Zhang et al. (2005), the axenic culture from Nguyen et al. (2005) and the non-axenic culture from Henderson et al. (2008).

	Extinction coefficients ($E_{\lambda \text{ nm}}$) ($\text{L g}^{-1} \text{ cm}^{-1}$)				
	E_{270}	E_{350}	E_{254}	E_{280}	E_{355}
Model component A	69.3	30.0	77.1	63.9	27.9
Model component B	15.4	0.0	21.3	12.0	0.0
Model component C	0.0	0.0	0.0	0.0	0.0
Algal derived DOM*	4.9 (± 2.9)	1.1 (± 1.1)	4.3 (± 3.0)	3.2 (± 4.1)	1.0 (± 1.0)
Open ocean DOM	6.4	1.0	8.2	4.9	0.7
Yangtze Basin	-	-	-	6.5	1.5
Axenic lab culture	-	-	4.8 (± 1.3)	-	-
Non-axenic lab culture	-	-	4.2 (± 2.4)	-	-

* The algal derived DOM was derived from the mesocosm time series. These were the parameters used for the new variable component C2.

Table 6.3. Calculated fractions of A, B and C2 using the new parameters derived from the mesocosm experiments and the corresponding proportions of [DOC] in mg L⁻¹. Samples are listed by their specific ID – site names and locations can be found in Appendix 6.1.

Sample ID	[DOC] measured mg L ⁻¹	f_A	f_B	f_{C2}	[DOC _A] mg L ⁻¹	[DOC _B] mg L ⁻¹	[DOC _{C2}] mg L ⁻¹
RTB1(b)	2.67	0.31	0.69	0.00	0.82	1.85	0.00
RTB1(a)	2.44	0.65	0.35	0.00	1.58	0.86	0.00
RES2	8.91	0.83	0.17	0.00	7.41	1.50	0.00
RES4	8.89	0.42	0.58	0.00	3.73	5.16	0.00
FY3	28.7	0.33	0.67	0.00	9.61	19.09	0.00
RES3	9.63	0.84	0.16	0.00	8.12	1.51	0.00
RES1	8.34	0.70	0.30	0.00	5.87	2.47	0.00
SCM7(a) *	13.8	1.00	0.00	0.00	13.80	0.00	0.00
FY5	32.4	0.67	0.33	0.00	21.80	10.60	0.00
RIV2(a)	2.81	0.40	0.57	0.02	1.13	1.61	0.07
SCM9(a)	9.89	0.17	0.81	0.01	1.71	8.05	0.13
LD4	2.19	0.26	0.68	0.07	0.56	1.48	0.14
RTB3(a)	3.47	0.36	0.54	0.10	1.24	1.89	0.34
RTB2(a)	3.65	0.22	0.65	0.13	0.80	2.39	0.46
LD10	2.13	0.24	0.54	0.23	0.51	1.14	0.49
LD9	3.86	0.38	0.44	0.19	1.45	1.69	0.72
RIV2(b)	2.34	0.25	0.42	0.32	0.60	0.99	0.76
LD1	3.57	0.24	0.53	0.22	0.87	1.91	0.79
LD2	1.67	0.32	0.20	0.48	0.54	0.33	0.81
LD7	1.93	0.18	0.40	0.42	0.35	0.77	0.82
LD3	2.94	0.19	0.51	0.31	0.56	1.49	0.90
RIV2(c)	3.74	0.29	0.46	0.26	1.07	1.71	0.96
RTB1(c)	3.65	0.28	0.43	0.29	1.02	1.58	1.04
RTB2(c)	3.72	0.24	0.47	0.28	0.90	1.76	1.06
LD6	2.18	0.33	0.16	0.51	0.72	0.35	1.10
RTB2(b)	3.66	0.25	0.43	0.32	0.91	1.57	1.18
RTB3(c)	3.56	0.31	0.32	0.37	1.10	1.15	1.30
FY1	15.3	0.30	0.60	0.09	4.64	9.23	1.43
SCM6(a)	10	0.19	0.66	0.15	1.86	6.59	1.54
RIV1(c)	6.57	0.26	0.50	0.24	1.73	3.27	1.56
RIV1(a)	5.1	0.57	0.12	0.31	2.90	0.62	1.58
RTB3(b)	4.7	0.23	0.43	0.34	1.09	2.00	1.60
LD8	2.81	0.19	0.22	0.59	0.54	0.62	1.64
SCM13	7.43	0.16	0.58	0.26	1.18	4.29	1.96
FY4	14.5	0.23	0.64	0.14	3.29	9.24	1.98
LD5	5.15	0.28	0.31	0.40	1.45	1.62	2.08
YB8	2.7	0.03	0.19	0.78	0.09	0.51	2.10
SCM8	20.1	0.22	0.64	0.14	4.39	12.96	2.76
SCM14	7.46	0.18	0.45	0.37	1.32	3.35	2.79
SCM3	7.69	0.13	0.50	0.37	1.03	3.83	2.83
SCM16(a)	11.3	0.11	0.64	0.25	1.22	7.21	2.87
RIV1(b)	7.3	0.19	0.41	0.40	1.42	2.99	2.88
YB10	3.7	0.02	0.18	0.79	0.09	0.68	2.93
YB22	4.1	0.03	0.17	0.79	0.13	0.71	3.25

Table 6.3. (Continued)

Sample ID	[DOC] measured mg L ⁻¹	f_A	f_B	f_{C2}	[DOC _A] mg L ⁻¹	[DOC _B] mg L ⁻¹	[DOC _{C2}] mg L ⁻¹
SCM5	10.7	0.12	0.58	0.31	1.25	6.17	3.28
YB5	4.1	0.02	0.13	0.84	0.10	0.54	3.46
SCM17 *	6.2	0.08	0.35	0.57	0.50	2.18	3.52
YB2	4.9	0.03	0.23	0.74	0.16	1.11	3.64
YB16	4.4	0.03	0.14	0.83	0.13	0.63	3.64
SCM9(b)	10.9	0.13	0.54	0.34	1.37	5.88	3.66
FY2	17.8	0.29	0.50	0.21	5.09	8.99	3.72
YB19	4.7	0.00	0.19	0.81	0.00	0.90	3.79
SCM15	11.5	0.13	0.53	0.33	1.54	6.15	3.81
SCM12	16.7	0.13	0.63	0.24	2.13	10.48	4.09
YB3	4.3	0.00	0.04	0.96	0.00	0.15	4.15
YB7	5.6	0.03	0.23	0.74	0.16	1.27	4.17
SCM10 *	7.38	0.08	0.34	0.58	0.56	2.54	4.28
YB4	4.9	0.00	0.12	0.88	0.02	0.57	4.31
YB18	5	0.00	0.11	0.89	0.01	0.53	4.46
SCM4 *	8.42	0.07	0.40	0.53	0.59	3.37	4.46
SCM16(b) *	11.5	0.09	0.52	0.39	1.07	5.93	4.50
YB9	5.6	0.04	0.16	0.81	0.20	0.88	4.52
YB13	6.7	0.05	0.27	0.67	0.36	1.81	4.52
SCM11	7.79	0.07	0.35	0.58	0.53	2.72	4.54
YB6	5.5	0.01	0.15	0.84	0.05	0.85	4.60
YB14	5.8	0.01	0.15	0.84	0.03	0.90	4.87
SCM6(b) *	11.3	0.09	0.48	0.43	1.01	5.39	4.89
YB1	6.4	0.01	0.21	0.78	0.07	1.34	4.99
SCM1	27.7	0.26	0.56	0.19	7.16	15.39	5.15
SCM7(b) *	15.1	0.12	0.53	0.35	1.82	7.98	5.29
YB15	5.6	0.00	0.03	0.97	0.00	0.17	5.43
YB20	6.5	0.00	0.12	0.88	0.01	0.79	5.70
YB21	7.7	0.00	0.18	0.82	0.04	1.37	6.29
YB17	7.5	0.01	0.15	0.84	0.08	1.10	6.32
YB11	8.4	0.06	0.14	0.80	0.47	1.21	6.72
YB12	10.1	0.09	0.12	0.80	0.89	1.18	8.03
SCM2	63.5	0.47	0.40	0.13	30.09	25.14	8.27

* Samples that were not satisfactorily explained by the original model.

**SCM= Shropshire Cheshire meres, LD = Lake District, RES = Reservoirs, FY = Fylde farm ponds, RIV = River, RTB= Tributary/small stream, YB= Yangtze basin.

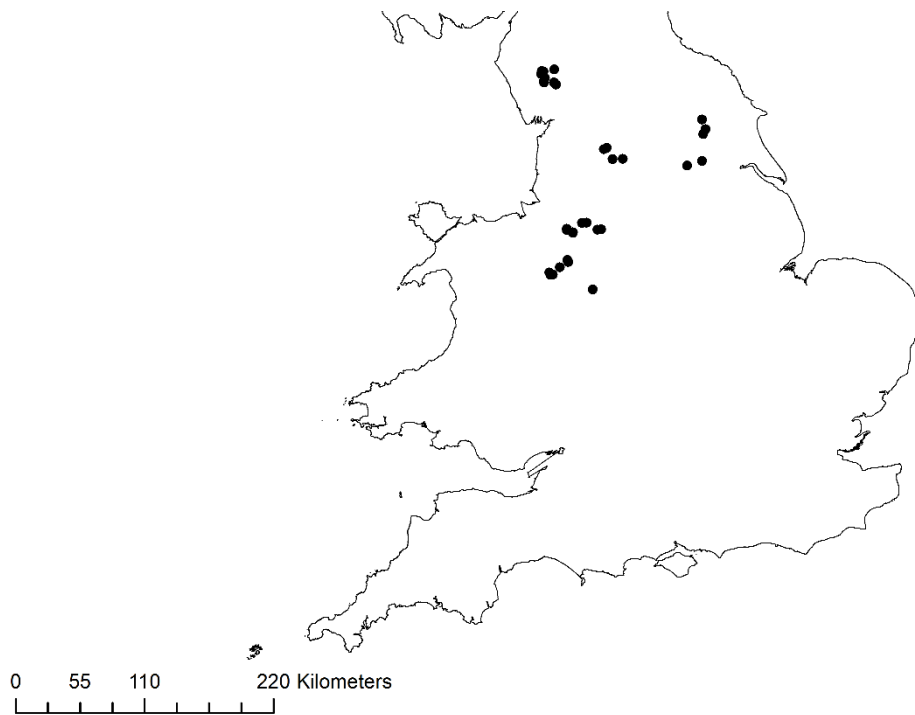


Figure 6.1. Locations of the sites where surface water samples were collected. Site Co-ordinates are provided in Appendix 6.1.

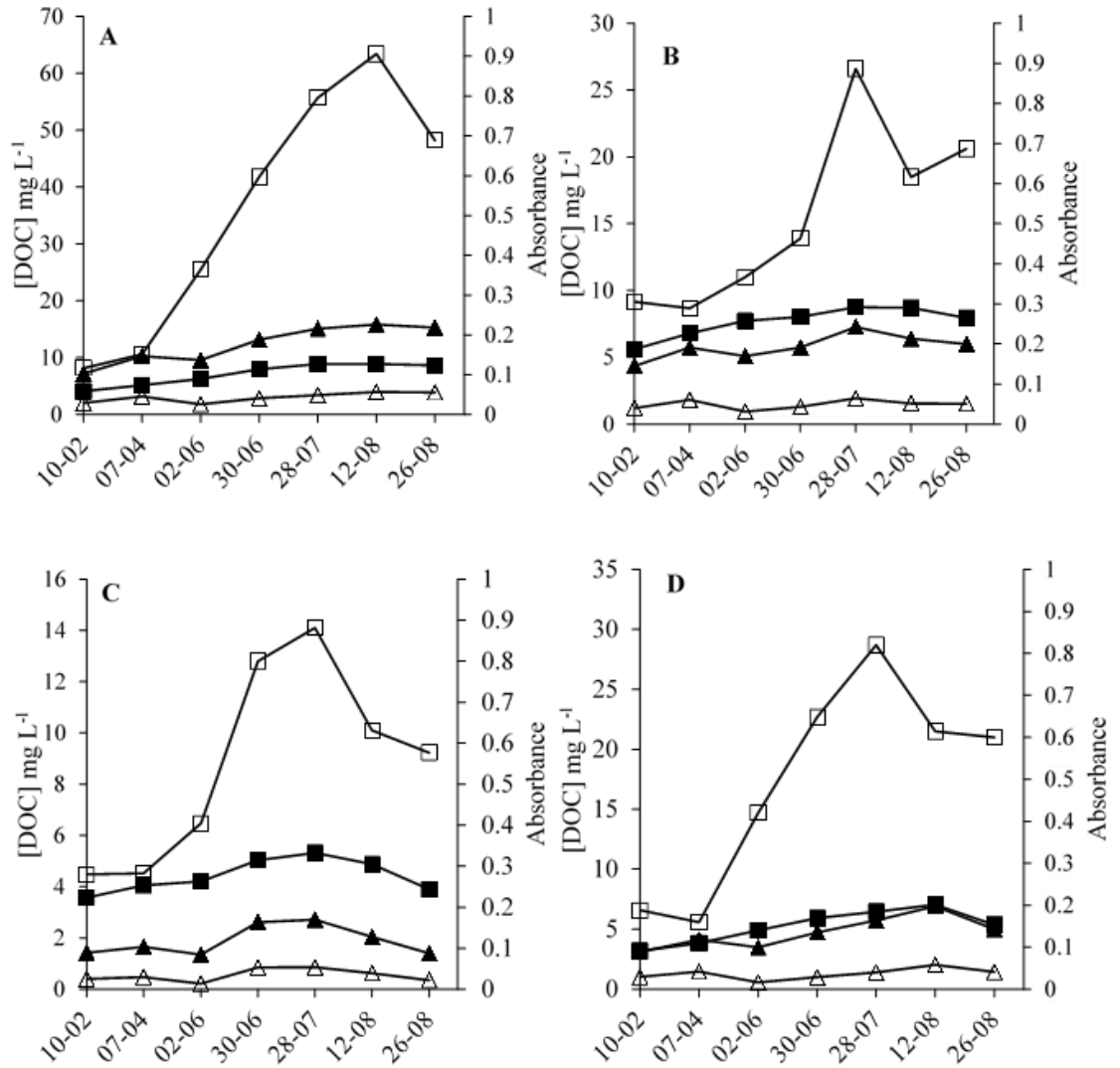


Figure 6.2. [DOC] and absorbance plotted through time for A) mesocosm 4, B) mesocosm 7, C) mesocosm 15 and D) mesocosm 20. [DOC] measured and [DOC] modelled are shown on the primary axis and are represented by the hollow and filled squares respectively. Absorbance at 270 nm and 350 nm are on the secondary axis and are represented by the filled and hollow triangles respectively.

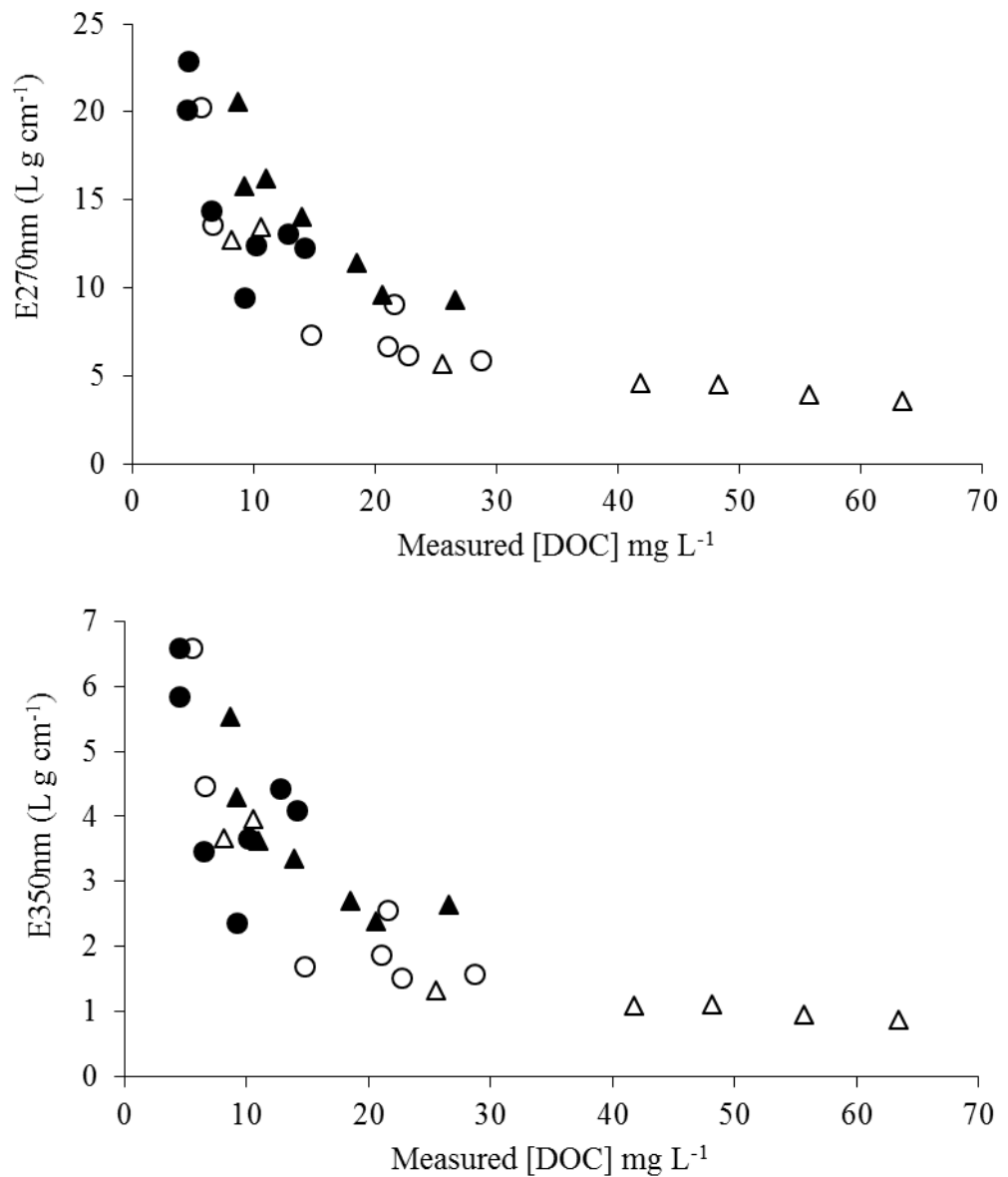


Figure 6.3. Extinction coefficients (E) at 270 nm (upper panel) and 350 nm (lower panel) against [DOC] measured across the entire sampling period for the mesocosms. Mesocosm 4 is marked by the hollow triangle, the black triangle represents mesocosm 7, the black circle mesocosm 15 and the hollow circle mesocosm 20.

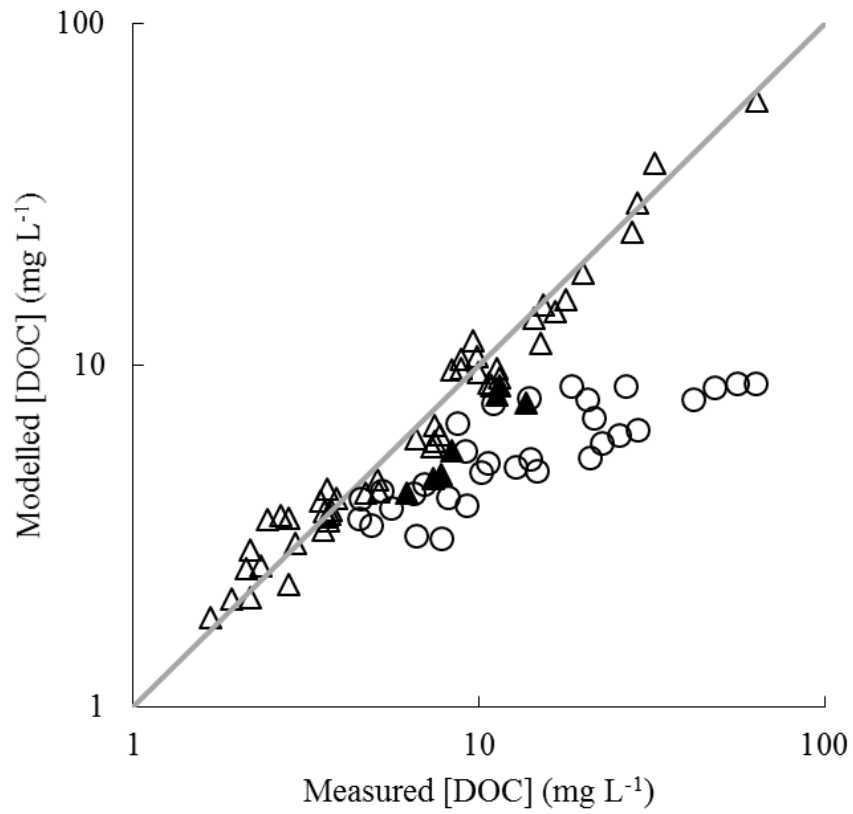


Figure 6.4. Modelled [DOC] plotted against the measured [DOC] for all samples collected in this study. Hollow circles represent the mesocosm samples and triangles for the field sites. Filled triangles show seven Shropshire – Cheshire meres sites that were not satisfactorily explained by the model. The 1:1 line is shown.

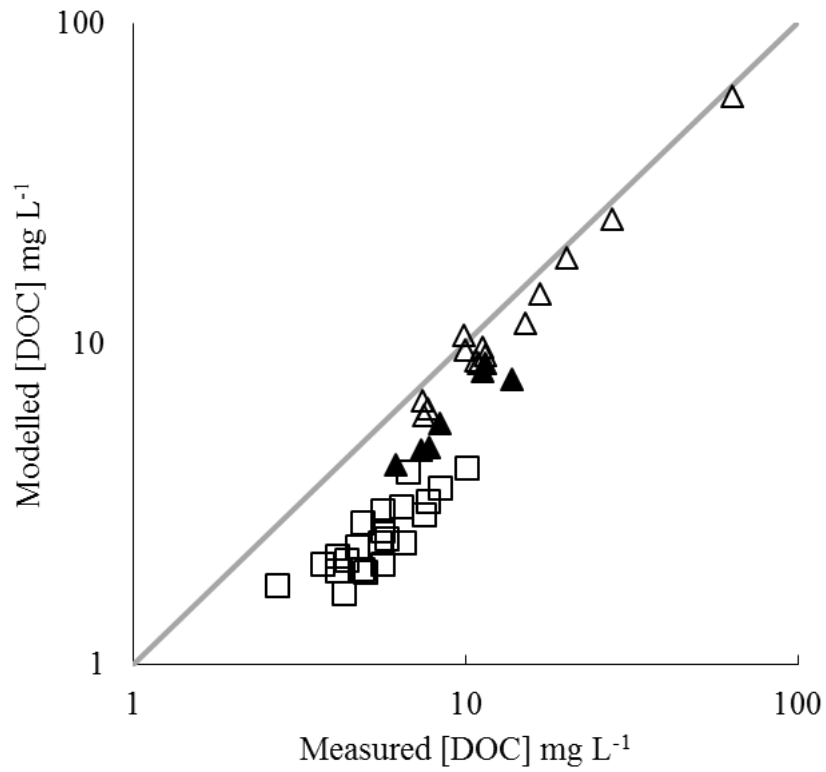


Figure 6.5. Modelled [DOC] plotted against measured [DOC] for the Shropshire – Cheshire mere water samples (triangles). Filled triangles show the seven sites that were unsatisfactorily predicted. Data collected for Chinese lakes are shown by the hollow squares (Zhang et al. 2005). The 1:1 line is shown.

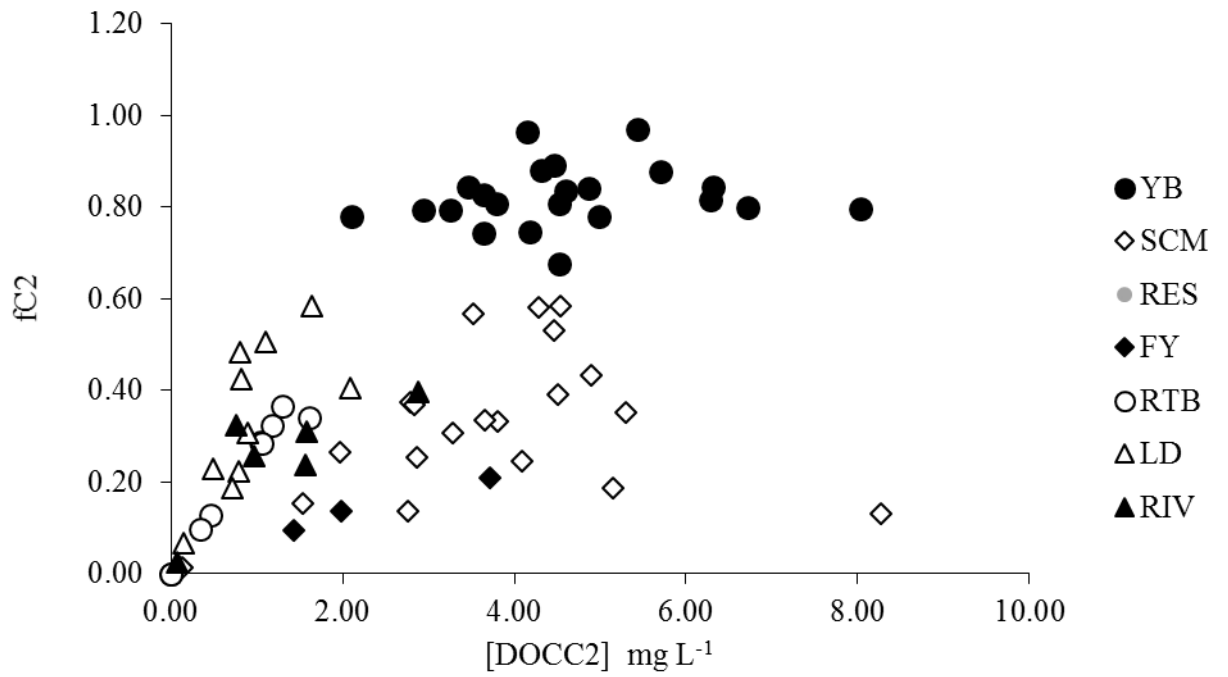


Figure 6.6. The fraction of the variable component C2 (f_{C2}), vs the $[DOCC_2]$ for the whole sample set, including the Yangtze basin samples.

7. Discussion

In recent decades, there has been a burgeoning database regarding the composition and behaviour of natural organic matter, which has enhanced our understanding of NOM cycling. However, applying this knowledge on a larger scale, and linking different ecosystems remains incomplete due to the lack of available information across a wider range of nutrient elements, and a lack of breadth in land use, catchment type and soil classification. This study aimed to increase the understanding of NOM function over large scales, between terrestrial and aquatic ecosystems. Specifically, the association of the macronutrient elements C, N and P with different SOM pools was explored using a laboratory based density fractionation method. In rivers, the enrichment of ^{14}C in dissolved and particulate organic matter was investigated across watersheds not well represented in the literature, providing necessary constraints in the modelling of soil organic matter transport into freshwater ecosystems. Finally, the efficacy of a multi component model for quantifying freshwater DOC through UV-Vis absorbance was tested, highlighting the implications involved in accurately predicting DOC concentrations in highly eutrophic systems. Wider knowledge of the processes involved in SOM formation, degradation, and transport to aquatic systems is advantageous for future integrated modelling approaches to nutrient cycling. Several key findings have emerged, all of which contribute towards the large scale understanding of natural organic matter, and addresses three implications, as described in the introduction:

7.1: Quantification of natural organic matter

Significant findings have recently emerged that qualitatively describe the physical components of NOM on the molecular scale, particularly for plants, microbes and soil

(Simpson & Simpson 2012; Kögel-Knabner 2002). However, quantifying the processes involved in SOM cycling remains incomplete due a lack of information available for macronutrients other than carbon and nitrogen. In chapter 3, we sought to explore the distribution of organic phosphorus across density fractionated soil organic matter, and its enrichment relative to C and N. Until now, the organic phosphorus content of density fractionated soil has only been demonstrated in the organic (light) fraction, which makes it difficult to model oP over different SOM pools. The results in chapter 3 demonstrated that an average 90% of organic P was present in the mineral (heavy) fraction of semi natural soils, showing that organic phosphorus is favoured by mineral matter due to the strong adsorbing properties. This confirmed the suggestions of a stoichiometric SOM model based on >2000 international soils (Tipping, Somerville and Luster, 2016), which provided a new quantitative framework for SOM classification and characterisation. As argued in Tipping et al. (2016), to improve models of SOM dynamics, it is important to quantitatively account for different pool sizes, concentrations and turnover, and the variation between different soil types. The findings in chapter 3 therefore contributes to the wider understanding of SOM stability, and provides necessary constraints to terrestrial models of soil carbon dynamics and nutrient cycles.

However, the low recovery of oP raises doubts over the use of sodium polytungstate as the density separation matrix. This therefore highlighted potential implications in applying common fractionation techniques to the oP pools, and gave important suggestions for future methodological adaptations.

7.2: Large scale data

For effective large scale modelling, it is important to consider the diverse range of soil types, land uses and ecosystems, and considerable gaps in the literature still remain. In density fractionation studies, most only focus on arable and agricultural soil (Kirkby *et al.*, 2011; Schrumpf *et al.*, 2013), with limited information available on grassland and forested soil (Zimmermann *et al.*, 2007). Chapter 3 provided the first investigation using a method that was adapted and applied to a range of different soils, which were taken from an extensive UK soil survey, and included arable, semi natural and managed land. The procedure yielded 96% of the total material. However, there were implications involved in the recovery of material where the quantity of the light fraction was low, which resulted in the arable soil being omitted from the sample set. While the findings in chapter 3 contributed new information on macronutrient cycling, the procedure should be adapted, to be applied over a wider range of soil types. In doing so, samples sizes would have to be increased, which introduces complications with the volume of sodium polytungstate needed, and the necessary centrifugation equipment. Further discussion on future research needs are presented in section 6.5.

Radiocarbon dating riverine OC gives information on the time elapsed between the fixing of C by plants and entry into the water course, which gives the ability to model the terrestrial-freshwater C cycle. Globally, there are approximately 466 published data points of $PO^{14}C$, as synthesised by Marwick *et al.* (2015), most of which were exclusive to catchments with high particulate export and erosion rates. In the UK, no data was available on lowland watersheds, and chapter 4 provided the first insight into the ^{14}C content of POC transported in four predominantly rural catchments. In line

with the global dataset, the PO^{14}C values for the UK catchments were mostly ^{14}C depleted, with the overall apparent age of the sample decreasing with decreasing OC content. One catchment was particularly aged and was attributed to industrial and mining activity in the drainage area, which contrasted the global average. Organic C contents of the samples tended to be higher than the global average, which reflects the typically higher OC contents of UK soil. The data presented in chapter 4 will therefore contribute towards improved modelling of terrestrial-freshwater C cycling, which is important for global measurements of C sequestration, terrestrial nutrient losses and thus future ecosystem management.

While the dataset available for DO^{14}C is more extensive, there were again significant gaps in the breadth that the data covers. The global synthesis by Marwick et al. (2015) revealed that arable and urban dominant catchments were lacking in the global dataset, which could have implications when applying terrestrial-aquatic C cycles to the world. However, data was missing from the synthesis, and a repeat of the global literature search found data from an extra 13 studies, and showed a lack of lowland watersheds from the UK. New data collected from arable watersheds were more depleted than the global average, while urban catchments also contained depleted ^{14}C . The new data for the UK in Chapters 4 and 5 showed contrasting average enrichments. PO^{14}C tended to be depleted on average, while DO^{14}C was enriched, suggesting the release of OC from different sources. In semi natural ecosystems, overland flow will release enriched DOC and POC from the upper areas of the catchment soil profile, while the physical erosion of sub-surface soil and parent material from exposed banks will contribute significantly aged ^{14}C to the POC pool. Globally, the contrasting ^{14}C contents of POC and DOC follow the same pattern as

the UK data on average. However, considerably depleted sources from catchments draining arable and urban land are found in both DOC and POC.

Variation of atmospheric ^{14}C resulting from the weapons testing period causes complications when interpreting ^{14}C data collected over several decades, as the apparent ages and enrichments are not directly comparable. The most recent global O^{14}C synthesis of Marwick et al. (2015) did not consider temporal changes, which complicates model constraining of OM turnover and transport. In chapter 5, we applied modelled SOM pools to the global dataset, which enabled quantitative estimates of topsoil and subsoil sources to the bulk DO^{14}C , for each individual data point. We added previously unpublished data from the 1960s, which provided a useful comparison between samples of similar value collected decades apart, and revealed a paucity of samples available for the 1960s, 70s and 80s. The modelled SOM pools fitted 88% of the data, with some samples more enriched than the average topsoil pool with fast turnovers (1 and 20 years). The modelled SOM pools could better constrain the dataset if more data from previous decades were made available. The data presented in chapter 5 therefore provides both a temporal and spatial perspective of global ^{14}C . Further development will enhance terrestrial-aquatic modelling of C cycling as the data presented considerably expands the current dataset.

However, for both PO^{14}C and DO^{14}C , in stream processes may distort the true value of the enrichment of material entering the river. Preferential mineralisation of labile OC could make the material we measure seem more depleted, which could lead to the conclusion that more of the material originates from sub-surface sources. Further, the single ^{14}C value of a sample will represent a mixture of OC from different sources in the catchment. Therefore, any values measured can only be approximate, which complicates the modelling of multiple SOM pools, cycles and timescales.

7.3: Technological advances: past, present and future

An underlying theme throughout this thesis is the opportunities that technological advances have given to the field of NOM cycling. The development of the ^{13}C NMR techniques has dramatically improved our understanding of the properties of NOM, and its origins. For the analysis of ^{14}C , the accelerator mass spectrometer improved the precision of radiocarbon dating, reduced the size of the sample needed, and ultimately made the analysis more accessible. The data presented in chapters 4 and 5 were part of the NERC funded project LTLS (Long Term, Large Scale), which gathered approximately 250 soil and water ^{14}C values, making it one of the largest surveys of its kind. However, there is an increasing demand for real time, reliable and affordable monitoring of aquatic nutrient concentrations, that will benefit time and cost efficient catchment management, especially in industry.

In chapter 6, a multi component model algorithm of UV-Vis absorbance by Carter et al. (2012) was tested in freshwaters where algal derived DOM may be the dominant producer of DOC. The model, if successfully applied to all freshwaters, could provide in situ measurements of DOC concentration, eliminating the need for laboratory analysis using total organic carbon analysers, thereby reducing labour, cost and data delivery time. Previous analysis of ~1700 freshwater samples showed a good agreement between the measured and modelled DOC concentrations ($r^2 = 0.98$). New measurements on controlled mesocosms and field samples in chapter 6, showed that DOC concentration was considerably underestimated in areas where algal DOM was the dominant producer of DOC. Sampling the mesocosms through time showed that as the production of algal DOM increased, the ability to accurately predict the DOC concentration decreased i.e, the difference between the measured and modelled DOC

concentrations increased. This therefore demonstrates that autochthonous processing of OM produces components with different characteristics to terrestrially derived material. In an attempt to quantify the contribution of algal DOM, a third, variable component replaced the fixed component C value, which showed that algal DOM can account for up to 97% of the total, with high contributions also observed in Chinese lakes of the Yangtze Basin (Zhang *et al.*, 2005), which were previously identified by Carter *et al.* (2012). Algal DOM in rivers and streams accounted for an average 22% of the total, probably due to the shorter residence times of the river water. Though the contribution of algal DOM to riverine DOC is not considerably high, DOC produced within the water body could also have implications on the interpretation of the DO^{14}C in chapter 5, where only terrestrial sources were considered.

Testing of the multi component UV-Vis model in chapter 6 was carried out as part of the NERC CLASPDOG project, which aimed to develop a UV miniaturised fourier transform spectrometer that could eventually be field deployable, providing on demand data with no need for laboratory analysis. However, the model in its current state raises doubts on the feasibility of a universally applicable algorithm. At present, the model could not be applied to highly eutrophic systems without confirmatory analysis in the laboratory. Further testing of the model across different algal species would give an indication of any species dependent variation of DOM, raising the possibility of an expansion of the model to account for other wavelengths. Further discussion of potential future research is presented in section 6.5.

7.4 Conclusions

This thesis identified several barriers to understanding the large scale function of NOM, and provided new information for terrestrial and aquatic ecosystems. Organic

phosphorus was found to be highly enriched, more so than carbon and nitrogen, in the heavy SOM fraction of semi natural and managed soils. This is the first time that a density fractionation method has been used to display the distribution of organic phosphorus across both organic and mineral SOM pools. Enrichment of organic phosphorus in mineral soil has previously only been suggested, and not proven in soil fractions. This therefore provides valuable information and data for more complete modelling of macronutrient cycles. Measurements of riverine PO^{14}C and DO^{14}C measured in lowland, larger UK catchments, found a higher concentration of SPM than the global average, and more depleted ^{14}C values from industrial, urban and agricultural catchments, which highlighted the importance of collecting data over larger scales that covers a wider range of land uses and soil characteristics. Finally, the testing of the multi compartment model of UV-Vis absorbance presented in chapter 6 showed that the contribution of algae to the overall DOC concentration can be considerable, raising doubts over the efficacy of the model when applied to eutrophic freshwaters, and highlighted important areas for future development.

7.5 Future work

The findings presented in this thesis have raised several potential opportunities for further research:

- The density fractionation method presented in chapter 3 could not be applied to arable soils, and the low recovery of oP throws into question the feasibility of the procedure. Improving the density fractionation on larger quantities of soil, and on a wider range of soil types, may reduce the uncertainty of the method. Other dense solutions should be explored that may improve the recovery of the P fractions. It was not possible to provide information on the

forms of P present in the different fractions. Using a Hedley fractionation procedure on the different fractions would provide a better indication of the distribution of the different forms of oP.

- In chapter 4, new information was provided on lowland, larger catchments in the UK. There is no known PO^{14}C data for arable catchments, which may contain more depleted material, due to the typically more depleted surface soil O^{14}C . More data therefore needs to be collected on systems not well presented in the database.
- Globally, there is a wealth of data available on rivers with some of the largest exports of DOC in the world. In the UK, almost all of the data available on riverine DO^{14}C were in small, upland, peat dominated catchments, and the new UK data presented in chapter 5 significantly expanded the database. For more effective large scale modelling for the UK, further sampling of arable and urban catchments should be considered. Archived data for the 1960s, 70s and 80s could be obtained to provide better constraints on the modelled SOM turnover pools for estimating DO^{14}C sources.
- Quantifying the contribution of algal derived DOC in freshwaters provided indication of the extent to which DOC could be underestimated by a multi-component model of UV-Vis absorbance. More measurements are needed that account for a wider range of systems. Further, variations between different algal species needs to be measured, to determine any species dependent DOM variation. If algal DOM had an identifiable spectrum at known wavelengths, the model could be expanded to account for this. Re-testing of the model can then be carried out.

- Testing the model of Carter et al. (2012) was carried out as part of the NERC funded CLASPDOG project, which aimed to manufacture a miniaturised fourier transform (FT) UV-Vis spectrometer that could be field deployable in the future. Once fully tested and adjusted, the model algorithm of Carter et al. (2012) should therefore be ultimately used to provide rapid measurements of DOC concentration in situ. Further developments of the FT spectrometer in future projects are therefore necessary for long term field deployment.

8. References

- Adams, J. L., Tipping, E., Bryant, C. L., Helliwell, R. C., Toberman, H. and Quinton, J. (2015) 'Aged riverine particulate organic carbon in four UK catchments', *Science of The Total Environment*. Elsevier B.V., 536, pp. 648–654. doi: 10.1016/j.scitotenv.2015.06.141.
- Agbenin, J. O., Iwuafor, E. N. O. and Ayuba, B. (1998) 'A critical assessment of methods for determining organic phosphorus in savanna soils', *Biology and Fertility of Soils*. Springer-Verlag, 28(2), pp. 177–181. doi: 10.1007/s003740050481.
- Aiken, G., McKnight, D., Harnish, R. and Wershaw, R. (1996) 'Geochemistry of aquatic humic substances in the Lake Fryxell Basin, Antarctica', *Biogeochemistry*, 34(3), pp. 157–188. doi: 10.1007/BF00000900.
- Aiken G.R, Spencer R.G.M, Striegl R.G, S. P. . and R. P. . (2014) 'Influences of glacier melt and permafrost thaw on the age of dissolved organic carbon in the Yukon River basin', *Global Biogeochemical Cycles*, pp. 525–537. doi: 10.1002/2013GB004764.Received.
- Almendros, G., Guadalix, M. E., González-Vila, F. J. and Martin, F. (1996) 'Preservation of aliphatic macromolecules in soil humins', in *Organic Geochemistry*, pp. 651–659. doi: 10.1016/0146-6380(96)00056-3.
- Amelung, W. (2003) 'Nitrogen biomarkers and their fate in soil', *Journal of Plant Nutrition and Soil Science*. WILEY-VCH Verlag, 166(6), pp. 677–686. doi: 10.1002/jpln.200321274.
- Amelung, W., Brodowski, S., Sandhage-Hofmann, A. and Bol, R. (2008) 'Chapter 6

Combining Biomarker with Stable Isotope Analyses for Assessing the Transformation and Turnover of Soil Organic Matter’, *Advances in Agronomy*, 100, pp. 155–250. doi: 10.1016/S0065-2113(08)00606-8.

Amundson, R. (2001) ‘The Carbon Budget in Soils’, *Annual Review of Earth and Planetary Sciences*. Annual Reviews 4139 El Camino Way, P.O. Box 10139, Palo Alto, CA 94303-0139, USA , 29(1), pp. 535–562. doi: 10.1146/annurev.earth.29.1.535.

André J. Simpson, *,†, William L. Kingery, ‡ and and Hatcher§, P. G. (2002) ‘The Identification of Plant Derived Structures in Humic Materials Using Three-Dimensional NMR Spectroscopy’. American Chemical Society . doi: 10.1021/ES025956J.

Aufdenkampe, A. K., Mayorga, E., Raymond, P. a, Melack, J. M., Doney, S. C., Alin, S. R., Aalto, R. E. and Yoo, K. (2011) ‘Riverine coupling of biogeochemical cycles between land, oceans, and atmosphere’, *Frontiers in Ecology and the Environment*. Ecological Society of America, 9(1), pp. 53–60. doi: 10.1890/100014.

Baker, A. R., Jickells, T. D., Witt, M. and Linge, K. L. (2006) ‘Trends in the solubility of iron, aluminium, manganese and phosphorus in aerosol collected over the Atlantic Ocean’, *Marine Chemistry*, 98(1), pp. 43–58. doi: 10.1016/j.marchem.2005.06.004.

Batjes, N. H. (2014) ‘Total carbon and nitrogen in the soils of the world’, *European Journal of Soil Science*. Blackwell Publishing Ltd, 65(1), pp. 10–21. doi: 10.1111/ejss.12114_2.

Battin, T. J., Kaplan, L. a., Findlay, S., Hopkinson, C. S., Marti, E., Packman, A. I., Newbold, J. D. and Sabater, F. (2008) ‘Biophysical controls on organic carbon fluxes in fluvial networks’, *Nature Geoscience*, 1(2), pp. 95–100. doi: 10.1038/ngeo101.

Benner, R. (2004) 'Export of young terrigenous dissolved organic carbon from rivers to the Arctic Ocean', *Geophysical Research Letters*, 31(5), pp. 10–13. doi: 10.1029/2003GL019251.

Bennett, E.M, Carpenter, S.R. and Caraco, N.F. (2001) 'Human Impact on Erodeable Phosphorus and Eutrophication: A Global Perspective', *BioScience*, 51(3), p. 227. doi: 10.1641/0006-3568(2001)051[0227:HIOEPA]2.0.CO;2.

Biddanda, B. and Benner, R. (1997) 'Carbon, nitrogen, and carbohydrate fluxes during the production of particulate and dissolved organic matter by marine phytoplankton', *Limnology and Oceanography*, 42(3), pp. 506–518. doi: 10.4319/lo.1997.42.3.0506.

Billett, M. F., Dinsmore, K. J., Smart, R. P., Garnett, M. H., Holden, J., Chapman, P., Baird, a. J., Grayson, R. and Stott, a. W. (2012) 'Variable source and age of different forms of carbon released from natural peatland pipes', *Journal of Geophysical Research: Biogeosciences*, 117(2), pp. 1–16. doi: 10.1029/2011JG001807.

Billett, M. F., Garnett, M. H., Dinsmore, K. J., Dyson, K. E., Harvey, F., Thomson, A. M., Piirainen, S. and Kortelainen, P. (2012) 'Age and source of different forms of carbon released from boreal peatland streams during spring snowmelt in E. Finland', *Biogeochemistry*, 111(1–3), pp. 273–286. doi: 10.1007/s10533-011-9645-4.

Billett, M. F., Garnett, M. H. and Harvey, F. (2007) 'UK peatland streams release old carbon dioxide to the atmosphere and young dissolved organic carbon to rivers', *Geophysical Research Letters*, 34(23), p. n/a-n/a. doi: 10.1029/2007GL031797.

Blair, N. E., Leithold, E. L., Ford, S. T., Peeler, K. A., Holmes, J. C. and Perkey, D. W. (2003) 'The persistence of memory: the fate of ancient sedimentary organic carbon in a modern sedimentary system', *Geochimica et Cosmochimica Acta*, 67(1), pp. 63–73.

doi: 10.1016/S0016-7037(02)01043-8.

Blough, N. V. and Del Vecchio, R. (2002) 'Chromophoric DOM in the Coastal Environment', in *Biogeochemistry of Marine Dissolved Organic Matter*. Elsevier, pp. 509–546. doi: 10.1016/B978-012323841-2/50012-9.

Boehme, J. R. and Coble, P. G. (2000) 'Characterization of colored dissolved organic matter using high-energy laser fragmentation', *Environmental Science and Technology*. American Chemical Society, 34(15), pp. 3283–3290. doi: 10.1021/es9911263.

Bol, R. a, Harkness, D. D., Huang, Y. and Howard, D. M. (1999) 'The influence of soil processes on carbon isotope distribution and turnover in the British uplands', *European Journal of Soil Science*, 50(March), pp. 41–51.

Bouchez, J., Galy, V., Hilton, R. G., Gaillardet, J., Moreira-Turcq, P., Pérez, M. A., France-Lanord, C. and Maurice, L. (2014) 'Source, transport and fluxes of Amazon River particulate organic carbon: Insights from river sediment depth-profiles', *Geochimica et Cosmochimica Acta*, 133, pp. 280–298. doi: 10.1016/j.gca.2014.02.032.

Bouillon, S., Korntheuer, M., Baeyens, W. and Dehairs, F. (2006) 'A new automated setup for stable isotope analysis of dissolved organic carbon', *Limnology and Oceanography: Methods*, 4(7), pp. 216–226. doi: 10.4319/lom.2006.4.216.

Boutton, T. W., Wong, W. W., Hachey, D. L., Lee, L. S., Cabrera, M. P. and Klein, P. D. (1983) 'Comparison of quartz and Pyrex tubes for combustion of organic samples for stable carbon isotope analysis', *Analytical Chemistry*. American Chemical Society, 55(11), pp. 1832–1833. doi: 10.1021/ac00261a049.

van Breemen, N., Boyer, E. W., Goodale, C. L., Jaworski, N. A., Paustian, K.,

Seitzinger, S. P., Lajtha, K., Mayer, B., van Dam, D., Howarth, R. W., Nadelhoffer, K. J., Eve, M. and Billen, G. (2002) 'Where did all the nitrogen go? Fate of nitrogen inputs to large watersheds in the northeastern U.S.A.', *Biogeochemistry*. Kluwer Academic Publishers, 57(1), pp. 267–293. doi: 10.1023/A:1015775225913.

Butman, D. E., Wilson, H. F., Barnes, R. T., Xenopoulos, M. a. and Raymond, P. a. (2015) 'Increased mobilization of aged carbon to rivers by human disturbance', *Nature Geoscience*, 8(February), pp. 112–116. doi: 10.1038/NGEO2322.

Butman, D., Raymond, P. A., Butler, K. and Aiken, G. (2012) 'Relationships between $\delta^{14}\text{C}$ and the molecular quality of dissolved organic carbon in rivers draining to the coast from the conterminous United States', *Global Biogeochemical Cycles*, 26(4), pp. 1–15. doi: 10.1029/2012GB004361.

Caraco, N., Bauer, J. E., Cole, J. J., Petsch, S. and Raymond, P. (2010) 'Millennial-aged organic carbon subsidies to a modern river food web', *Ecology*. Ecological Society of America, 91(8), pp. 2385–2393. doi: 10.1890/09-0330.1.

Carpenter, S. R., Caraco, N. F., Correll, D. L., Howarth, R. W., Sharpley, A. N. and Smith, V. H. (1998) 'NONPOINT POLLUTION OF SURFACE WATERS WITH PHOSPHORUS AND NITROGEN', *Ecological Applications*. Ecological Society of America, 8(3), pp. 559–568. doi: 10.1890/1051-0761(1998)008[0559:NPOSWW]2.0.CO;2.

Carter, H. T., Tipping, E., Koprivnjak, J.-F., Miller, M. P., Cookson, B. and Hamilton-Taylor, J. (2012) 'Freshwater DOM quantity and quality from a two-component model of UV absorbance.', *Water research*. Elsevier Ltd, 46(14), pp. 4532–42. doi: 10.1016/j.watres.2012.05.021.

Cathalot, C., Rabouille, C., Tisnérat-Laborde, N., Toussaint, F., Kerhervé, P., Buscail, R., Loftis, K., Sun, M.-Y., Tronczynski, J., Azoury, S., Lansard, B., Treignier, C., Pastor, L. and Tesi, T. (2013) 'The fate of river organic carbon in coastal areas: A study in the Rhône River delta using multiple isotopic ($\delta^{13}\text{C}$, $\Delta^{14}\text{C}$) and organic tracers', *Geochimica et Cosmochimica Acta*, 118, pp. 33–55. doi: 10.1016/j.gca.2013.05.001.

Cerli, C., Celi, L., Kalbitz, K., Guggenberger, G. and Kaiser, K. (2012) 'Separation of light and heavy organic matter fractions in soil - Testing for proper density cut-off and dispersion level', *Geoderma*. Elsevier B.V., 170, pp. 403–416. doi: 10.1016/j.geoderma.2011.10.009.

Chapman, A. S., Foster, I. D. L., Lees, J. A., Hodgkinson, R. A. and Jackson, R. H. (2001) 'Particulate phosphorus transport by sub-surface drainage from agricultural land in the UK. Environmental significance at the catchment and national scale', in *Science of the Total Environment*, pp. 95–102. doi: 10.1016/S0048-9697(00)00734-8.

Chen, J., LeBoeuf, E. J., Dai, S. and Gu, B. (2003) 'Fluorescence spectroscopic studies of natural organic matter fractions', *Chemosphere*, 50(5), pp. 639–647. doi: 10.1016/S0045-6535(02)00616-1.

Chen, Q., Sun, Y., Shen, C., Peng, S., Yi, W., Li, Z. and Jiang, M. (2002) 'Organic matter turnover rates and CO₂ flux from organic matter decomposition of mountain soil profiles in the subtropical area, south China', *Catena*, 49(3), pp. 217–229. doi: 10.1016/S0341-8162(02)00044-9.

Christensen, B. T. (2001) 'Physical fractionation of soil and structural and functional complexity in organic matter turnover', *European Journal of Soil Science*. Blackwell Science Ltd, 52(3), pp. 345–353. doi: 10.1046/j.1365-2389.2001.00417.x.

Cleveland, C. C. and Liptzin, D. (2007) 'C:N:P stoichiometry in soil: Is there a "Redfield ratio" for the microbial biomass?', *Biogeochemistry*, 85(3), pp. 235–252. doi: 10.1007/s10533-007-9132-0.

Cole, J. J., Prairie, Y. T., Caraco, N. F., McDowell, W. H., Tranvik, L. J., Striegl, R. G., Duarte, C. M., Kortelainen, P., Downing, J. a., Middelburg, J. J. and Melack, J. (2007) 'Plumbing the global carbon cycle: Integrating inland waters into the terrestrial carbon budget', *Ecosystems*, 10(1), pp. 171–184. doi: 10.1007/s10021-006-9013-8.

Collins, A. L. and Walling, D. E. (2007) 'Fine-grained bed sediment storage within the main channel systems of the Frome and Piddle catchments, Dorset, UK', *Hydrological Processes*. John Wiley & Sons, Ltd., 21(11), pp. 1448–1459. doi: 10.1002/hyp.6269.

Crow, S. E., Swanston, C. W., Lajtha, K., Brooks, J. R. and Keirstead, H. (2007) 'Density fractionation of forest soils: Methodological questions and interpretation of incubation results and turnover time in an ecosystem context', *Biogeochemistry*, 85(1), pp. 69–90. doi: 10.1007/s10533-007-9100-8.

da Cunha, L. C., Serve, L., Gadel, F. and Blazi, J. L. (2000) 'Characterisation of riverine particulate organic matter by pyrolysis-gas chromatography-mass spectrometry.', *The Science of the total environment*, 256(2–3), pp. 191–204.

Curtin, D., McCallum, F. M. and Williams, P. H. (2003) 'Phosphorus in light fraction organic matter separated from soils receiving long-term applications of superphosphate', *Biology and Fertility of Soils*, 37(5), pp. 280–287. doi: 10.1007/s00374-003-0598-1.

Davies, J. A. C., Tipping, E., Rowe, E. C., Boyle, J. F., Pannatier, E. G. and Martinsen, V. (2016) 'Long-term P weathering and recent N deposition control contemporary

plant-soil C, N, and P', *Global Biogeochemical Cycles*, 30, pp. 231–249. doi: 10.1002/2015GB005167.Received.

Deasy, C., Brazier, R. E., Heathwaite, A. L. and Hodgkinson, R. (2009) 'Pathways of runoff and sediment transfer in small agricultural catchments', *Hydrological Processes*. John Wiley & Sons, Ltd., 23(9), pp. 1349–1358. doi: 10.1002/hyp.7257.

Derenne, S. and Largeau, C. (2001) 'a Review of Some Important Families of Refractory Macromolecules: Composition, Origin, and Fate in Soils and Sediments', *Soil Science*, 166(11), pp. 833–847. doi: 10.1097/00010694-200111000-00008.

Donahue, W. F., Schindler, D. W., Page, S. J. and Stainton, M. P. (1998) 'Acid-induced changes in DOC quality in an experimental whole-lake manipulation', *Environmental Science and Technology*. American Chemical Society, 32(19), pp. 2954–2960. doi: 10.1021/es980306u.

Downing, J. A. and Duarte, C. M. (2006) 'Abundance and Size Distribution of Lakes, Ponds and Impoundments', *Limnol. Oceanogr*, 51(5), pp. 2388–2397. doi: 10.1016/B978-0-12-409548-9.03867-7.

Dungait, J. A. J., Hopkins, D. W., Gregory, A. S. and Whitmore, A. P. (2012) 'Soil organic matter turnover is governed by accessibility not recalcitrance', *Global Change Biology*, 18(6), pp. 1781–1796. doi: 10.1111/j.1365-2486.2012.02665.x.

E Tipping (2002) *Cation binding by humic substances*. Cambridge University Press.

Einsele, G., Yan, J. and Hinderer, M. (2001) 'Atmospheric carbon burial in modern lake basins and its significance for the global carbon budget', *Global and Planetary Change*, 30(3), pp. 167–195. doi: 10.1016/S0921-8181(01)00105-9.

Elser, J. and Bennett, E. (2011) 'Phosphorus cycle: A broken biogeochemical cycle', *Nature*. Nature Research, 478(7367), pp. 29–31. doi: 10.1038/478029a.

Elser, J. J., Bracken, M. E. S., Cleland, E. E., Gruner, D. S., Harpole, W. S., Hillebrand, H., Ngai, J. T., Seabloom, E. W., Shurin, J. B. and Smith, J. E. (2007) 'Global analysis of nitrogen and phosphorus limitation of primary producers in freshwater, marine and terrestrial ecosystems', *Ecology Letters*, 10(12), pp. 1135–1142. doi: 10.1111/j.1461-0248.2007.01113.x.

ESTRANY, J., GARCIA, C. and Walling, D. E. (2010) 'An investigation of soil erosion and redistribution in a Mediterranean lowland agricultural catchment using caesium-137', *International Journal of Sediment Research*. International Research and Training Centre on Erosion and Sedimentation and the World Association for Sedimentation and Erosion Research, 25(1), pp. 1–16. doi: 10.1016/S1001-6279(10)60023-6.

Evans, C. D., Freeman, C., Cork, L. G., Thomas, D. N., Reynolds, B., Billett, M. F., Garnett, M. H. and Norris, D. (2007) 'Evidence against recent climate-induced destabilisation of soil carbon from ^{14}C analysis of riverine dissolved organic matter', *Geophysical Research Letters*, 34(7), p. L07407. doi: 10.1029/2007GL029431.

Evans, C. D., Page, S. E., Jones, T., Moore, S., Gauci, V., Laiho, R., Hruška, J., Allott, T. E. H., Billett, M. F., Tipping, E., Freeman, C. and Garnett, M. H. (2014) 'Contrasting vulnerability of drained tropical and high-latitude peatlands to fluvial loss of stored carbon', *Global Biogeochemical Cycles*, 28(11), pp. 1215–1234. doi: 10.1002/2013GB004782.

Falkowski, P. G., Scholes, R. J., Boyle, E., Canadell, J., Canfield, D., Elser, J., Gruber, N., Hibbard, K., Högberg, P., Linder, S., Mackenzie, F. T., Moore, B., Pedersen, T.,

Rosenthal, Y., Seitzinger, S., Smetacek, V. and Steffen, W. (2000) 'The global carbon cycle: a test of our knowledge of earth as a system.', *Science*, 290(5490), pp. 291–296. doi: 10.1126/science.290.5490.291.

Fellman, J. B., Spencer, R. G. M., Raymond, P. A., Pettit, N. E., Skrzypek, G., Hernes, P. J. and Grierson, P. F. (2014) 'Dissolved organic carbon biolability decreases along with its modernization in fluvial networks in an ancient landscape', *Ecology*, 95(9), pp. 2622–2632. doi: 10.1890/13-1360.1.

Feng, X., Simpson, A. J., Wilson, K. P., Dudley Williams, D. and Simpson, M. J. (2008) 'Increased cuticular carbon sequestration and lignin oxidation in response to soil warming', *Nature Geoscience*. Nature Publishing Group, 1(12), pp. 836–839. doi: 10.1038/ngeo361.

Fisher, J., Barker, T., James, C. and Clarke, S. (2009) 'Water quality in chronically nutrient-rich lakes : the example of the Shropshire-Cheshire meres', pp. 79–99. doi: 10.1608/FRJ-2.1.5.

Foster, G. D., Roberts, E. C., Gruessner, B. and Velinsky, D. J. (2000) 'Hydrogeochemistry and transport of organic contaminants in an urban watershed of Chesapeake Bay (USA)', *Applied Geochemistry*, 15(7), pp. 901–915. doi: 10.1016/S0883-2927(99)00107-9.

Fry, B., Hopkinson, C. S., Nolin, A. and Wainright, S. C. (1998) '¹³C/¹²C composition of marine dissolved organic carbon', *Chemical Geology*, 152(1), pp. 113–118. doi: 10.1016/S0009-2541(98)00100-4.

Gaillardet, J., Dupré, B. and Allègre, C. J. (1999) 'Geochemistry of large river suspended sediments: silicate weathering or recycling tracer?', *Geochimica et*

Cosmochimica Acta, 63(23–24), pp. 4037–4051. doi: 10.1016/S0016-7037(99)00307-5.

Galloway, J. N., Dentener, F. J., Capone, D. G., Boyer, E. W., Howarth, R. W., Seitzinger, S. P., Asner, G. P., Cleveland, C. C., Green, P. A., Holland, E. A., Karl, D. M., Michaels, A. F., Porter, J. H., Townsend, A. R. and Vörösmarty, C. J. (2004) ‘Nitrogen Cycles: Past, Present, and Future’, *Source: Biogeochemistry*, 70(2), pp. 153–226.

Galloway, N., Schlesinger, W. H., Ii, H. L., Schnoor, L. and Tg, N. (1995) ‘Nitrogen fixation: Anthropogenic enhancement-environmental response’, *Global Biogeochemical Cycles*, 9(2), pp. 235–252.

Galy, V., France-Lanord, C. and Lartiges, B. (2008) ‘Loading and fate of particulate organic carbon from the Himalaya to the Ganga–Brahmaputra delta’, *Geochimica et Cosmochimica Acta*, 72(7), pp. 1767–1787. doi: 10.1016/j.gca.2008.01.027.

Gandhi, H., Wiegner, T. N., Ostrom, P. H., Kaplan, L. A. and Ostrom, N. E. (2004) ‘Isotopic (^{13}C) analysis of dissolved organic carbon in stream water using an elemental analyzer coupled to a stable isotope ratio mass spectrometer’, *RAPID COMMUNICATIONS IN MASS SPECTROMETRY Rapid Commun. Mass Spectrom.*, 18, pp. 903–906. doi: 10.1002/rcm.1426.

Golchin, A., Oades, J., Skjemstad, J., Clarke, P., Golchin, A., Oades, J., Skjemstad, J. and Clarke, P. (1994) ‘Study of free and occluded particulate organic matter in soils by solid state ^{13}C Cp/MAS NMR spectroscopy and scanning electron microscopy’, *Australian Journal of Soil Research*. CSIRO PUBLISHING, 32(2), p. 285. doi: 10.1071/SR9940285.

Goldstone, J. V., Del Vecchio, R., Blough, N. V. and Voelker, B. M. (2004) 'A Multicomponent Model of Chromophoric Dissolved Organic Matter Photobleaching', *Photochemistry and Photobiology*, 80(1), p. 52. doi: 10.1562/TM-03-17.1.

Gondar, D., Thacker, S. A., Tipping, E. and Baker, A. (2008) 'Functional variability of dissolved organic matter from the surface water of a productive lake', 42, pp. 81–90. doi: 10.1016/j.watres.2007.07.006.

Griffith, D. R., Barnes, R. T. and Raymond, P. A. (2009a) 'Inputs of Fossil Carbon from Wastewater Treatment Plants to U.S. Rivers and Oceans', *Environmental Science & Technology*. American Chemical Society, 43(15), pp. 5647–5651. doi: 10.1021/es9004043.

Griffith, D. R., Barnes, R. T. and Raymond, P. A. (2009b) 'Inputs of Fossil Carbon from Wastewater Treatment Plants to U.S. Rivers and Oceans', *Environmental Science & Technology*, 43(15), pp. 5647–5651. doi: 10.1021/es9004043.

Gruszowski, K. E., Foster, I. D. L., Lees, J. a. and Charlesworth, S. M. (2003) 'Sediment sources and transport pathways in a rural catchment, Herefordshire, UK', *Hydrological Processes*, 17(13), pp. 2665–2681. doi: 10.1002/hyp.1296.

Gu, B., Schmitt, J., Chen, Z., Liang, L. and McCarthy, J. F. (1994) 'Adsorption and desorption of natural organic matter on iron oxide: mechanisms and models', *Environmental Science & Technology*, 28(1), pp. 38–46. doi: 10.1021/es00050a007.

Guo, L., Ping, C. L. and Macdonald, R. W. (2007) 'Mobilization pathways of organic carbon from permafrost to arctic rivers in a changing climate', *Geophysical Research Letters*, 34(13), pp. 1–5. doi: 10.1029/2007GL030689.

Guo, L., Santschi, P. H. and Warnken, K. W. (1995) 'Dynamics of dissolved organic carbon (DOC) in oceanic environments', 40(8), pp. 1392–1403.

Gustafsson, J. P. (2003) 'Modelling molybdate and tungstate adsorption to ferrihydrite', *Chemical Geology*, 200(1–2), pp. 105–115. doi: 10.1016/S0009-2541(03)00161-X.

De Haan, H. and De Boer, T. (1987) 'Applicability of light absorbance and fluorescence as measures of concentration and molecular size of dissolved organic carbon in humic Lake Tjeukemeer', *Water Research*. Elsevier , 21(6), pp. 731–734. doi: 10.1016/0043-1354(87)90086-8.

Hagedorn, F., Spinnler, D. and Siegwolf, R. (2003) 'Increased N deposition retards mineralization of old soil organic matter', *Soil Biology and Biochemistry*, 35(12), pp. 1683–1692. doi: 10.1016/j.soilbio.2003.08.015.

Hatcher, P. G., Dria, K. J., Kim, S. and Frazier, S. W. (2001) 'Modern Analytical Studies of Humic Substances', *Soil Science*, 166(11), pp. 770–794. doi: 10.1097/00010694-200111000-00005.

Hedges, J. I., Eglinton, G., Hatcher, P. G., Kirchman, D. L., Arnosti, C., Derenne, S., Evershed, R. P., Kögel-Knabner, I., De Leeuw, J. W., Littke, R., Michaelis, W. and Rullkötter, J. (2000) 'The molecularly-uncharacterized component of nonliving organic matter in natural environments', *Organic Geochemistry*, 31(10), pp. 945–958. doi: 10.1016/S0146-6380(00)00096-6.

Hedley, M. J. J. and Stewart, J. W. B. W. B. (1982) 'Method to measure microbial phosphate in soils', *Soil Biology and Biochemistry*, 14(4), pp. 377–385. doi: 10.1016/0038-0717(82)90009-8.

Heinze, C., Meyer, S., Goris, N., Anderson, L., Steinfeldt, R., Chang, N., Le Quéré, C. and Bakker, D. C. E. (2015) ‘The ocean carbon sink – impacts, vulnerabilities and challenges’, *Earth Syst. Dynam.*, 6, pp. 327–358. doi: 10.5194/esd-6-327-2015.

Helms, J. R., Stubbins, A., Ritchie, J. D., Minor, E. C., Kieber, D. J. and Mopper, K. (2008) ‘Absorption spectral slopes and slope ratios as indicators of molecular weight, source, and photobleaching of chromophoric dissolved organic matter’, *Limnology and Oceanography*, 53(3), pp. 955–969.

Henderson, R. K., Baker, A., Parsons, S. A. and Jefferson, B. (2008) ‘Characterisation of algogenic organic matter extracted from cyanobacteria, green algae and diatoms’, *Water Research*, 42(13), pp. 3435–3445. doi: 10.1016/j.watres.2007.10.032.

Hesshaimer, V., Heimann, M. and Levin, I. (1994) ‘Radiocarbon evidence for a smaller oceanic carbon dioxide sink than previously believed’, *Letters to Nature*, 370, pp. 201–203. doi: 10.1038/370201a0.

Higuera, M., Kerhervé, P., Sanchez-Vidal, A., Calafat, A., Ludwig, W., Verdoit-Jarraya, M., Heussner, S. and Canals, M. (2014) ‘Biogeochemical characterization of the riverine particulate organic matter transferred to the NW Mediterranean Sea’, *Biogeosciences*. Copernicus GmbH, 11(1), pp. 157–172. doi: 10.5194/bg-11-157-2014.

Hilton, R. G., Galy, A. and Hovius, N. (2008) ‘Riverine particulate organic carbon from an active mountain belt: Importance of landslides’, *Global Biogeochemical Cycles*, 22(1), p. n/a-n/a. doi: 10.1029/2006GB002905.

Hilton, R. G., Galy, A., Hovius, N., Chen, M.-C., Horng, M.-J. and Chen, H. (2008) ‘Tropical-cyclone-driven erosion of the terrestrial biosphere from mountains’, *Nature Geoscience*. Nature Publishing Group, 1(11), pp. 759–762. doi: 10.1038/ngeo333.

Hood, E., Fellman, J., Spencer, R. G. M., Hernes, P. J., Edwards, R., D'Amore, D. and Scott, D. (2009) 'Glaciers as a source of ancient and labile organic matter to the marine environment.', *Nature*. Nature Publishing Group, 462(7276), pp. 1044–7. doi: 10.1038/nature08580.

Hossler, K. and Bauer, J. E. (2012) 'Estimation of riverine carbon and organic matter source contributions using time-based isotope mixing models', *Journal of Geophysical Research: Biogeosciences*, 117(3), pp. 1–15. doi: 10.1029/2012JG001988.

Hua, Q. (2009) 'Radiocarbon: A chronological tool for the recent past', *Quaternary Geochronology*. Elsevier Ltd, 4(5), pp. 378–390. doi: 10.1016/j.quageo.2009.03.006.

Hua, Q., Barbetti, M. and Rakowski, A. Z. (2013) 'Atmospheric Radiocarbon for the Period 1950–2010', *Radiocarbon*, 55(4), pp. 2059–2072. doi: 10.2458/azu_js_rc.v55i2.16177.

Huang, P. M., Bollag, J.-M. (Jean-M. and Senesi, N. (Nicola) (2002) *Interactions between soil particles and microorganisms: impact on the terrestrial ecosystem, Interactions between soil particles and microorganisms*. Edited by J. . B. & N. S. P.M Huang. John Wiley & Sons, Ltd.

V. Ittekkot, R. W. P. . L. (1991) 'Fate of riverine particulate organic matter', in E.T. Degens, S. Kempe, and J. E. R. (ed.) *Biogeochemistry of major world rivers*. 42nd edn. John Wiley, Chichester.

Jarvie, H. P., Neal, C. and Withers, P. J. A. (2006) 'Sewage-effluent phosphorus: A greater risk to river eutrophication than agricultural phosphorus?', *Science of The Total Environment*, 360(1), pp. 246–253. doi: 10.1016/j.scitotenv.2005.08.038.

Jenkinson, D. S., Andrew, S. P. S., Lynch, J. M., Goss, M. J. and Tinker, P. B. (1990) 'The Turnover of Organic Carbon and Nitrogen in Soil [and Discussion] The turnover of organic carbon and nitrogen in soil', *Source: Philosophical Transactions: Biological Sciences*, 329(29), pp. 361–368.

Jenkinson, D. S., Poulton, P. R. and Bryant, C. (2008) 'The turnover of organic carbon in subsoils. Part 1. Natural and bomb radiocarbon in soil profiles from the Rothamsted long-term field experiments', *European Journal of Soil Science*, 59(2), pp. 391–399. doi: 10.1111/j.1365-2389.2008.01025.x.

Jespersen, A. M. and Christoffersen, K. (1987) 'Measurements of Chlorophyll-a From Phytoplankton Using Ethanol As Extraction Solvent', *Archiv Fur Hydrobiologie*, 109(3), pp. 445–454.

Jiao, N., Herndl, G. J., Hansell, D. A., Benner, R., Kattner, G., Wilhelm, S. W., Kirchman, D. L., Weinbauer, M. G., Luo, T., Chen, F. and Azam, F. (2010) 'Microbial production of recalcitrant dissolved organic matter: long-term carbon storage in the global ocean', *Nature Reviews Microbiology*, 8(8), pp. 593–599. doi: 10.1038/nrmicro2386.

Jobbágy, E. G. and Jackson, R. B. (2000) 'THE VERTICAL DISTRIBUTION OF SOIL ORGANIC CARBON AND ITS RELATION TO CLIMATE AND VEGETATION', *Ecological Applications*. Ecological Society of America, 10(2), pp. 423–436. doi: 10.1890/1051-0761(2000)010[0423:TVDOSO]2.0.CO;2.

Johnson, A. H., Frizano, J. and Vann, D. R. (2003) 'Biogeochemical Implications of Labile Phosphorus in Forest Soils Determined by the Hedley', *Oecologia*, 135(4), pp. 487–499.

Jørgensen, C. (2015) 'Identification of inositol hexakisphosphate binding sites in soils by selective extraction and solution ^{31}P NMR spectroscopy', *Geoderma*, 257, pp. 22–28. doi: 10.1016/j.geoderma.2015.03.021.

Kaiser, K. and Guggenberger, G. (2003) 'Mineral surfaces and soil organic matter', *European Journal of Soil Science*. Blackwell Science Ltd, 54(2), pp. 219–236. doi: 10.1046/j.1365-2389.2003.00544.x.

Kaiser, M., Ellerbrock, R. H. and Sommer, M. (2009) 'Separation of Coarse Organic Particles from Bulk Surface Soil Samples by Electrostatic Attraction', *Soil Science Society of America Journal*. Soil Science Society, 73(6), p. 2118. doi: 10.2136/sssaj2009.0046.

Kalbitz, K., Schmerwitz, J., Schwesig, D. and Matzner, E. (2003) 'Biodegradation of soil-derived dissolved organic matter as related to its properties', *Geoderma*, 113(3–4), pp. 273–291. doi: 10.1016/S0016-7061(02)00365-8.

Kalbitz, K., Schwesig, D., Rethemeyer, J. and Matzner, E. (2005) 'Stabilization of dissolved organic matter by sorption to the mineral soil', *Soil Biology and Biochemistry*, 37(7), pp. 1319–1331. doi: 10.1016/j.soilbio.2004.11.028.

Kalbitz, K., Schwesig, D., Schmerwitz, J., Kaiser, K., Haumaier, L., Glaser, B., Ellerbrock, R. and Leinweber, P. (2003) 'Changes in properties of soil-derived dissolved organic matter induced by biodegradation', *Soil Biology and Biochemistry*, 35(8), pp. 1129–1142. doi: 10.1016/S0038-0717(03)00165-2.

Kang, S. H., Amarasiriwardena, D., Veneman, P. and Xing, B. S. (2003) 'Characterization of ten sequentially extracted humic acids and a humin from a soil in western Massachusetts', *Soil Science*, 168(12), pp. 880–887. doi: DOI

10.1097/01.ss.0000106404.84926.b0.

Kellerman, A. M., Kothawala, D. N., Dittmar, T. and Tranvik, L. J. (2015) 'Persistence of dissolved organic matter in lakes related to its molecular characteristics', *Nature Geoscience*. Nature Research, 8(6), pp. 454–457. doi: 10.1038/ngeo2440.

Kendall, C., Silva, S. R. and Kelly, V. J. (2001) 'Carbon and nitrogen isotopic compositions of particulate organic matter in four large river systems across the United States', *Hydrological Processes*. John Wiley & Sons, Ltd., 15(7), pp. 1301–1346. doi: 10.1002/hyp.216.

Kiem, R. and Kögel-Knabner, I. (2003) 'Contribution of lignin and polysaccharides to the refractory carbon pool in C-depleted arable soils', *Soil Biology and Biochemistry*, 35(1), pp. 101–118. doi: 10.1016/S0038-0717(02)00242-0.

Kirkby, C. A., Kirkegaard, J. A., Richardson, A. E., Wade, L. J., Blanchard, C. and Batten, G. (2011) 'Stable soil organic matter: A comparison of C:N:P:S ratios in Australian and other world soils', *Geoderma*. Elsevier B.V., 163(3–4), pp. 197–208. doi: 10.1016/j.geoderma.2011.04.010.

Kirkby, C. A., Richardson, A. E., Wade, L. J., Batten, G. D., Blanchard, C. and Kirkegaard, J. A. (2013) 'Carbon-nutrient stoichiometry to increase soil carbon sequestration', *Soil Biology and Biochemistry*, 60, pp. 77–86. doi: 10.1016/j.soilbio.2013.01.011.

Klages, M. G. and Hsieh, Y. P. (1975) 'Suspended Solids Carried by the Gallatin River of Southwestern Montana: II. Using Mineralogy for Inferring Sources¹', *Journal of Environment Quality*, 4(1), p. 68. doi: 10.2134/jeq1975.00472425000400010016x.

Kleber, M. and Johnson, M. G. (2010) 'Chapter 3 – Advances in Understanding the Molecular Structure of Soil Organic Matter: Implications for Interactions in the Environment', in *Advances in Agronomy*, pp. 77–142. doi: 10.1016/S0065-2113(10)06003-7.

Knicker, H. (2011) 'Soil organic N - An under-rated player for C sequestration in soils?', *Soil Biology and Biochemistry*, 43(6), pp. 1118–1129. doi: 10.1016/j.soilbio.2011.02.020.

Kögel-Knabner, I. (2000) 'Analytical approaches for characterizing soil organic matter', *Organic Geochemistry*, 31(7), pp. 609–625. doi: 10.1016/S0146-6380(00)00042-5.

Kögel-Knabner, I. (2002) 'The macromolecular organic composition of plant and microbial residues as inputs to soil organic matter', *Soil Biology and Biochemistry*, 34(2), pp. 139–162. doi: 10.1016/S0038-0717(01)00158-4.

Kögel-Knabner, I. (2006) 'Chemical Structure of Organic N and Organic P in Soil', in *Nucleic Acids and Proteins in Soil*. Springer Berlin Heidelberg, pp. 23–48. doi: 10.1007/3-540-29449-X_2.

Kögel-Knabner, I., Guggenberger, G., Kleber, M., Kandeler, E., Kalbitz, K., Scheu, S., Eusterhues, K. and Leinweber, P. (2008) 'Organo-mineral associations in temperate soils: Integrating biology, mineralogy, and organic matter chemistry', *Journal of Plant Nutrition and Soil Science*. WILEY-VCH Verlag, 171(1), pp. 61–82. doi: 10.1002/jpln.200700048.

Kölbl, A. and Kögel-Knabner, I. (2004) 'Content and composition of free and occluded particulate organic matter in a differently textured arable Cambisol as revealed by solid-

state ^{13}C NMR spectroscopy', *Journal of Plant Nutrition and Soil Science*. WILEY-VCH Verlag, 167(1), pp. 45–53. doi: 10.1002/jpln.200321185.

Kramer, M. G., Sollins, P., Sletten, R. S. and Swart, P. K. (2003) 'N isotope fractionation and measures of organic matter alteration during decomposition', *Ecology*. Ecological Society of America, 84(8), pp. 2021–2025. doi: 10.1890/02-3097.

Lal, R. (2003) 'Soil erosion and the global carbon budget', *Environment International*, 29(4), pp. 437–450. doi: 10.1016/S0160-4120(02)00192-7.

Lam, B., Baer, A., Alaee, M., Lefebvre, B., Moser, A., Williams, A. and Simpson, A. J. (2007) 'Major structural components in freshwater dissolved organic matter.', *Environ. Sci. Technol.*, 41(24), pp. 8240–8247. doi: 10.1021/es0713072.

Lehmann, J. and Kleber, M. (2015) 'The contentious nature of soil organic matter', *Nature*, 528(7580), pp. 60–8. doi: 10.1038/nature16069.

LEIFELD, J., ZIMMERMANN, M., FUHRER, J. and CONEN, F. (2009) 'Storage and turnover of carbon in grassland soils along an elevation gradient in the Swiss Alps', *Global Change Biology*. Blackwell Publishing Ltd, 15(3), pp. 668–679. doi: 10.1111/j.1365-2486.2008.01782.x.

Libby, W. F., Anderson, E. C. and Arnold, J. R. (1949) 'Age Determination by Radiocarbon Content: World-Wide Assay of Natural Radiocarbon', *Science*, 109(2827).

Longworth, B. E., Petsch, S. T., Raymond, P. a. and Bauer, J. E. (2007) 'Linking lithology and land use to sources of dissolved and particulate organic matter in headwaters of a temperate, passive-margin river system', *Geochimica et Cosmochimica*

Acta, 71(17), pp. 4233–4250. doi: 10.1016/j.gca.2007.06.056.

Lu, Y. H., Bauer, J. E., Canuel, E. a., Chambers, R. M., Yamashita, Y., Jaffé, R. and Barrett, A. (2014) ‘Effects of land use on sources and ages of inorganic and organic carbon in temperate headwater streams’, *Biogeochemistry*, 119(1–3), pp. 275–292. doi: 10.1007/s10533-014-9965-2.

Lundström, U. ., van Breemen, N. and Bain, D. (2000) ‘The podzolization process. A review’, *Geoderma*, 94(2), pp. 91–107. doi: 10.1016/S0016-7061(99)00036-1.

Lutzow, M. v., Kogel-Knabner, I., Ekschmitt, K., Matzner, E., Guggenberger, G., Marschner, B. and Flessa, H. (2006) ‘Stabilization of organic matter in temperate soils: mechanisms and their relevance under different soil conditions - a review’, *European Journal of Soil Science*. Blackwell Publishing Ltd, 57(4), pp. 426–445. doi: 10.1111/j.1365-2389.2006.00809.x.

M. Stuiver & HA. Polach (1977) ‘Reporting of ¹⁴C data’, *Radiocarbon*, 19, pp. 355–363.

Maberly, S. C., King, L., Dent, M. M., Jones, R. I. and Gibson, C. E. (2002) ‘Nutrient limitation of phytoplankton and periphyton growth in upland lakes’, *Freshwater Biology*. Blackwell Science Ltd, 47(11), pp. 2136–2152. doi: 10.1046/j.1365-2427.2002.00962.x.

Mahieu, N., Randall, E. W. and Powlson, D. S. (1999) ‘Statistical Analysis of Published Carbon-13 CPMAS NMR Spectra of Soil Organic Matter’, *Soil Science Society of America Journal*. Soil Science Society of America, 63(2), p. 307. doi: 10.2136/sssaj1999.03615995006300020008x.

Mahowald, N., Jickells, T. D., Baker, A. R., Artaxo, P., Benitez-Nelson, C. R., Bergametti, G., Bond, T. C., Chen, Y., Cohen, D. D., Herut, B., Kubilay, N., Losno, R., Luo, C., Maenhaut, W., McGee, K. A., Okin, G. S., Siefert, R. L. and Tsukuda, S. (2008) 'Global distribution of atmospheric phosphorus sources, concentrations and deposition rates, and anthropogenic impacts', *Global Biogeochemical Cycles*, 22(4), p. n/a-n/a. doi: 10.1029/2008GB003240.

Marker, A. F. H., Nusch, E. A., Rai, H. and Riemann, B. (1978) 'The measurement of photosynthetic pigments in freshwaters and standardisation of methods: Conclusions and recommendations', *Arch. Hydrobiologie*, 14, pp. 91–106.

Marklein, A. R. and Houlton, B. Z. (2012) 'Nitrogen inputs accelerate phosphorus cycling rates across a wide variety of terrestrial ecosystems', *New Phytologist*. Blackwell Publishing Ltd, 193(3), pp. 696–704. doi: 10.1111/j.1469-8137.2011.03967.x.

Marwick, T. R., Tamoo, F., Teodoru, C. R., Borges, A. V., Darchambeau, F. and Bouillon, S. (2015) 'The age of river-transported carbon: A global perspective', *Global Biogeochemical Cycles*. doi: 10.1002/2014GB004911.

Mash, H., Westerhoff, P. K., Baker, L. A., Nieman, R. A. and Nguyen, M. L. (2004) 'Dissolved organic matter in Arizona reservoirs: Assessment of carbonaceous sources', *Organic Geochemistry*, 35(7), pp. 831–843. doi: 10.1016/j.orggeochem.2004.03.002.

Masiello, A. (2001) 'Carbon isotope geochemistry of the Santa Clara River', *Global Biogeochemical Cycles*, 15(2), pp. 407–416.

Mayorga, E., Aufdenkampe, A. K., Masiello, C. A., Krusche, A. V., Hedges, J. I., Quay, P. D., Richey, J. E. and Brown, T. A. (2005) 'Young organic matter as a source of

carbon dioxide outgassing from Amazonian rivers’, *Nature*. Nature Publishing Group, 436(7050), pp. 538–541. doi: 10.1038/nature03880.

Megens, L., van der Plicht, J., de Leeuw, J. ., L, M., J, V. D. P. and de Leeuw, W. (2001) ‘C and ¹⁴C concentrations in particulate organic matter from the southern North Sea’, *Geochimica et Cosmochimica Acta*, 65(17), pp. 2899–2911. doi: 10.1016/S0016-7037(01)00648-2.

Menzel, D. W. and Vaccaro, R. F. (1964) ‘THE MEASUREMENT OF DISSOLVED ORGANIC AND PARTICULATE CARBON IN SEAWATER¹’, *Limnology and Oceanography*, 9(1), pp. 138–142. doi: 10.4319/lo.1964.9.1.0138.

Messenger, M. L., Lehner, B., Grill, G., Nedeva, I. and Schmitt, O. (2016) ‘Estimating the volume and age of water stored in global lakes using a geo-statistical approach’, *Nature Communications*. Nature Publishing Group, 7, pp. 1–11. doi: 10.1038/ncomms13603.

Meybeck, M. (1982) ‘Carbon, nitrogen, and phosphorus transport by world rivers’, *American Journal of Science*. American Journal of Science, 282(4), pp. 401–450. doi: 10.2475/ajs.282.4.401.

Meybeck, M. and Vörösmarty, C. (1999) ‘Global transfer of carbon by rivers’, *Global Change Newsletter*, (8), pp. 18–19.

MHB Hayes, G Song, A. S. (2009) ‘Humic fractions and the nature of organic materials in intimate association with soil clays’, in *Carbon Stabilization by Clays*. Minerals Society, Chantilly, VA, pp. 1–31.

‘MICROWAVE ASSISTED ACID DIGESTION OF SEDIMENTS, SLUDGES,

SOILS, AND OILS SW-846' (2007).

Mills, R. T. E., Tipping, E., Bryant, C. L. and Emmett, B. a. (2013) 'Long-term organic carbon turnover rates in natural and semi-natural topsoils', *Biogeochemistry*, 118(1–3), pp. 257–272. doi: 10.1007/s10533-013-9928-z.

Monteith, D. T., Stoddard, J. L., Evans, C. D., de Wit, H. a, Forsius, M., Høgåsen, T., Wilander, A., Skjelkvåle, B. L., Jeffries, D. S., Vuorenmaa, J., Keller, B., Kopáček, J. and Vesely, J. (2007) 'Dissolved organic carbon trends resulting from changes in atmospheric deposition chemistry.', *Nature*, 450(7169), pp. 537–40. doi: 10.1038/nature06316.

Moore, S., Evans, C. D., Page, S. E., Garnett, M. H., Jones, T. G., Freeman, C., Hooijer, A., Wiltshire, A. J., Limin, S. H. and Gauci, V. (2013) 'Deep instability of deforested tropical peatlands revealed by fluvial organic carbon fluxes.', *Nature*. Nature Publishing Group, 493(7434), pp. 660–3. doi: 10.1038/nature11818.

Moss, B., Barker, T., Stephen, D., Williams, A. E., Balayla, D. J., Beklioglu, M. and Carvalho, L. (2005) 'Consequences of reduced nutrient loading on a lake system in a lowland catchment: Deviations from the norm?', *Freshwater Biology*, 50(10), pp. 1687–1705. doi: 10.1111/j.1365-2427.2005.01416.x.

Moyer, R. P., Bauer, J. E. and Grottoli, A. G. (2013) 'Carbon isotope biogeochemistry of tropical small mountainous river, estuarine, and coastal systems of Puerto Rico', *Biogeochemistry*, 112(1–3), pp. 589–612. doi: 10.1007/s10533-012-9751-y.

Mulder, J., Christophersen, N., Hauhs, M., Vogt, R. D., Andersen, S. and Andersen, D. O. (1990) 'Water flow paths and hydrochemical controls in the Birkenes Catchment as inferred from a rainstorm high in seasalts', *Water Resources Research*, 26(4), pp. 611–

622. doi: 10.1029/WR026i004p00611.

Nagao, S., Aramaki, T., Fujitake, N., Matsunaga, T. and Tkachenko, Y. (2004) 'Radiocarbon of dissolved humic substances in river waters from the Chernobyl area', *Nuclear Instruments and Methods in Physics Research, Section B: Beam Interactions with Materials and Atoms*, 223–224(SPEC. ISS.), pp. 848–853. doi: 10.1016/j.nimb.2004.04.156.

Neff, J. C., Finlay, J. C., Zimov, S. a., Davydov, S. P., Carrasco, J. J., Schuur, E. a. G. and Davydova, a. I. (2006) 'Seasonal changes in the age and structure of dissolved organic carbon in Siberian rivers and streams', *Geophysical Research Letters*, 33(23), pp. 1–5. doi: 10.1029/2006GL028222.

Nguyen, M., Westerhoff, P., Baker, L., Hu, Q., Esparza-Soto, M. and Sommerfeld, M. (2005) 'Characteristics and Reactivity of Algae-Produced Dissolved Organic Carbon', *Journal of Environmental Engineering*, 131(November), pp. 1574–1582. doi: doi:10.1061/(ASCE)0733-9372(2005)131:11(1574).

Nierop, K. G. J. ., Jansen, B. and Verstraten, J. M. (2002) 'Dissolved organic matter, aluminium and iron interactions: precipitation induced by metal/carbon ratio, pH and competition', *Science of The Total Environment*, 300(1), pp. 201–211. doi: 10.1016/S0048-9697(02)00254-1.

O'Hara, C. P., Bauhus, J. and Smethurst, P. J. (2006) 'Role of light fraction soil organic matter in the phosphorus nutrition of Eucalyptus globulus seedlings', *Plant and Soil*, 280(1–2), pp. 127–134. doi: 10.1007/s11104-005-2675-8.

Onstad, G. D., Canfield, D. E., Quay, P. D. and Hedges, J. I. (2000) 'Sources of particulate organic matter in rivers from the continental USA: Lignin phenol and stable

carbon isotope compositions', *Geochimica et Cosmochimica Acta*, 64(20), pp. 3539–3546. doi: 10.1016/S0016-7037(00)00451-8.

Osburn, C. L., Wigdahl, C. R., Fritz, S. C. and Saros, J. E. (2011) 'Dissolved organic matter composition and photoreactivity in prairie lakes of the U.S. Great Plains', *Limnology and Oceanography*, 56(6), pp. 2371–2390. doi: 10.4319/lo.2011.56.6.2371.

Otto, A. and Simpson, M. J. (2005) 'Degradation and Preservation of Vascular Plant-derived Biomarkers in Grassland and Forest Soils from Western Canada', *Biogeochemistry*. Kluwer Academic Publishers, 74(3), pp. 377–409. doi: 10.1007/s10533-004-5834-8.

Otto, A. and Simpson, M. J. (2007) 'Analysis of soil organic matter biomarkers by sequential chemical degradation and gas chromatography – mass spectrometry', *Journal of Separation Science*. WILEY-VCH Verlag, 30(2), pp. 272–282. doi: 10.1002/jssc.200600243.

Owens, P. N., Walling, D. E. and Leeks, G. J. . (1999) 'Use of floodplain sediment cores to investigate recent historical changes in overbank sedimentation rates and sediment sources in the catchment of the River Ouse, Yorkshire, UK', *Catena*, 36(1–2), pp. 21–47. doi: 10.1016/S0341-8162(99)00010-7.

Palmer, S. M., Hope, D., Billett, M. F., Dawson, J. J. C. and Bryant, C. L. (2001) 'Sources of organic and inorganic carbon in a headwater stream : Evidence from carbon isotope studies', *Biogeochemistry*, 52, pp. 321–338.

Parton, W. . (1996) 'Ecosystem model comparisons: science or fantasy world?', in D.S Powlson, P. S. and J. . S. (ed.) *Evaluation of soil organic matter models*. Springer-Verlag, pp. 133–142.

Peñuelas, J., Poulter, B., Sardans, J., Ciais, P., van der Velde, M., Bopp, L., Boucher, O., Godderis, Y., Hinsinger, P., Llusia, J., Nardin, E., Vicca, S., Obersteiner, M. and Janssens, I. A. (2013) 'Human-induced nitrogen–phosphorus imbalances alter natural and managed ecosystems across the globe', *Nature Communications*. Nature Publishing Group, 4, pp. 153–226. doi: 10.1038/ncomms3934.

Pereira, R., Isabella Bovolo, C., Spencer, R. G. M., Hernes, P. J., Tipping, E., Vieth-Hillebrand, A., Pedentchouk, N., Chappell, N. A., Parkin, G. and Wagner, T. (2014) 'Mobilization of optically invisible dissolved organic matter in response to rainstorm events in a tropical forest headwater river', *Geophysical Research Letters*, 41(4), pp. 1202–1208. doi: 10.1002/2013GL058658.

Phiri, S., Barrios, E., Rao, I. M. and Singh, B. R. (2001) 'Changes in soil organic matter and phosphorus fractions under planted fallows and a crop rotation system on a Colombian volcanic-ash soil', *Plant and Soil*. Kluwer Academic Publishers, 231(2), pp. 211–223. doi: 10.1023/A:1010310300067.

Piccolo, A. (2002) 'The supramolecular structure of humic substances: A novel understanding of humus chemistry and implications in soil science', *Advances in Agronomy*, 75, pp. 57–134. doi: 10.1016/S0065-2113(02)75003-7.

Raich, J. W. and Potter, C. S. (1995) 'Global Patterns of Carbon-Dioxide Emissions From Soils', *Global Biogeochemical Cycles*, 9(1), pp. 23–36. doi: 10.1029/94gb02723.

Randerson, J. T., Chapin, F. S., Harden, J. W., Neff, J. C. and Harmon, M. E. (2002) 'NET ECOSYSTEM PRODUCTION: A COMPREHENSIVE MEASURE OF NET CARBON ACCUMULATION BY ECOSYSTEMS', *Ecological Applications*. Ecological Society of America, 12(4), pp. 937–947. doi: 10.1890/1051-

0761(2002)012[0937:NEPACM]2.0.CO;2.

Raymond, P. A. and Bauer, J. E. (2001) 'DOC cycling in a temperate estuary: A mass balance approach using natural', *Limnol. Oceanogr*, 46(3), pp. 655–667. doi: 10.4319/lo.2001.46.3.0655.

Raymond, P. a., McClelland, J. W., Holmes, R. M., Zhulidov, a. V., Mull, K., Peterson, B. J., Striegl, R. G., Aiken, G. R. and Gurtovaya, T. Y. (2007) 'Flux and age of dissolved organic carbon exported to the Arctic Ocean: A carbon isotopic study of the five largest arctic rivers', *Global Biogeochemical Cycles*, 21(4), pp. 1–9. doi: 10.1029/2007GB002934.

Raymond, P. a and Bauer, J. E. (2001) 'Riverine export of aged terrestrial organic matter to the North Atlantic Ocean.', *Nature*, 409(6819), pp. 497–500. doi: 10.1038/35054034.

Raymond, P. a, Hartmann, J., Lauerwald, R., Sobek, S., McDonald, C., Hoover, M., Butman, D., Striegl, R., Mayorga, E., Humborg, C., Kortelainen, P., Durr, H., Meybeck, M., Ciais, P. and Guth, P. (2013) 'Global carbon dioxide emissions from inland waters', *Nature*, 503(7476), pp. 355–359. doi: 10.1038/nature12760.

Redfield, A. C. (1958) 'The biological control of chemical factors in the environment', *American Scientis*, 46(3), pp. 205–221.

Reynolds, C. . (1979) 'The limnology of the eutrophic meres of the Shropshire-Cheshire plain: A review', pp. 93–173.

Rice, J. A. (2001) 'Humins', *Soil Science*, 166(11), pp. 848–857.

Richter, D. D., Markewitz, D., Trumbore, S. E. and Wells, C. G. (1999) 'Rapid

accumulation and turnover of soil carbon in a re-establishing forest', *Nature*. Nature Publishing Group, 400(6739), pp. 56–58. doi: 10.1038/21867.

Rodkey, K. S., Kaczmarek, D. J. and Pope, P. E. (1995) 'The distribution of nitrogen and phosphorus in forest floor layers of oak-hickory forests of varying productivity.', *Proceedings 10th Central Hardwood Forest Conference.*, Gen. Tech., pp. 94–108.

Rosenheim, B. E. and Galy, V. (2012) 'Direct measurement of riverine particulate organic carbon age structure', *Geophysical Research Letters*, 39(19), p. n/a-n/a. doi: 10.1029/2012GL052883.

Rumpel, C., Eusterhues, K. and Kögel-Knabner, I. (2004) 'Location and chemical composition of stabilized organic carbon in topsoil and subsoil horizons of two acid forest soils', *Soil Biology and Biochemistry*, 36(1), pp. 177–190. doi: 10.1016/j.soilbio.2003.09.005.

Rumpel, C. and Kögel-Knabner, I. (2011) 'Deep soil organic matter—a key but poorly understood component of terrestrial C cycle', *Plant and Soil*. Springer Netherlands, 338(1–2), pp. 143–158. doi: 10.1007/s11104-010-0391-5.

Sachleben, J. R. and Hatcher, P. G. (2004) 'Solid-State NMR Characterization of Pyrene - Cuticular Matter Interactions', *Environmental Science and Technology*, (614), pp. 4369–4376.

Saggar, S., Parshotam, A., Sparling, G. P., Feltham, C. W. and Hart, P. B. S. (1996) '14C-labelled ryegrass turnover and residence times in soils varying in clay content and mineralogy', *Soil Biology and Biochemistry*, 28(12), pp. 1677–1686. doi: 10.1016/S0038-0717(96)00250-7.

Salas, a M., Elliott, E. T., Westfall, D. G., Cole, C. V and Six, J. (2003) 'The Role of Particulate Organic Matter in Phosphorus Cycling', *Soil Science Society of America Journal*, 67(1), p. 181. doi: 10.2136/sssaj2003.0181.

S Xu, R Anderson, C Bryant, G T Cook, A Dougans, S Freeman, P Naysmith, C Schnabel, E. M. S. (2004) 'Performance Tests on Solid Samples', *Radiocarbon*, 46(1), pp. 59–64.

Schachtman, D. P., Reid, R. J. and Ayling, S. M. (1998) 'Update on Phosphorus Uptake Phosphorus Uptake by Plants: From Soil to Cell', pp. 447–453. doi: 10.1104/pp.116.2.447.

Scharlemann, J. P., Tanner, E. V., Hiederer, R. and Kapos, V. (2014) 'Global soil carbon: understanding and managing the largest terrestrial carbon pool', *Carbon Management*. Future Science Ltd London, UK, 5(1), pp. 81–91. doi: 10.4155/cmt.13.77.

Schiff, S. L., Aravena, R., Trumbore, S. E. and Hinton, M. J. (1997) 'Export of DOC from forested catchments on the Precambrian Shield of Central Ontario : Clues from ^{13}C ', (Figure 1), pp. 43–65.

Schlesinger, W. H. (1997) *Biogeochemistry: an analysis of global change*. Academic Press.

Schlesinger, W. H. and Andrews, J. A. (2000) 'Soil Respiration and the Global Carbon Cycle', *Source: Biogeochemistry*, 48(1), pp. 7–20.

Schlünz, B. and Schneider, R. R. (2000) 'Transport of terrestrial organic carbon to the oceans by rivers: re-estimating flux- and burial rates', *International Journal of Earth Sciences*, 88(4), pp. 599–606. doi: 10.1007/s005310050290.

Schmidt, M. W. I., Torn, M. S., Abiven, S., Dittmar, T., Guggenberger, G., Janssens, I. A., Kleber, M., Kögel-Knabner, I., Lehmann, J., Manning, D. A. C., Nannipieri, P., Rasse, D. P., Weiner, S. and Trumbore, S. E. (2011) 'Persistence of soil organic matter as an ecosystem property', *Nature*. Nature Research, 478(7367), pp. 49–56. doi: 10.1038/nature10386.

Schrumpf, M., Kaiser, K., Guggenberger, G., Persson, T., Kögel-Knabner, I. and Schulze, E. D. (2013) 'Storage and stability of organic carbon in soils as related to depth, occlusion within aggregates, and attachment to minerals', *Biogeosciences*, 10(3), pp. 1675–1691. doi: 10.5194/bg-10-1675-2013.

Schulten, H.-R. and Schnitzer, M. (1997) 'The chemistry of soil organic nitrogen: a review', *Biology and Fertility of Soils*. Springer-Verlag, 26(1), pp. 1–15. doi: 10.1007/s003740050335.

Schulze, K., Borken, W., Muhr, J. and Matzner, E. (2009) 'Stock, turnover time and accumulation of organic matter in bulk and density fractions of a Podzol soil', *European Journal of Soil Science*. Blackwell Publishing Ltd, 60(4), pp. 567–577. doi: 10.1111/j.1365-2389.2009.01134.x.

Seitzinger, S., Harrison, J., Bohlke, J., Bouwman, A., Lowrance, R., Peterson, B., Tobias, C. and Van Drecht, G. (2006) 'Denitrification across landscapes and waterscapes: a synthesis', *Ecological Applications*, 16(6), pp. 2064–2090. doi: 10.1890/1051-0761(2006)016[2064:DALAWA]2.0.CO;2.

Selberg, A., Viik, M., Ehapalu, K. and Tenno, T. (2011) 'Content and composition of natural organic matter in water of Lake Pitkjärv and mire feeding Kuke River (Estonia)', *Journal of Hydrology*. Elsevier B.V., 400(1–2), pp. 274–280. doi:

10.1016/j.jhydrol.2011.01.035.

Sickman, J. O., DiGiorgio, C. L., Lee Davisson, M., Lucero, D. M. and Bergamaschi, B. (2009) 'Identifying sources of dissolved organic carbon in agriculturally dominated rivers using radiocarbon age dating: Sacramento–San Joaquin River Basin, California', *Biogeochemistry*, 99(1–3), pp. 79–96. doi: 10.1007/s10533-009-9391-z.

Sickman, J. O., Zanolli, M. J. and Mann, H. L. (2007) 'Effects of urbanization on organic carbon loads in the Sacramento River, California', *Water Resources Research*, 43(11), pp. 1–15. doi: 10.1029/2007WR005954.

Simpson, A. J., McNally, D. J. and Simpson, M. J. (2011) 'NMR spectroscopy in environmental research: From molecular interactions to global processes', *Progress in Nuclear Magnetic Resonance Spectroscopy*, 58(3–4), pp. 97–175. doi: 10.1016/j.pnmrs.2010.09.001.

Simpson, A. J., Simpson, M. J., Smith, E. and Kelleher, B. P. (2007) 'Microbially derived inputs to soil organic matter: Are current estimates too low?', *Environmental Science and Technology*, 41(23), pp. 8070–8076. doi: 10.1021/es071217x.

Simpson, M. J. and Johnson, P. C. E. (2006) 'IDENTIFICATION OF MOBILE ALIPHATIC SORPTIVE DOMAINS IN SOIL HUMIN BY SOLID-STATE ¹³C NUCLEAR MAGNETIC RESONANCE', *Environmental Toxicology and Chemistry*. Wiley Periodicals, Inc., 25(1), p. 52. doi: 10.1897/05-152R.1.

Simpson, M. J. and Simpson, A. J. (2012) 'The Chemical Ecology of Soil Organic Matter Molecular Constituents', *Journal of Chemical Ecology*, 38(6), pp. 768–784. doi: 10.1007/s10886-012-0122-x.

Six, J., Conant, R. T., Paul, E. A. and Paustian, K. (2002) 'Stabilization mechanisms of soil organic matter: Implications for C-saturation of soils', *Plant and Soil*. Kluwer Academic Publishers, 241(2), pp. 155–176. doi: 10.1023/A:1016125726789.

Six, J., Elliott, E. T. and Paustian, K. (2000) 'Soil macroaggregate turnover and microaggregate formation: A mechanism for C sequestration under no-tillage agriculture', *Soil Biology and Biochemistry*, 32(14), pp. 2099–2103. doi: 10.1016/S0038-0717(00)00179-6.

Six, J., Elliott, E. T., Paustian, K. and Doran, J. W. (1998) 'Aggregation and Soil Organic Matter Accumulation in Cultivated and Native Grassland Soils', *Soil Science Society of America Journal*. Soil Science Society of America, 62(5), p. 1367. doi: 10.2136/sssaj1998.03615995006200050032x.

Six, J. and Jastrow, J. D. (2002) 'Organic matter turnover', *Encyclopedia of Soil Science*, pp. 936–942. doi: 10.1081/E-ESS-120001812.

Slota, P. J., Jull, A. J. T., Linick, T. W., Toolin, L. J., Beukens, R. P., Kromer, B., Van Der Plicht, J., Kromer, B., Junghans, C. and Münnich, K. O. (1987) 'Preparation of Small Samples for ¹⁴C Accelerator Targets by Catalytic Reduction of CO', *Radiocarbon*. Cambridge University Press, 29(2), pp. 303–306. doi: 10.1017/S0033822200056988.

Smith, J. C., Galy, A., Hovius, N., Tye, A. M., Turowski, J. M. and Schleppe, P. (2013) 'Runoff-driven export of particulate organic carbon from soil in temperate forested uplands', *Earth and Planetary Science Letters*. Elsevier, 365, pp. 198–208. doi: 10.1016/j.epsl.2013.01.027.

Smith, V. H., Tilman, G. D. and Nekola, J. C. (1998) 'Eutrophication: Impacts of excess

nutrient inputs on freshwater, marine, and terrestrial ecosystems’, *Environmental Pollution*, 100(1–3), pp. 179–196. doi: 10.1016/S0269-7491(99)00091-3.

Sohi, S. P., Mahieu, N., Arah, J. R. M., Powlson, D. S., Madari, B. and Gaunt, J. L. (2001) ‘A Procedure for Isolating Soil Organic Matter Fractions Suitable for Modeling’, *Soil Science Society of America Journal*. Soil Science Society, 65(4), pp. 1121–1128. doi: 10.2136/sssaj2001.6541121x.

Spencer, R. G. M., Butler, K. D. and Aiken, G. R. (2012) ‘Dissolved organic carbon and chromophoric dissolved organic matter properties of rivers in the USA’, *Journal of Geophysical Research: Biogeosciences*, 117(3), p. n/a-n/a. doi: 10.1029/2011JG001928.

Stevenson, F. J. and Cole, M. A. (Michael A. . (1999) *Cycles of soil : carbon, nitrogen, phosphorus, sulfur, micronutrients*. Wiley.

Still, C. J., Berry, J. A., Collatz, G. J. and DeFries, R. S. (2003) ‘Global distribution of C3 and C4 vegetation: Carbon cycle implications’, *Global Biogeochemical Cycles*, 17(1), pp. 6-1-6–14. doi: 10.1029/2001GB001807.

Swanston, C. W., Caldwell, B. A., Homann, P. S., Ganio, L. and Sollins, P. (2002) ‘Carbon dynamics during a long-term incubation of separate and recombined density fractions from seven forest soils’, *Soil Biology and Biochemistry*, 34(8), pp. 1121–1130. doi: 10.1016/S0038-0717(02)00048-2.

Swanston, C. W., Torn, M. S., Hanson, P. J., Southon, J. R., Garten, C. T., Hanlon, E. M. and Ganio, L. (2005) ‘Initial characterization of processes of soil carbon stabilization using forest stand-level radiocarbon enrichment’, *Geoderma*, 128(1), pp. 52–62. doi: 10.1016/j.geoderma.2004.12.015.

Tan, Z., Lal, R., Owens, L. and Izaurralde, R. C. (2007) 'Distribution of light and heavy fractions of soil organic carbon as related to land use and tillage practice', *Soil and Tillage Research*, 92(1), pp. 53–59. doi: 10.1016/j.still.2006.01.003.

Thacker, S. A., Tipping, E., Gondar, D. and Baker, A. (2008) 'Functional properties of DOM in a stream draining blanket peat', *Science of The Total Environment*, 407(1), pp. 566–573. doi: 10.1016/j.scitotenv.2008.09.011.

Tilman, D., Fargione, J., Wolff, B., D'Antonio, C., Dobson, A., Howarth, R., Schindler, D., Schlesinger, W. H., Simberloff, D. and Swackhamer, D. (2001) 'Forecasting Agriculturally Driven Global Environmental Change', *Science*, 292(5515).

Tipping, E., Benham, S., Boyle, J. F., Crow, P., Davies, J., Fischer, U., Guyatt, H., Helliwell, R. C., Jackson-Blake, L., Lawlor, A. J., Monteith, D. T., Rowe, E. C. and Toberman, H. (2014) 'Atmospheric deposition of phosphorus to land and freshwater', *Environ. Sci.: Processes Impacts*. The Royal Society of Chemistry, 16(7), pp. 1608–1617. doi: 10.1039/C3EM00641G.

Tipping, E., Billett, M. F., Bryant, C. L., Buckingham, S. and Thacker, S. a. (2010) 'Sources and ages of dissolved organic matter in peatland streams: Evidence from chemistry mixture modelling and radiocarbon data', *Biogeochemistry*, 100(1), pp. 121–137. doi: 10.1007/s10533-010-9409-6.

Tipping, E., Corbishley, H. T., Koprivnjak, J.-F., Lapworth, D. J., Miller, M. P., Vincent, C. D. and Hamilton-Taylor, J. (2009) 'Quantification of natural DOM from UV absorption at two wavelengths', *Environmental Chemistry*. CSIRO PUBLISHING, 6(6), p. 472. doi: 10.1071/EN09090.

Tipping, E., Marker, A., Butterwick, C., Collett, G. D., Cranwell, P. A., Ingram, J. K.

G., Leach, D. V., Lishman, J. P., Pinder, A. C., Rigg, E. and Simon, B. M. (1997) 'Organic carbon in the Humber rivers', *Science of The Total Environment*, 194–195(96), pp. 345–355. doi: 10.1016/S0048-9697(96)05374-0.

Tipping, E., Rowe, E. C., Evans, C. D., Mills, R. T. E., Emmett, B. A., Chaplow, J. S. and Hall, J. R. (2012) 'N14C: A plant-soil nitrogen and carbon cycling model to simulate terrestrial ecosystem responses to atmospheric nitrogen deposition', *Ecological Modelling*. Elsevier B.V., 247, pp. 11–26. doi: 10.1016/j.ecolmodel.2012.08.002.

Tipping, E., Smith, E. J., Bryant, C. L. and Adamson, J. K. (2007) 'The organic carbon dynamics of a moorland catchment in N. W. England', *Biogeochemistry*, 84(2), pp. 171–189. doi: 10.1007/s10533-007-9117-z.

Tipping, E., Somerville, C. J. and Luster, J. (2016) 'The C:N:P:S stoichiometry of soil organic matter', *Biogeochemistry*, (Amundson 2001). doi: 10.1007/s10533-016-0247-z.

Tittel, J., Büttner, O., Freier, K., Heiser, A., Sudbrack, R. and Ollesch, G. (2013) 'The age of terrestrial carbon export and rainfall intensity in a temperate river headwater system', *Biogeochemistry*, 115(1–3), pp. 53–63. doi: 10.1007/s10533-013-9896-3.

Toberman H, Adams J, Tipping E, Schillereff D, Somerville C, Coull M, Helliwell R, Carter H, Guyatt H, Keenan P, Lawlor A, Pereira MG, Patel M, Tanna B, Thacker S, Thomson N, Owens J, Gibbs S, Smith D, Bryant C, Elliot F, Gulliver P
Toberman H, Adams J, Ti, G. P. (2016) *Soil survey in England, Scotland and Wales carried out during 2013 and 2014 [LTLS]. NERC Environmental Information Data Centre*. doi: <https://doi.org/10.5285/17bebd7e-d342-49fd-b631-841ff148ecb0>.

Tranvik, L. J., Downing, J. A., Cotner, J. B., Loiselle, S. A., Striegl, R. G., Ballatore, T. J., Dillon, P., Finlay, K., Fortino, K., Knoll, L. B., Kortelainen, P. L., Kutser, T., Larsen, S., Laurion, I., Leech, D. M., McCallister, S. L., McKnight, D. M., Melack, J. M., Overholt, E., Porter, J. A., Prairie, Y., Renwick, W. H., Roland, F., Sherman, B. S., Schindler, D. W., Sobek, S., Tremblay, A., Vanni, M. J., Verschoor, A. M., von Wachenfeldt, E. and Weyhenmeyer, G. A. (2009) 'Lakes and reservoirs as regulators of carbon cycling and climate', *Limnology and Oceanography*, 54(6), pp. 2298–2314. doi: 10.4319/lo.2009.54.6_part_2.2298.

Trumbore, S. (2000) 'AGE OF SOIL ORGANIC MATTER AND SOIL RESPIRATION: RADIOCARBON CONSTRAINTS ON BELOWGROUND C DYNAMICS', *Ecological Applications*. Ecological Society of America, 10(2), pp. 399–411. doi: 10.1890/1051-0761(2000)010[0399:AOSOMA]2.0.CO;2.

Trumbore, S. (2009) 'Radiocarbon and Soil Carbon Dynamics', *Annual Review of Earth and Planetary Sciences*, 37(1), pp. 47–66. doi: 10.1146/annurev.earth.36.031207.124300.

Trumbore, S. E. (1993) 'Comparison of carbon dynamics in tropical and temperate soils using radiocarbon measurements', *Global Biogeochemical Cycles*, 7(2), pp. 275–290. doi: 10.1029/93GB00468.

Turner, B. L., Cade-Menun, B. J., Condon, L. M. and Newman, S. (2005) 'Extraction of soil organic phosphorus', *Talanta*, 66(2), pp. 294–306. doi: 10.1016/j.talanta.2004.11.012.

Turner, B. L., Cheesman, A. W., Godage, H. Y., Riley, A. M. and Potter, B. V. L. (2012) 'Determination of *neo* - and *d* - *chiro* -Inositol Hexakisphosphate in Soils by

Solution ³¹ P NMR Spectroscopy', *Environmental Science & Technology*. American Chemical Society, 46(9), pp. 4994–5002. doi: 10.1021/es204446z.

Turner, B. L., Papházy, M. J., Haygarth, P. M. and McKelvie, I. D. (2002) 'Inositol phosphates in the environment.', *Philosophical transactions of the Royal Society of London. Series B, Biological sciences*, 357(1420), pp. 449–69. doi: 10.1098/rstb.2001.0837.

Del Vecchio, R. and Blough, N. V. (2004) 'On the origin of the optical properties of humic substances', *Environmental Science and Technology*, 38(14), pp. 3885–3891. doi: 10.1021/es049912h.

Verpoorter, C., Kutser, T., Seekell, D. A. and Tranvik, L. J. (2014) 'A global inventory of lakes based on high-resolution satellite imagery', *Geophysical Research Letters*, 41(18), pp. 6396–6402. doi: 10.1002/2014GL060641.

Vitousek, P. M., Mooney, H. a, Lubchenco, J. and Melillo, J. M. (1997) 'Human Domination of Earth' s Ecosystems', *Science*, 277(5325), pp. 494–499. doi: 10.1126/science.277.5325.494.

Vitousek, P. M., Porder, S., Houlton, B. Z. and Chadwick, O. A. (2010) 'Terrestrial phosphorus limitation: mechanisms, implications, and nitrogen–phosphorus interactions', *Ecological Applications*. Ecological Society of America, 20(1), pp. 5–15. doi: 10.1890/08-0127.1.

Waiser, M. J., Waiser, M. J. and Robarts, R. D. (2000) 'Changes in composition and reactivity of allochthonous DOM in a prairie saline lake', *Limnology and Oceanography*, 45(4), pp. 763–774. doi: 10.4319/lo.2000.45.4.0763.

WAKSMAN, S. A. (1936) 'Humus Origin, Chemical Composition, and Importance in Nature', *Soil Science*, 41(5), p. 395. doi: 10.1097/00010694-193605000-00010.

WALKER, T. W. and ADAMS, A. F. R. (1958) 'STUDIES ON SOIL ORGANIC MATTER', *Soil Science*, 85(6), pp. 307–318. doi: 10.1097/00010694-195806000-00004.

Walker, T. W. and Syers, J. K. (1976) 'The Fate of Phosphorus During Pedogenesis', *Geoderma*, 15, pp. 1–19.

Walling, D. (2013) 'Sediment source: a key parameter of catchment sediment yield', in Fukuoka, H Nakagawa, S. T. and H. Z. (ed.) *Advances in River Sediment Research , Proc. 12th International Symposium on River Sedimentation, ISRS 2013, Kyoto, Japan*. CRC press, pp. 37–47.

Walling, D. E. (2005) 'Tracing suspended sediment sources in catchments and river systems.', *The Science of the total environment*, 344(1–3), pp. 159–84. doi: 10.1016/j.scitotenv.2005.02.011.

Wang, X., Ma, H., Li, R., Song, Z. and Wu, J. (2012) 'Seasonal fluxes and source variation of organic carbon transported by two major Chinese Rivers: The Yellow River and Changjiang (Yangtze) River', *Global Biogeochemical Cycles*, 26(2), pp. 1–10. doi: 10.1029/2011GB004130.

WARDLE, D. A. (1992) 'a Comparative Assessment of Factors Which Influence Microbial Biomass Carbon and Nitrogen Levels in Soil', *Biological Reviews*. Blackwell Publishing Ltd, 67(3), pp. 321–358. doi: 10.1111/j.1469-185X.1992.tb00728.x.

Watanabe, F. S. and Olsen, S. R. (1965) 'Test of an Ascorbic Acid Method for

Determining Phosphorus in Water and NaHCO₃ Extracts from Soil¹, *Soil Science Society of America Journal*. Soil Science Society of America, 29(6), p. 677. doi: 10.2136/sssaj1965.03615995002900060025x.

Weishaar, J. L., Aiken, G. R., Bergamaschi, B. A., Fram, M. S., Fujii, R. and Mopper, K. (2003) 'Evaluation of specific ultraviolet absorbance as an indicator of the chemical composition and reactivity of dissolved organic carbon', *Environmental Science and Technology*. American Chemical Society, 37(20), pp. 4702–4708. doi: 10.1021/es030360x.

Wetzel, R. G. (2001) *Limnology : lake and river ecosystems*. Academic Press.

Wick, B. and Tiessen, H. (2008) 'Organic Matter Turnover in Light Fraction and Whole Soil Under Silvopastoral Land Use in Semiarid Northeast Brazil', *Rangeland Ecology & Management*, 61(3), pp. 275–283. doi: 10.2111/07-038.1.

Wilkinson, J., Reynolds, B., Neal, C., Hill, S., Neal, M. and Harrow, M. (1997) 'Major, minor and trace element composition of cloudwater and rainwater at Plynlimon', *Hydrology and Earth System Sciences*. Copernicus GmbH, 1(3), pp. 557–569. doi: 10.5194/hess-1-557-1997.

Willey, D., Kieber, R. J., Eyman, M. S., Brooks, G. and Jr, A. (2000) 'Rainwater dissolved organic carbon: Concentrations and global flux', *Global Biogeochemical Cycles*, 14(1), pp. 139–148.

William H. Schlesinger, E. S. B. (2013) *Biogeochemistry : an analysis of global change - Lancaster University (Alma)*. Amsterdam; Oxford : Elsevier/Academic Press, 2013 .

Withers, P. J. A. and Jarvie, H. P. (2008) 'Delivery and cycling of phosphorus in rivers:

A review', *Science of The Total Environment*, 400(1), pp. 379–395. doi: 10.1016/j.scitotenv.2008.08.002.

Worrall, F., Burt, T. P. and Howden, N. J. K. (2014) 'The fluvial flux of particulate organic matter from the UK: Quantifying in-stream losses and carbon sinks', *Journal of Hydrology*, 519, pp. 611–625. doi: 10.1016/j.jhydrol.2014.07.051.

Wu, Z., Huang, N. E., Wallace, J. M., Smoliak, B. V and Chen, X. (2011) 'On the time-varying trend in global-mean surface temperature', *Climate Dynamics*, 37(3), pp. 759–773. doi: 10.1007/s00382-011-1128-8.

Yang, X. and Post, W. M. (2011) 'Phosphorus transformations as a function of pedogenesis: A synthesis of soil phosphorus data using Hedley fractionation method', *Biogeosciences*. Copernicus GmbH, 8(10), pp. 2907–2916. doi: 10.5194/bg-8-2907-2011.

Zhang, Y. L., Qin, B. Q., Zhang, L., Zhu, G. W. and Chen, W. M. (2005) 'Spectral absorption and fluorescence of chromophoric dissolved organic matter in shallow lakes in the middle and lower reaches of the Yangtze River', *Journal of Freshwater Ecology*, 20(3), pp. 451–459. doi: 10.1080/02705060.2005.9664760.

Zimmermann, M., Leifeld, J., Schmidt, M. W. I., Smith, P. and Fuhrer, J. (2007) 'Measured soil organic matter fractions can be related to pools in the RothC model', *European Journal of Soil Science*. Blackwell Publishing Ltd, 58(3), pp. 658–667. doi: 10.1111/j.1365-2389.2006.00855.x.

Zysset, M. and Berggren, D. (2001) 'Retention and release of dissolved organic matter in Podzol B horizons', *European Journal of Soil Science*. Blackwell Science Ltd, 52(3), pp. 409–421. doi: 10.1046/j.1365-2389.2001.00399.x.

